IN-SITU BURNING OF

UNCONTAINED OIL SLICKS

EE-60 revised

IN-SITU BURNING OF UNCONTAINED OIL SLICKS

by

S.L. Ross Environmental Research Limited
Ottawa, Ontario

and

Energetex Engineering
Waterloo, Ontario

Environmental Emergencies Technology Division
Technology Development and Technical Services Branch
Environmental Protection Directorate
Conservation & Protection
Ottawa, Ontario
K1A 0E7

EE-60 revised

July 1986

ABSTRACT

This report presents the methodology, results, conclusions and recommendations arising from a study on the use of in-situ burning as a countermeasure for uncontained batch oil spills. It is concluded that this technique has the potential to remove a considerable percentage of the oil from such spills, providing ignition can be effected within several hours of the incident.

The research has shown that removal efficiency increases with increasing spill volume. The maximum value is about 96% for a spill of 10^4 m^3 ignited immediately. At a certain delay time, different for each size of spill, the removal efficiency of the combustion decreases quickly, and the possibility of burning any significant fraction of the spilled oil is sharply reduced.

These critical delay times can be approximated by a simple expression which can then be used to predict the critical ignition delay time for spills of any size. That expression is:

delay time (hours) = 0.1 $V_s^{1/2}$, V_s in m^3

This means that a spill of 10^4 m^3 can still be ignited 10 hours after it occurs, but a spill of 1 m^3 must be ignited in 6 minutes.

Delayed ignition of a spill can be achieved by deploying igniters around the periphery. Experimental data from one test indicate that there should be one igniter for every three metres of slick periphery. Combining this number with the radius of the slick at the critical ignition delay time gives the number of igniters required to achieve ignition at the latest possible time: 30 are required for a spill of $1 m^3$, 238 for 10^2 m^3, and 1,875 for a spill of 10^4 m^3.

Further research to test the developed models, including large scale field trials, is recommended.

RESUME

FOREWORD

This study was conducted by Mr. I.A. Buist of S.L. Ross Environmental Research Limited, with the assistance of Mr. E. Twardus of Energetex Engineering, under contract to the Environmental Protection Service.

ACKNOWLEDGEMENTS

This study was funded by Environment Canada, through the Arctic Marine Transportation Program, and the United States Coast Guard. Sohio Alaska Petroleum Company provided funds and logistics to support the large-scale testing phase of the study.

In particular, Ms. Francine Laperriere and Mr. Harry Whittaker of Environment Canada, LTJG Michele Fitzpatrick of the U.S. Coast Guard and Ms. Sharon Hillman of Sohio Alaska Petroleum are thanked for their invaluable assistance.

TABLE OF CONTENTS

LIST OF FIGURES

LIST OF TABLES

LIST OF PLATES

1.0 INTRODUCTION

Although Canada has never suffered from a massive marine oil spill, a finite probability exists that one might occur as a result of current or proposed offshore petroleum related activities (Figure 1.1). This study assessed in-situ burning as a countermeasure for large, batch oil spills (i.e. from tanker accidents).

1.1 TANKER TRAFFIC

Medium size tankers (MSTs) in the size range of 45,000 to 160,000 DWT and very large crude carriers (VLCCs) in the size range of 160,000 to 320,000 DWT already represent a threat to Canada in terms of massive oil spills. On the west coast VLCCs are being used to transport Alaskan crude from Valdez to Cherry Point through the Straits of Juan de Fuca and Rosario. On the East Coast MSTs and VLCCs transport crude oil from South America and the Middle East to Canadian deep water ports.

The shipment of Beaufort Sea crude oil to eastern Canadian markets has also been suggested. The icebreaking tankers proposed would be in the size ranges of 80,000 and 200,000 DWT. These tankers would steam from the Beaufort Sea, through Prince of Wales Strait into Viscount Melville Sound, then east through Lancaster Sound to Baffin Bay, and south through Davis Strait to the Maritimes. A plan to ship High Arctic crude from Cameron Island to southern markets has also been recently approved.

A major oil spill could occur at any point along any of the existing and proposed tanker routes.

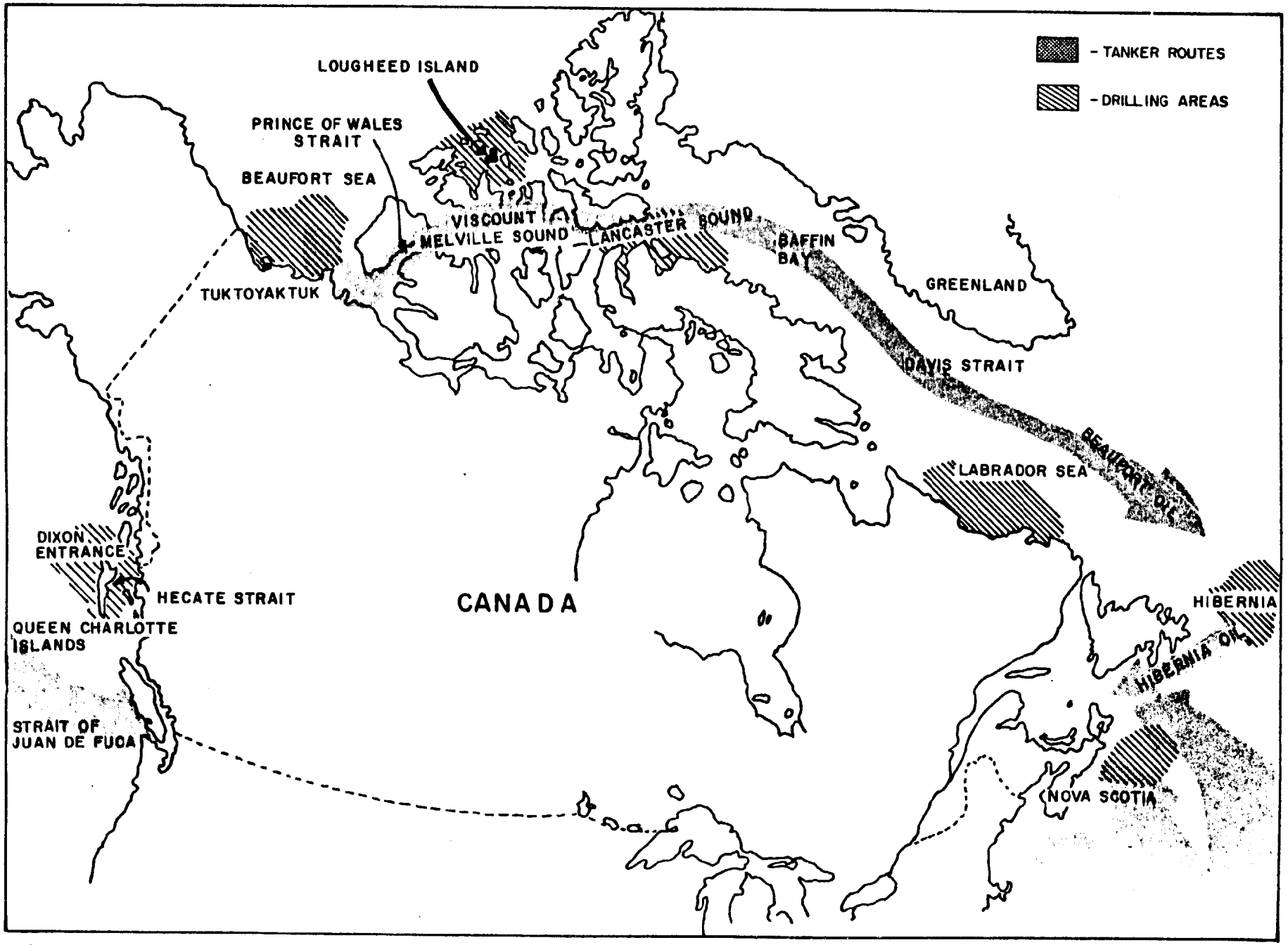

FIGURE 1.1: LOCATION OF POTENTIAL OFFSHORE PETROLEUM RELATED ACTIVITIES IN CANADA

1.2 TANKER SPILL STATISTICS

In the four year period, 1969 to 1973, there were in excess of 3,000 recorded accidents involving tankers worldwide. Fifty-one of these accidents involved the discharge of a total of over 770,000 tons of oil into the sea (Butler, 1978). From 1974 to 1980 it is estimated that 2,731,000 tons of oil entered the sea following tanker accidents (IMO, 1981). This represents an average of 390,000 tons a year.

Table 1.1 illustrates the size range and relative frequency of tanker oil spills in the period 1968 to 1978 for ships greater than 10,000 DWT and spills larger than 200 tons. More than half these incidents involved spills larger than 5,000 tons (DNV, 1979).

In 1980 there were 54 tanker spills recorded. Of the 31 of these for which the spill volume is known, 28 involved spills greater than 75,000 litres (about 650 tons) totalling some 235,000 cubic metres (about 205,000 tons) (OSIR, 1981).

1.3 EXISTING TANKER SPILL CLEANUP TECHNOLOGY

Conventional response to a major tanker spill can include the steps of source control, offshore oil containment and recovery, offshore dispersant application and in-situ burning, and shoreline protection and cleanup. Each of these operations must involve equipment and personnel being sent to the spill from a shore base, since no tanker in use today carries spill response equipment capable of cleaning up a major spill (S.L. Ross, 1983).

TABLE 1.1

TANKER OIL SPILL SIZES

Size Range of Oil Spill (Tons)	Accidents			Total Oil Spilled
	No.	% of Total	Tons	% of Total
200 - 1,000	17	21.8	9,750	0.6
1,000 - 2,000	5	6.4	6,620	0.4
2,000 - 5,000	13	16.7	47,255	2.9
5,000 - 15,000	11	14.1	118,250	7.2
15,000 - 30,000	19	24.3	444,880	27.0
30,000 - 50,000	6	7.7	232,819	14.2
50,000 - 100,000	4	5.1	327,000	19.9
100,000+	3	3.8	457,000	27.8
TOTAL	78	TOTAL	1,643,574	

Source: DNV, 1979

1.3.1 Source Control

The purpose of this highly specialized operation is to minimize the escape of oil from the stricken vessel by lightening the cargo into another vessel and attempting to patch the damage. For many spills these actions are not practicable because of time restraints; the hydrostatic pressure of the oil in the damaged cargo tank is such that large volumes of oil are often spilled in just a few minutes or hours after the accident occurs (S.L. Ross, 1983)

1.3.2 Offshore Containment and Recovery

The offshore containment and recovery equipment available for response to major tanker spills is generally located at populated coastal centres because of maintenance, logistics, and other practical reasons. It is unlikely that the equipment could be mobilized at a tanker spill site in less than 10 to 24 hours. By this time the oil will have spread to cover a considerable area, greatly minimizing the effectiveness of containment and recovery operations.

Additionally, available offshore oil containment booms and skimmers are limited to operating in open water conditions in waves less than 1. to 1.5 m in height and currents less than 0.5 m/s. With the exception of summer conditions in the southern Beaufort Sea and the Northwest Passage, these open water conditions are not the Canadian norm. The available equipment is severely limited by even light ice conditions.

Thus, offshore oil spill containment and recovery equipment has a limited application for tanker spills in Canadian waters (S.L. Ross, 1982a).

1.3.3 Offshore Dispersant Application and In-Situ Burning in Ice

Dispersants

Presently available oil spill dispersants can be applied to a slick either aerially from fixed or rotary-wing aircraft, or from vessels. Dispersant dosages are normally in the range of 5 to 10 parts dispersant per 100 parts of oil. Even for moderate sized oil releases, thousands of litres of dispersant would be required. In addition, conventional dispersants are only effective on relatively non-viscous oils and on oil spilled in open water conditions.

Oil slicks on water very quickly evaporate and usually form water-in-oil emulsions. These weathering processes result in an increase in viscosity of the oil, beyond which point the dispersants are ineffective. It is generally believed that dispersants must be applied to spilled oil at least within 24 to 48 hours of the release.

In much of Canada's coastal waters, particularly in the Arctic this would be impossible to achieve. Unless large volumes of dispersant and spray aircraft are stockpiled around Canada the potential effectiveness of dispersants on tanker spills is likely to be low (S.L. Ross, 1982b).

In-Situ Burning

Oil spilled on or under solid sea ice is amenable to removal by in-situ burning (Dickins and Buist, 1981; NORCOR, 1975). The spreading of oil spills in these cases is considerably reduced compared to its spreading on water because the oil is contained by the ice and snow. Thick pools of oil on ice can be ignited and burned with removal efficiencies in excess of 90% (Dickins and Buist, 1981; Energetex, 1981a). Oil spilled in or under solid sea ice will be encapsulated by the growing ice and preserved in a fresh state until the ice melts. At this point the oil apppears in melt pools on the ice surface. Much of the oil can be ignited and burned using commercially available air-deployable

igniters dropped from helicopters (Dickins and Buist, 1981; S.L. Ross, 1981). The key to the potential success of this approach is the containment of the oil in thick pools by the ice.

1.3.4 Shoreline Cleanup

The end result of a tanker accident in coastal waters is usually the oiling of nearby shorelines. The cleanup of these shorelines, if possible at all, usually involves a labour intensive, costly operation. It is thus undeniably preferable to deal with the oil offshore, particularly near the source of the spill, soon after it occurs.

1.4 PROPOSED ON-BOARD SELF-HELP COUNTERMEASURES FOR ARCTIC TANKERS

A recent in-depth study of potential spills and on-board countermeasures for proposed Arctic tankers (S.L. Ross, 1983) concluded that several techniques could successfully reduce the size of a potential oil spill. These involved restricting the inflow of air and inert gas into the ullage space of a damaged cargo tank, directing oil from a damaged cargo tank to a sound ballast tank via a special valved pipe and the use of self-powered, portable deepwell pumps. The combination of these techniques could theoretically reduce the size of potential spills from Arctic tankers by 85% or more.

The study also addressed the possibility of carrying oil spill countermeasures equipment aboard Arctic tankers to remove oil spilled from the tanker in ice and open water conditions. It was concluded that, for large spills, only the use of air-deployable igniters dropped from a helicopter stationed on the tanker showed promise. For spills in a solid ice cover it was concluded that this technique could be extremely effective in removing spilled oil. It was strongly recommended that in-situ burning of the oil in broken ice and open water conditions be investigated as this is the only technique that seems feasible in these conditions.

1.5 SUMMARY

Conventional land-based response to a major tanker spill in Canadian coastal waters is unlikely to be successful. With the possible exception of the use of air-deployable igniters to burn oil in a solid ice cover, the end results would be a costly and labour intensive shoreline cleanup operation.

In the case of proposed Arctic VLCCs the implementation of on-board self-help countermeasures could reduce the size of potential oil spills; however, considerable quantities of oil could still be released. Although in a solid ice cover burning techniques could remove much of this oil, no proven technique exists to effectively deal with the oil in rough open water or broken ice conditions, even shortly after its release, when it is in a fresh and thick state. In-situ burning of uncontained oil slicks on open water or amongst broken ice could prove to be the solution to this difficult problem.

2.0 STUDY OBJECTIVE AND REPORT CONTENTS

This study was undertaken to investigate the capabilities and limitations of igniting and burning large uncontained oil slicks at sea. The objective was to determine whether or not in-situ combustion of oil released from damaged tankers is a technically feasible countermeasure for open water conditions. Key areas of the burning of uncontained oil slicks that were addressed included:

- oil spreading on water,
- flame spreading on oil,
- removal efficiency of spreading oil slicks,
- the effects of delays in ignition of the oil, and
- location of ignition.

Chapter 3 covers the state-of-the-art of in-situ burning as an oil spill countermeasures tool. Chapter 4 documents the methodology, results and conclusions of the small-scale wind tunnel studies of oil and flame spreading on water.

Chapter 5 discusses the mid-scale tank testing of two-dimensional oil and flame spreading, uncontained slick removal efficiency and slick combustion rates. Chapter 6 covers the large-scale testing, conducted at Prudhoe Bay, Alaska, to determine scaling effects and the impact of delayed ignition on burn efficiency.

Chapter 7 presents the development and results of a mathematical model to predict uncontained oil slick removal efficiencies as a function of spill volume, induced wind, and ignition delay. The model results are compared with the experimental data.

Chapter 8 presents the conclusions and recommendations arising from the study.

3.0 THE STATE-OF-THE-ART

The comsumption rate of large, thick oil fires on water or ice is about 5×10^{-5} m^3/m^2s (2.8 mm/min) (McAllister and Buist, 1981; Wakamiya et al, 1982) and ranges from 2 to 5×10^{-5} m^3/m^2s (Babrauskas, 1983). The volumetric efficiency (total volume burned versus initial volume) of crude oil in-situ burning is dependent primarily on the initial oil thickness and containment of the oil slick during combustion. Crude oil fires on water will extinguish when the heat transfer from the slick to the water or ice beneath exceeds the heat transfer to the slick from the flame and the oil cools to below its fire point (Wakamiya et al, 1982). For most crude oils this occurs when the slick is less than about 1 mm thick (Energetex, 1981b). When oil slicks are contained by a barrier, such as ice or a fireproof boom, the oil cannot spread and high removal efficiencies can be obtained, on the order of 80-99% (McAllister and Buist, 1981; Dickins and Buist, 1981). Wind, acting to hold the oil against a barrier usually inhibits the spread of flame upwind over the entire slick area, but over longer time periods high combustion efficienicies are achieved as the wind "feeds" oil to the localized burning area near the containing edge (Energetex, 1981a). In-situ burning of oil rapidly raises the oil temperature. This results in a large decrease in the viscosity of the oil, and a subsequent decrease in its tendency to resist spreading. Once the slick thickness approaches 1 mm the fire will extinguish.

For spills on open water historical evidence suggest that in-situ burning may be a countermeasure alternative since there have been several cases of tanker accidents where the oil accidentally caught fire and most of the spilled oil was consumed on-site before spreading to cover large areas (e.g., Goodier and Siclari, 1981; Horn and Neal, 1981). Some examples are shown in Plates 3.1 through 3.4. Research has determined that the combustion process in such spills does not seem to be severely affected by regular waves, such as a swell, although choppy seas may extinguish the fire (McAllister and Buist, 1981).

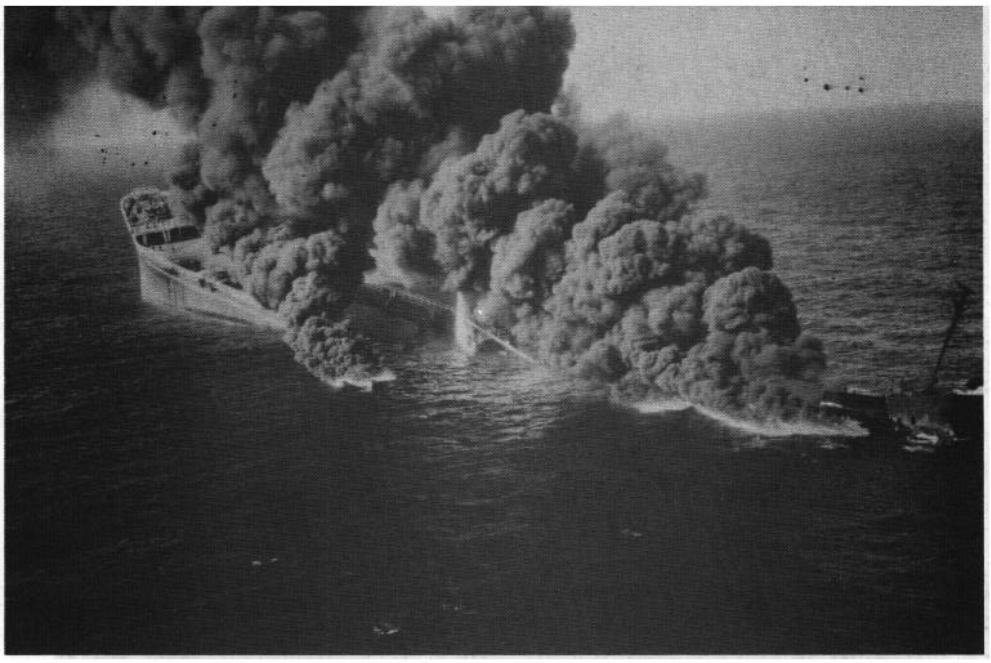

PLATE 3.1 - MT ASSIMI; 07/01/83; 52,000 TONNES IRANIAN LIGHT CRUDE

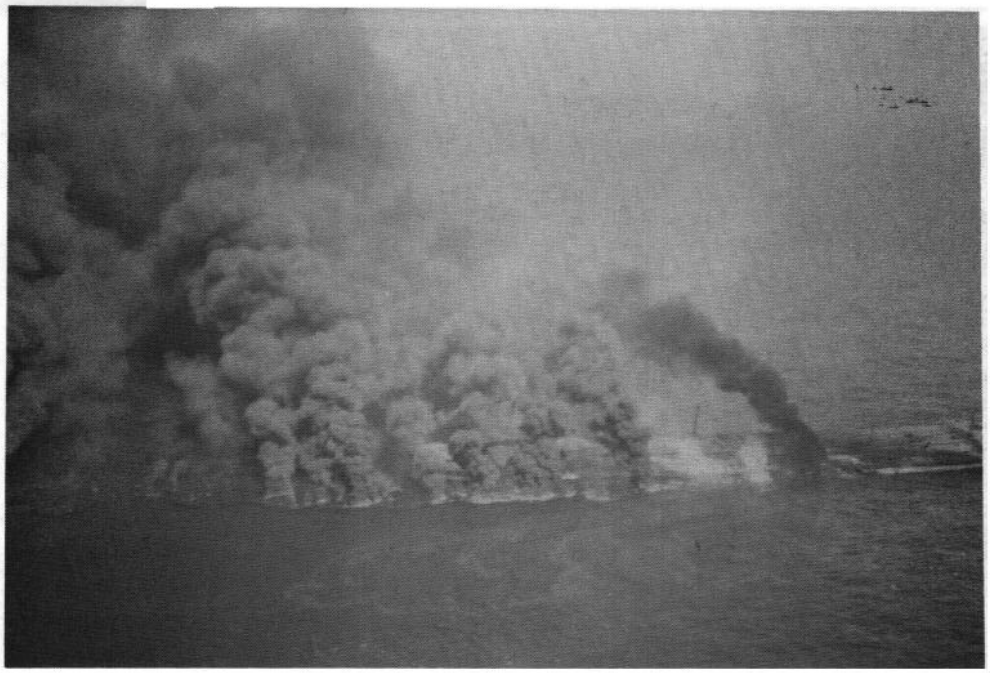

PLATE 3.2 - MT ATLANTIC EMPRESS; 19/07/79; 287,000 TONNES MURBAN, BERRI AND ARABIAN LIGHT CRUDES

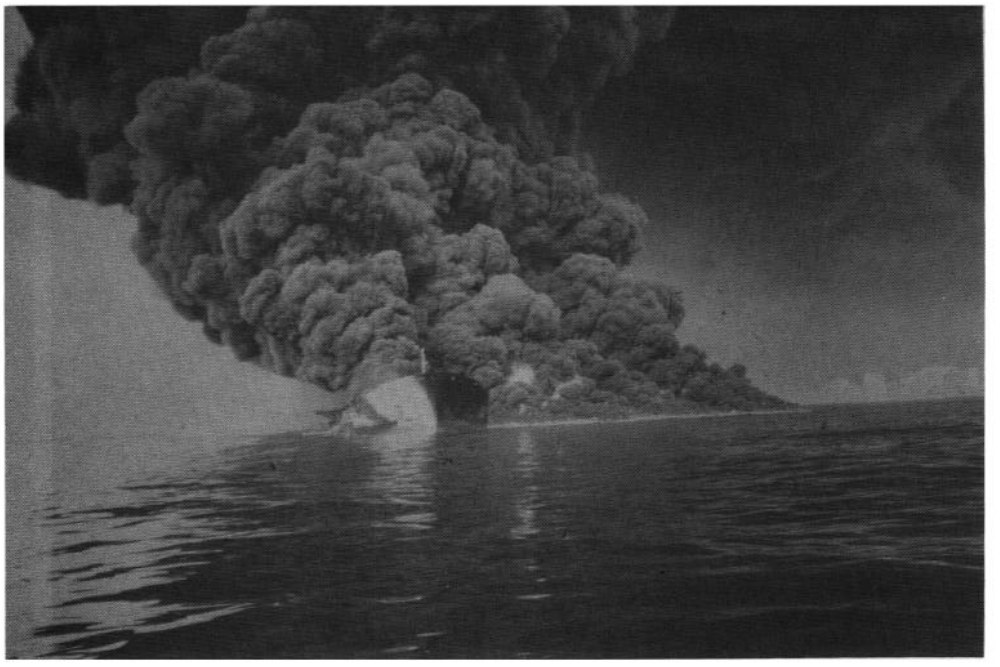

PLATE 3.3 - MT JAKOB MAERSK; 29/01/75; 88,000 TONNES ARABIAN LIGHT CRUDE

PLATE 3.4 - MT BETELGEUSE; 08/01/79; 40,000 TONNES LIGHT ARABIAN CRUDE

The key to successful open water in-situ combustion is to contain the oil at thicknesses much greater than 1 mm during the burning. An immediate response after a tanker accident will increase the chances for effective burning since the uncontained slick is thick and the oil fresh; thus, potential removal efficiency and flame spreading are enhanced.

One approach to containing the oil is to deploy a fireproof barrier around the slick. Although fireproof booms are available (e.g., Buist et al, 1983; Meikle, 1983) their use is limited to the same sea states as conventional offshore containment and recovery equipment. Their bulk makes swift mobilization unlikely.

The second approach is simply to set the free-floating slick(s) on fire. This technique has been tried on past tanker spills with varying success. For slicks of weathered crude oil or bunker, the oil is difficult to ignite. Also the combustion is not efficient, and leaves behind large volumes of heavy, viscous residue that is difficult to deal with (Thompson et al, 1980). However, in cases where large thick slicks of fresh crude oil or light distilled product have ignited, the combustion is intense and much of the oil burns (Horn and Neal, 1981). This would be the case for a burning operation initiated shortly after the tanker accident.

The premise of the study was based on the idea that, if a large, thick slick of oil is ignited, and the flames spread to cover the majority of the slick before it thins to less than one millimetre, very high oil removal efficiencies are possible. As the fire grows it can be postulated that the air entrained by the combustion and the thermal plume reduce the spreading rate of the oil and, at some critical fire diameter, stop the spreading, resulting in potentially very high oil removal efficiencies.

4.0 SMALL-SCALE OIL AND FLAME SPREADING TESTS

The goal of this phase of the study was to determine, experimentally, the following:

- the rate of spread of various oils on water,
- the rate of spread of flame over oil as a function of windspeed and direction, oil type, weathering and temperature,
- the rate of spread of burning oil.

4.1 METHODS

Small-scale experiments to investigate oil spreading and flame spreading were conducted in a small wind tunnel in Ottawa, (Plates 4.1 through 4.4 and Figure 4.1). A crude oil, Alberta Sweet Mixed Blend (provided by Petro-Canada), was weathered to three different degrees, simulating the exposure of a 3 cm thick slick in a 10 m/s wind for one, four and eight hours at 10°C. A fresh diesel oil was also used in the experiments. Table 4.1 gives the physical properties of the four oils.

The oil spreading experiments involved the placement of 600 cm^3 of oil in the upwind end of a 3m long x 10 cm wide water trough in the wind tunnel. The oil was retained, at an initial thickness of 2 cm, by a removable rubber dam. Prior to each run the wind speed was measured, using a thermal anemometer, (Plate 4.5) and air and water temperatures were recorded. (See Appendix 1 for the velocity profiles and conversions to atmospheric winds).

The spreading of the oil, released by raising the dam (Plate 4.6), was recorded on videotape and measured against a scale marked on the outside of the trough visible through the plexiglass windows of the wind-tunnel. Time, in hundredths of a second, was recorded by a built-in-display timer in the video-camera (Plate 4.7). The trough was cleaned and rinsed thoroughly after each run to minimize the effects of surface films on spreading rates.

PLATE 4.1 - UPWIND VIEW OF TUNNEL

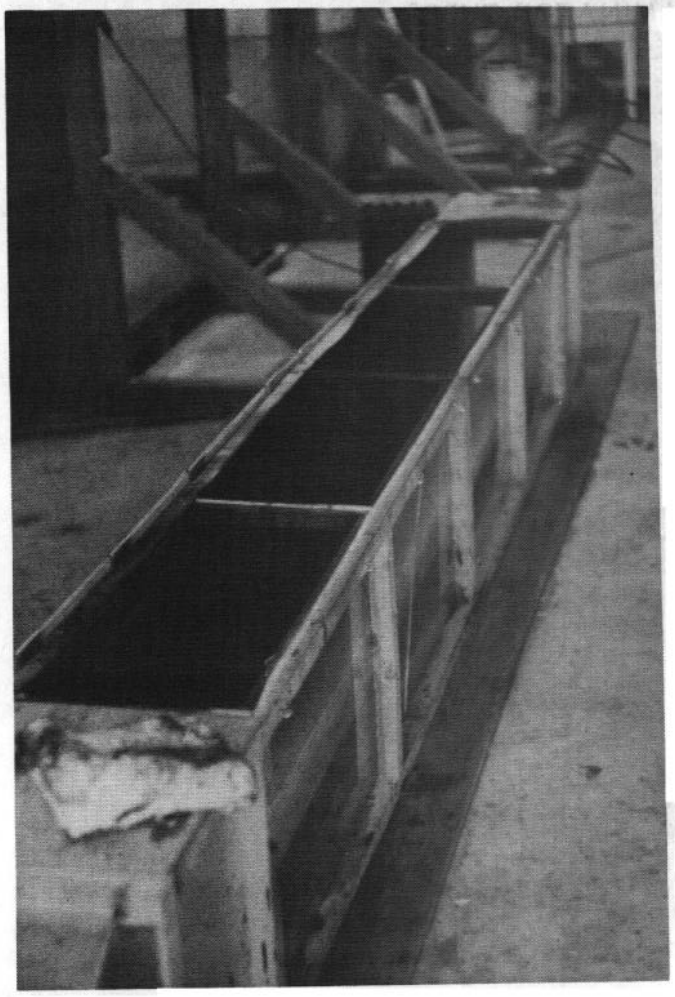

PLATE 4.2 - DOWNWIND VIEW OF TUNNEL & TROUGH (NOTE WATER THERMOMETER)

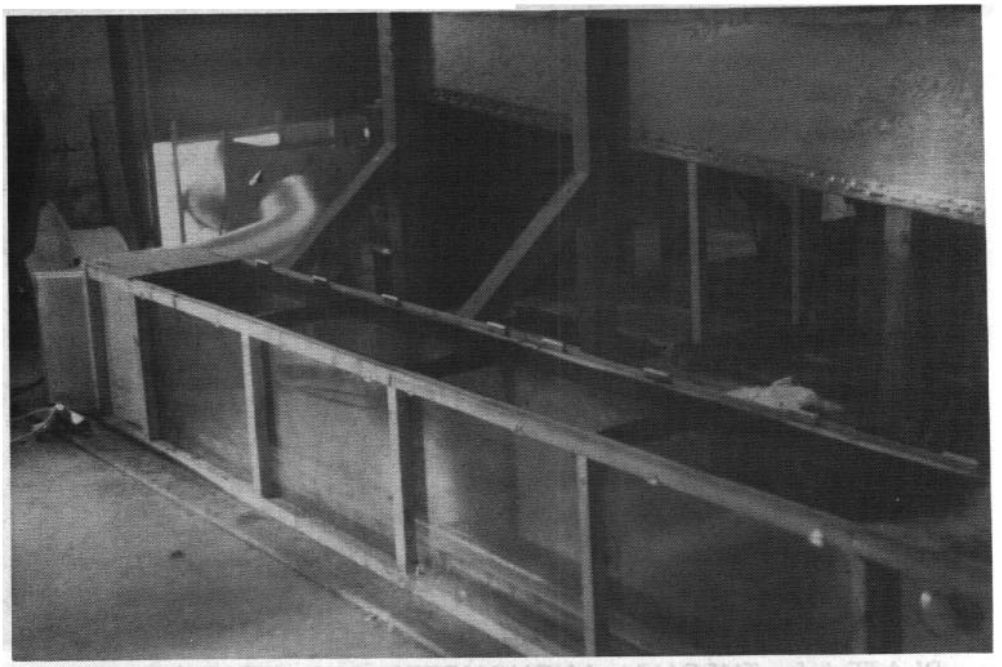

PLATE 4.3 - DOWNWIND VIEW OF TUNNEL SHOWING BELLMOUTH, DUCT AND 2,000 CFM FAN

PLATE 4.4 - DOWNWIND END OF TUNNEL SHOWING FLOW LAMINATOR TUBES

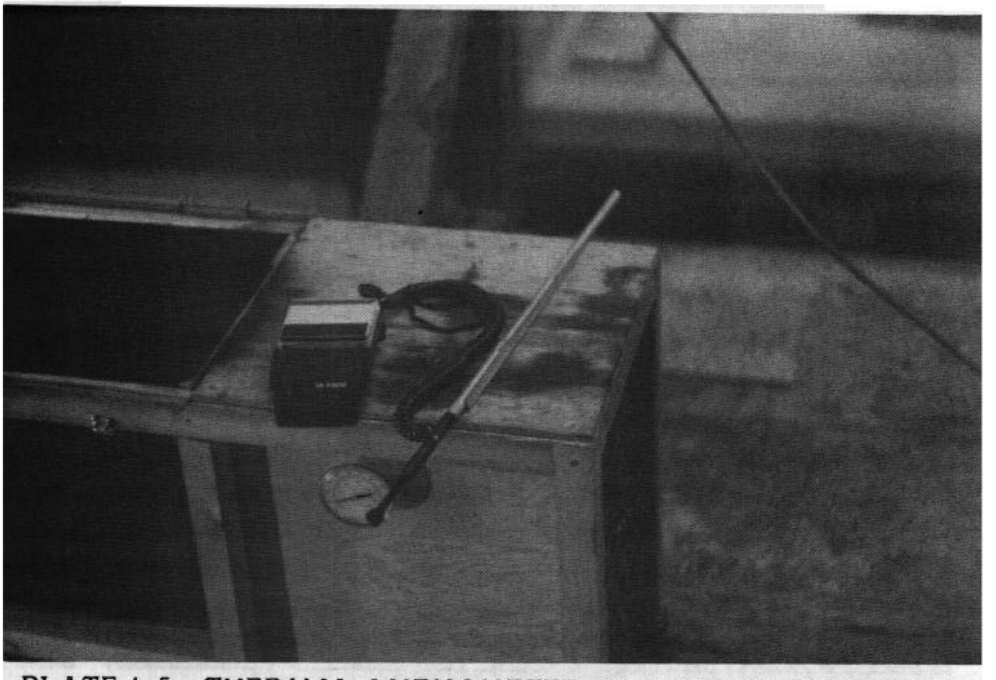

PLATE 4.5 - THERMAL ANEMOMETER AND AIR THERMOMETER

FIGURE 4.1 WIND TUNNEL LAYOUT

LEGEND

- A plastic inlet flow laminator
- B plexiglas windows
- C steel eavestrough
- D hinged access doors
- E instrument ports
- F steel outlets flow laminator bundle
- G steel bellmouth
- H flexible steel duct to 1m^3/s (2000cfm) fan

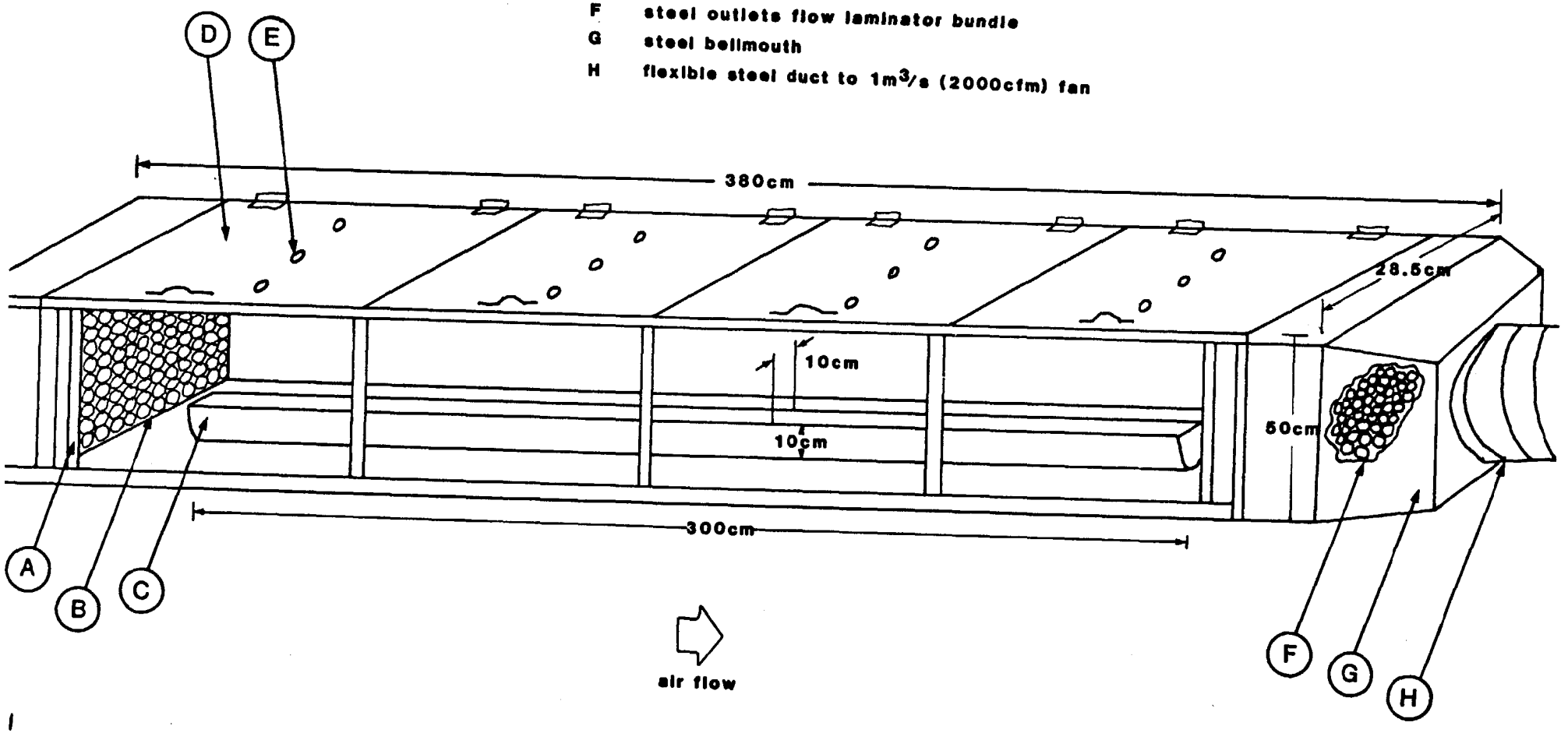

TABLE 4.1

PHYSICAL PROPERTIES OF OILS
USED IN SMALL-SCALE TESTS.

PROPERTY	OIL TYPE			
	ASMB CRUDE AGED 1 HR.	ASMB CRUDE AGED 4 HRS.	ASMB CRUDE AGED 8 HRS.	FRESH DIESEL
DENSITY @ 15°C (g/cm^3)	0.850	0.857	0.865	0.844
VISCOSITY @ 15°C (cSt)	8.6	11.4	16.2	4.0
INTERFACIAL TENSION* @ 15°C (dynes/cm)				
OIL/AIR	26.7	26.8	27.6	28.4
OIL/WATER	21.7	21.9	22.0	28.1
INITIAL BOILING+ POINT (°C)	27	29	33	61

* WATER/AIR = 70.6 dynes/cm
+ MODIFIED ASTM PROCEDURE; SEE APPENDIX 5

PLATE 4.6 - OIL HELD BEHIND REMOVABLE DAM PRIOR TO RUN

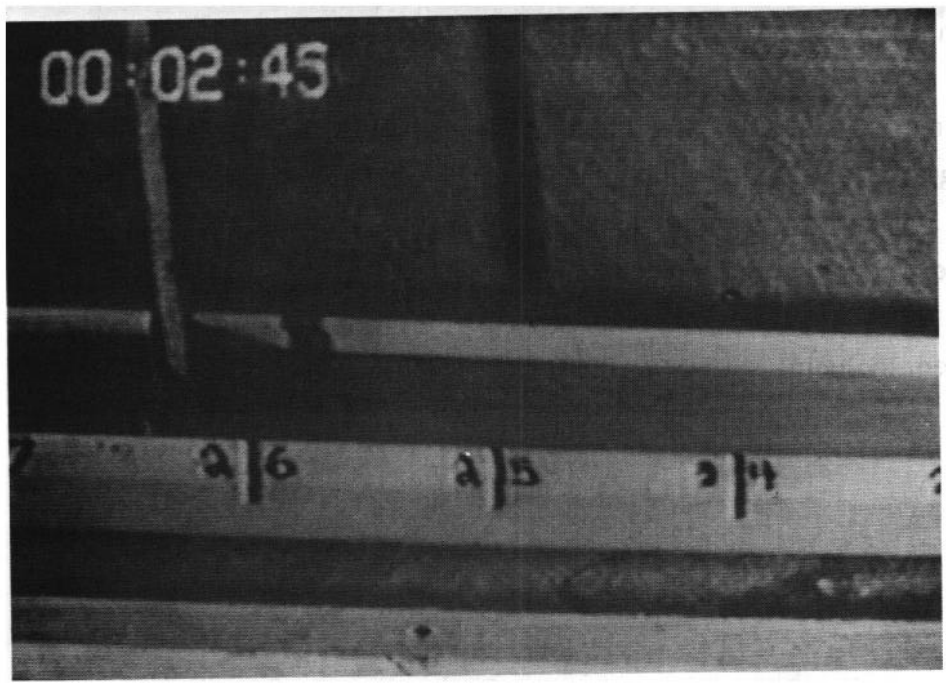

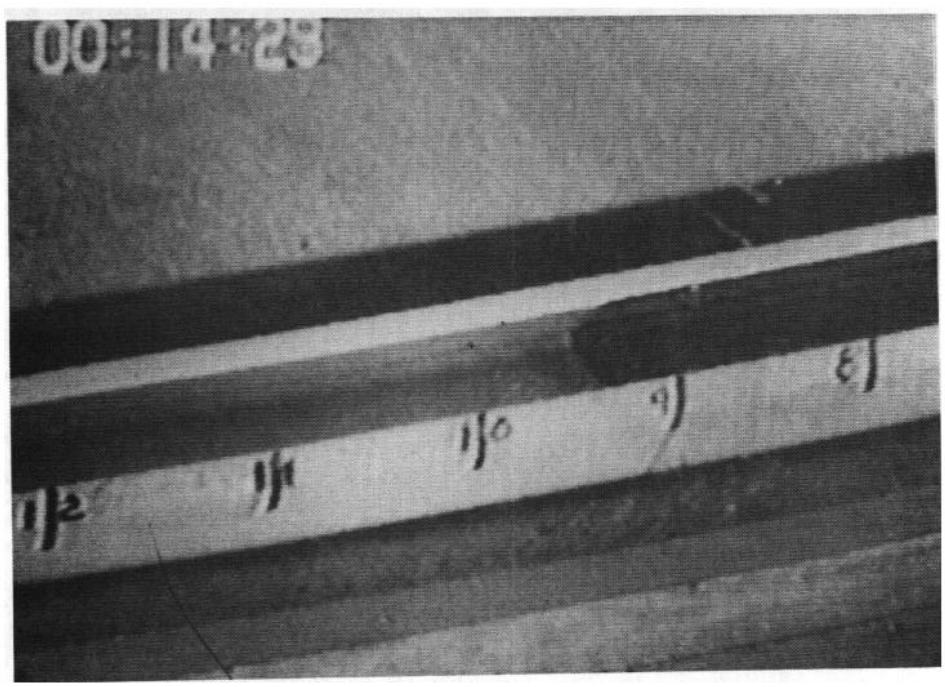

PLATE 4.7 - TIME AND SPREAD DISTANCE WERE VIDEO-RECORDED

Thirty-three runs involving the four oils at wind speeds of 0, 0.2, 0.6, 3.8 and 8.0 m/s (with spreading both up and downwind) were conducted.

Flame spreading on each of the four oils was investigated in two ways. Flame spreading as a function of wind speed (both upwind and downwind at 0.2, 0.5, 1.6 and 3.1 m/s) was measured using the videotaping technique for both a 3 mm thick slick covering the entire trough and ignited at one end (Plate 4.8), and a 2 cm thick slick of burning oil released as in the oil spreading experiments (Plate 4.9). A total of 39 runs were undertaken, including several at different temperatures (1°C, 10°C and 19°C).

PLATE 4.8 - FLAME SPREADING OVER 3mm THICK SLICK

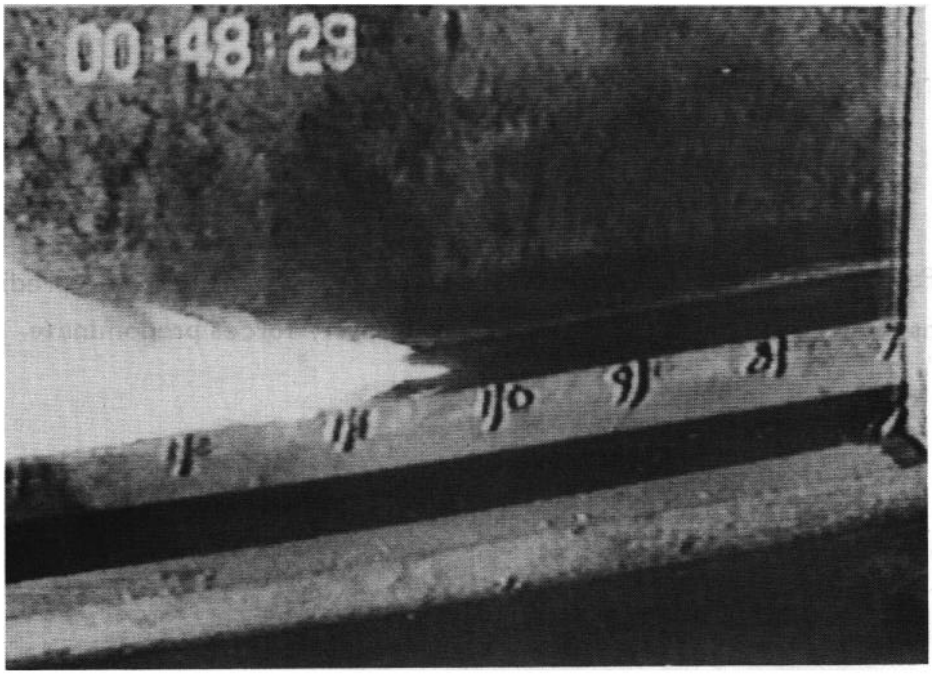

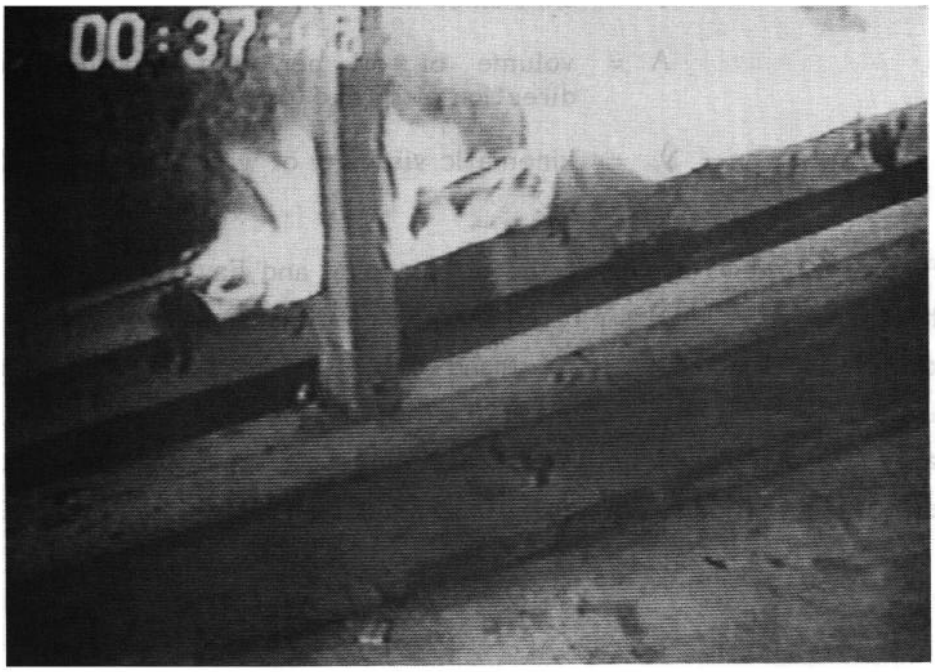

PLATE 4.9 - SPREADING OF BURNING OIL

4.2 RESULTS AND DISCUSSION

The raw data may be found in Appendix 2.

4.2.1 Oil Spreading

Fay (1971) has developed the following equations to predict one dimensional spreading in the regime where gravity forces predominate.

Gravity - Inertial

(4.1) $l = 1.5 (\Delta g A t^2)^{1/3}$

Gravity - Viscous

(4.2) $l = 1.5 (\Delta g A^2 t^{3/2} / \nu^{1/2})^{1/4}$

where

l	=	length of slick (cm)
Δ	=	ratio of density difference between water and oil to density of water
g	=	acceleration of gravity (981 cm/s^2)
t	=	time since initiation of spread (s)
A	=	volume of oil per unit length normal to direction of spread (cm^2)
ν	=	kinematic viscosity of water (10^{-2} cm^2/s)

Figure 4.2 shows a plot of the oil speading and Fay's prediction. Figure 4.3 shows the same results plotted in the non-dimensional form used by Fay. In both cases the data follows the trend of Fay's model but there is a definite oil viscosity effect not accounted for by the model. As the oil viscosity increases the difference between acutal and predicted spreading increases. This effect has been noted by others (e.g. Mackay, 1984; Tebeau et al, 1984).

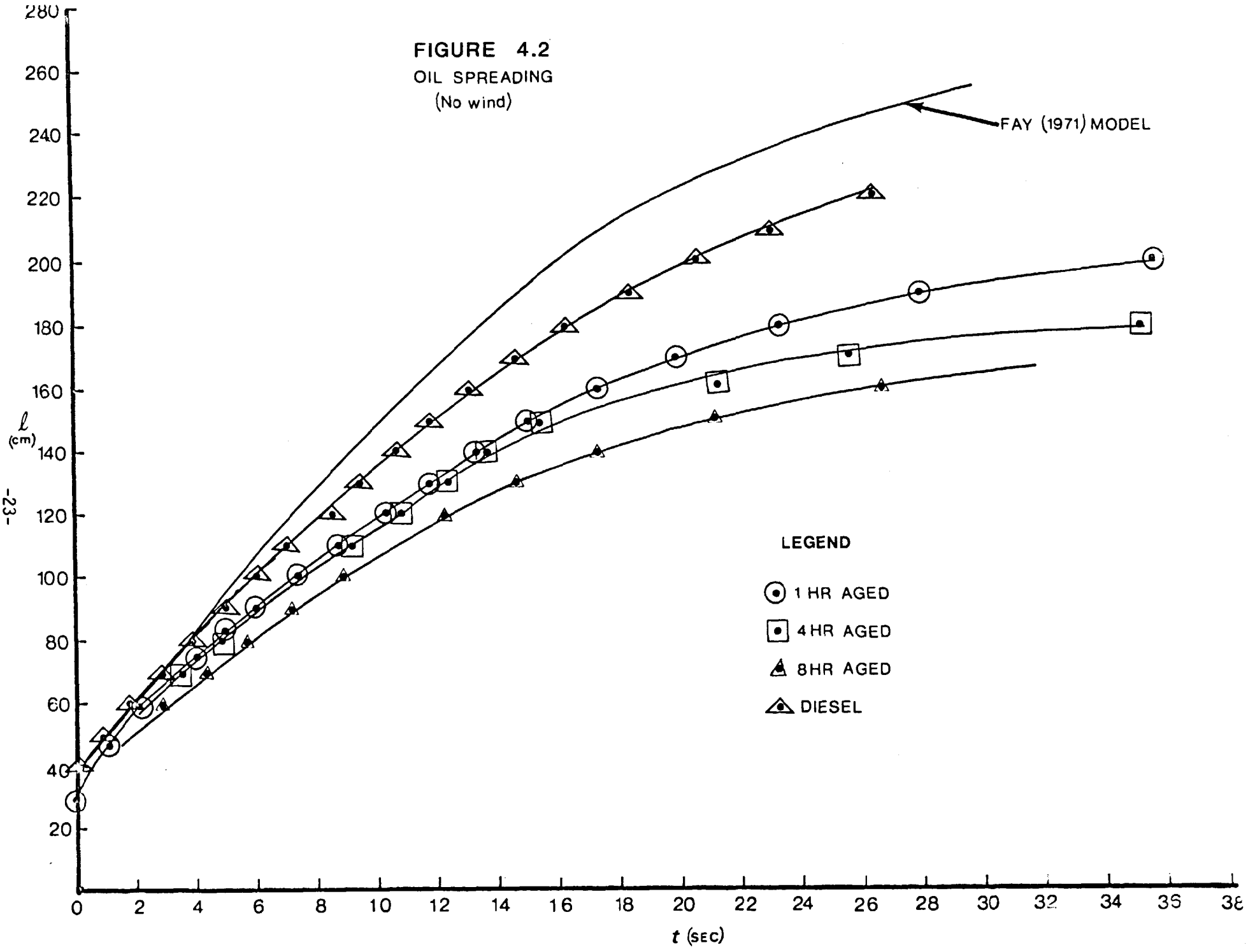
FIGURE 4.2
OIL SPREADING
(No wind)
FAY (1971) MODEL
LEGEND
1 HR AGED
4 HR AGED
8 HR AGED
DIESEL
ℓ (cm)
t (sec)
280
260
240
220
200
180
160
140
120
100
80
60
40
20
0
2
4
6
8
10
12
14
16
18
20
22
24
26
28
30
32
34
36
38

FIGURE 4.3

NON-DIMENSIONAL OIL SPREADING

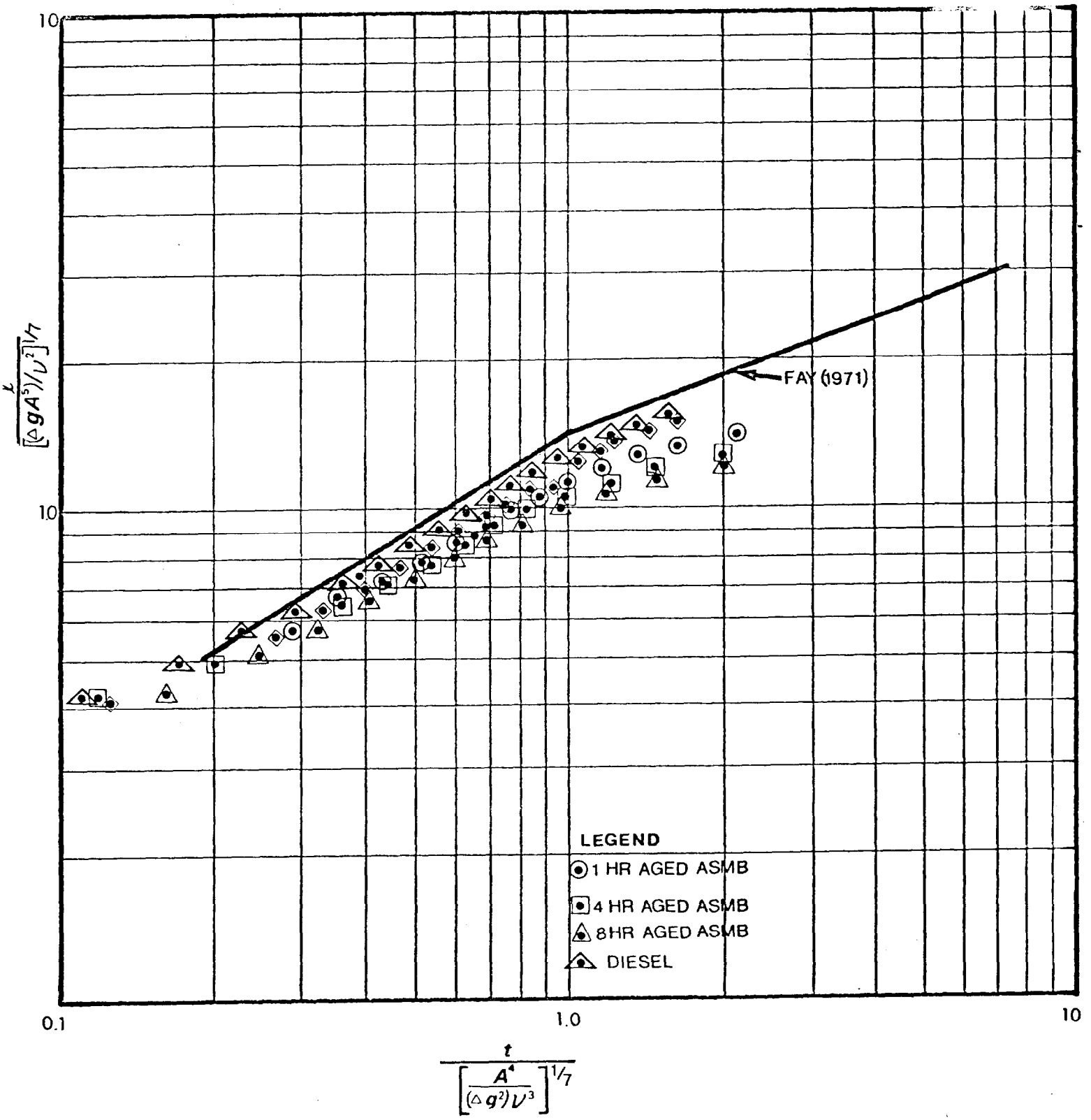

In order to attempt to quantify this phenomenon, plots of the ratio of actual to predicted spreading vs the ratio of the oil to water viscosity were prepared. These are shown in Figure 4.4 for both the gravity-inertia and gravity-viscous spreading regimes. It can be seen that the oil viscosity effect can be adequately described by an equation of the form:

(4.3) actual spread $= \left(\mu/\mu_\omega\right)^n$ x predicted spread

where μ = dynamic viscosity of oil

μ_ω = dynamic viscosity of water

n = a constant unique to each regieme

Thus, oil spreading in the gravity regimes can be more accurately predicted by:

Gravity - Inertia

(4.4) $$l = 1.5\left(\mu/\mu_\omega\right)^{-0.09} (\Delta g A)^{1/3} t^{2/3}$$

Gravity - Viscous

(4.5) $$l = 1.5\left(\mu/\mu_\omega\right)^{0.15} (\Delta g A^2/\nu^{1/2})^{1/4} t^{3/8}$$

4.2.2 Oil Spreading with Wind

An aerodynamic analysis of the wind tunnel has resulted in the following conversion from a wind tunnel speed (measured 10 cm above the oil) to an atmospheric wind (measured 10 m above sea level) - see Appendix I:

(4.6) $$V_{10} = 1.239\, V_{0.1}^{1.1275}$$

where $V_{0.1}$ = wind tunnel velocity (m/s)

V_{10} = atmospheric wind velocity (m/s)

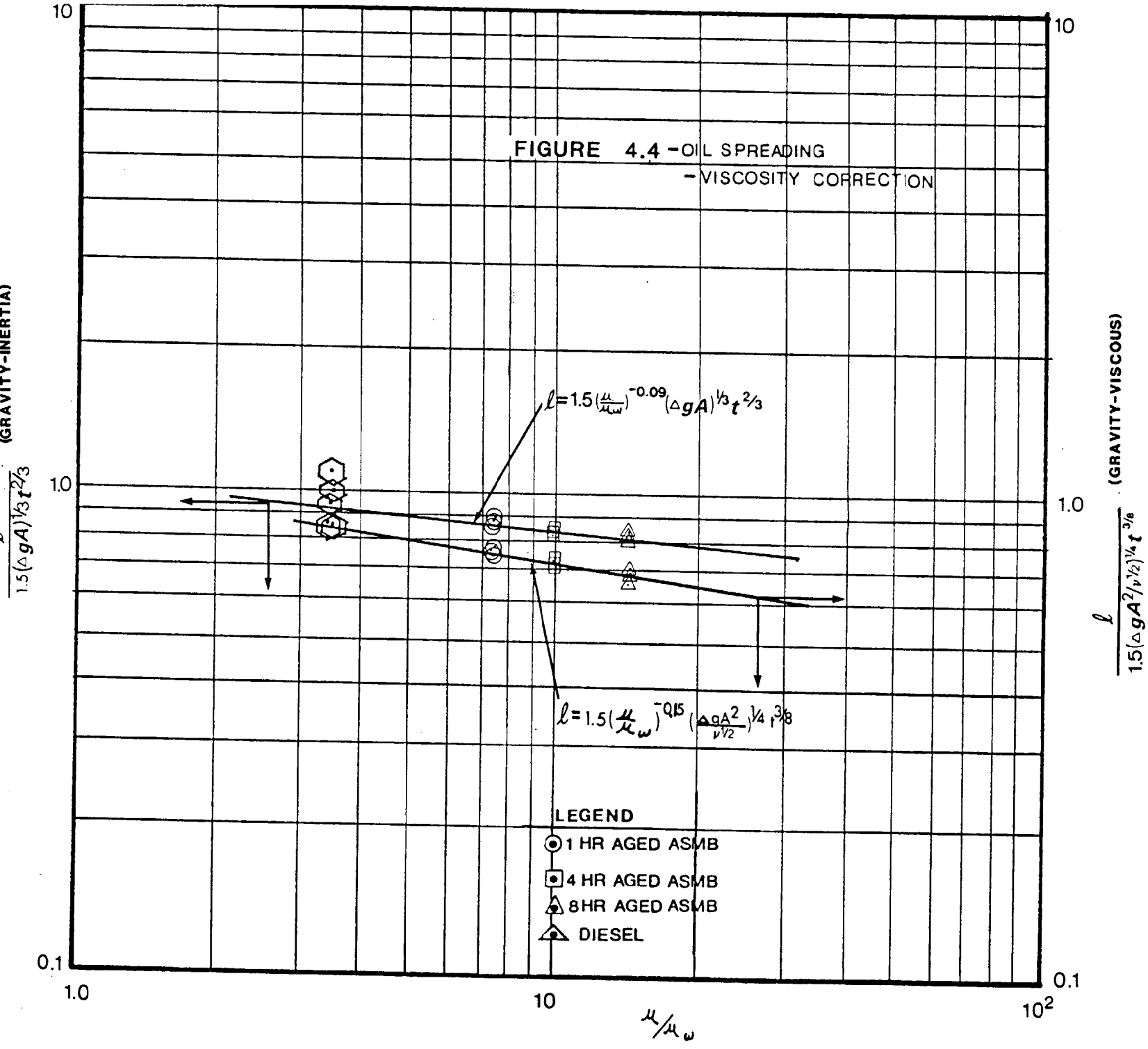

FIGURE 4.4 - OIL SPREADING - VISCOSITY CORRECTION

Figure 4.5 illustrates the data from a typical series of runs to investigate the effects of wind on oil spreading. The data points denoted as a run with a positive wind speed were obtained with the wind in the same direction as the oil spreading; those denoted as a run with a negative wind speed were obtained with the wind opposing the oil spreading.

Of particular importance to this study is the wind speed required to balance the spreading force of an oil slick. At the equilibrium point the spreading force of a one-dimensional oil slick in the gravity regime is:

$$(4.7)\quad F_s = (\rho - \rho_o)\, wgh^2$$

where F_s = spreading force
ρ = water density
ρ_o = oil density
w = slick width
h = slick thickness

and the force of the wind acting over the area of the slick is

$$(4.8)\quad F_w = \rho_A C_D V U^2/h$$

where F_w = wind retarding force
C_D = drag coefficient of slick
V = slick volume
ρ_A = air density
U = wind velocity

At equilibrium the two forces balance, i.e.:

$$(4.9)\quad C_D V \rho_A U^2/h = (\rho - \rho_o)\, wgh^2$$

or

$$h = (C_D V \rho_A / (\rho - \rho_o) g w)^{1/3}\, U^{2/3}$$

which can be rewritten as

$$(4.10)\quad h^3/V = (C_D \rho_A / (\rho - \rho_o)\, wg)\, U^2$$

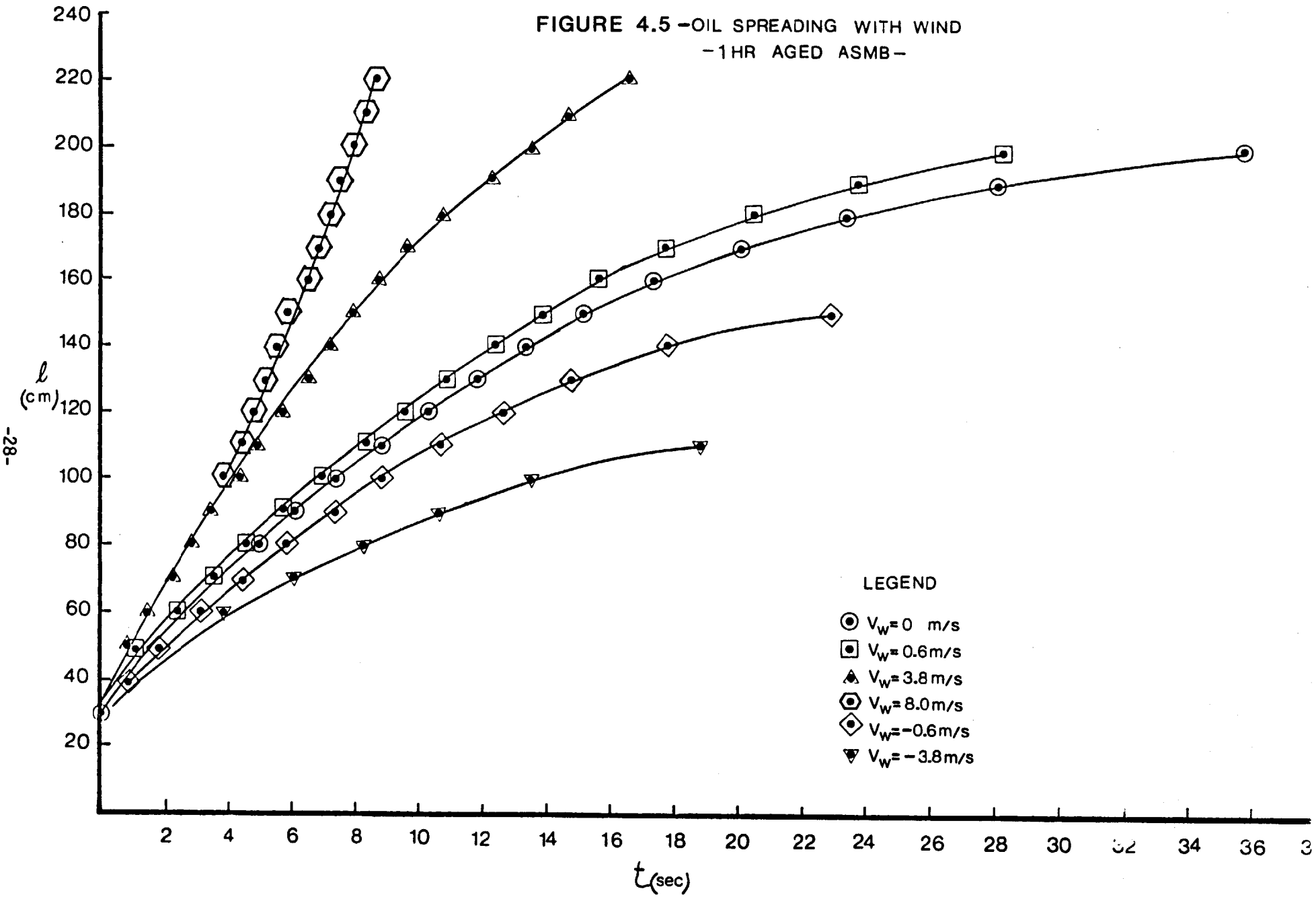
FIGURE 4.5 -OIL SPREADING WITH WIND
-1HR AGED ASMB-
240
220
200
180
160
140
120
100
80
60
40
20
ℓ (cm)
2
4
6
8
10
12
14
16
18
20
22
24
26
28
30
34
36
t (sec)
LEGEND
V_w= 0 m/s
V_w= 0.6m/s
V_w= 3.8m/s
V_w= 8.0m/s
V_w= -0.6m/s
V_w= -3.8m/s

Figure 4.6 shows a plot of h^3/V vs U. A plot of equation 4.10 with $C_D = 3.5 \times 10^{-3}$ is also given. The suggested equation fits the data except at low values of U where it is considerably underestimates the experimental values. This may be due to the end effects of the trough where spreading ceases due to surface tension in the finite test length at wind speed below 1m/s. Figure 4.7 compares the model (equation 4.10) with the experimental data. Further testing is needed to find a more accurate C_D value for the model.

4.2.3 Flame Spreading Over Oil

Figure 4.8 shows the length of the 3 mm thick slick of 1 hour aged Alberta Sweet Mixed Blend on fire as a function of time for various wind speeds. All the oils tested exhibited similar results. In all cases the data (Appendix 1) show that the flame velocity is constant for a given wind speed and oil type. Figure 4.9 shows the average flame velocity plotted against wind speed for each of the four oil types. The flame flashing velocity (the velocity at which flame propagates through a combustible mixture of vapours) was measured (by video techniques) at 1.3 m/s during Runs 28 and 29 (see Appendix 2).

The intercepts of the data at zero wind speed correlate well with experiments on flame spreading over 4 mm of decane at 10 - 15°C (Mackinven et al, 1969) which showed the quiescent flame spreading rate to be 0.026 m/s. This indicates that at zero wind, the flame propagation could be surface-tension-driven, as proposed by Sirignano and Glassman, 1969.

FIGURE 4.6 – WIND DRAG COEFFICIENT DETERMINATION

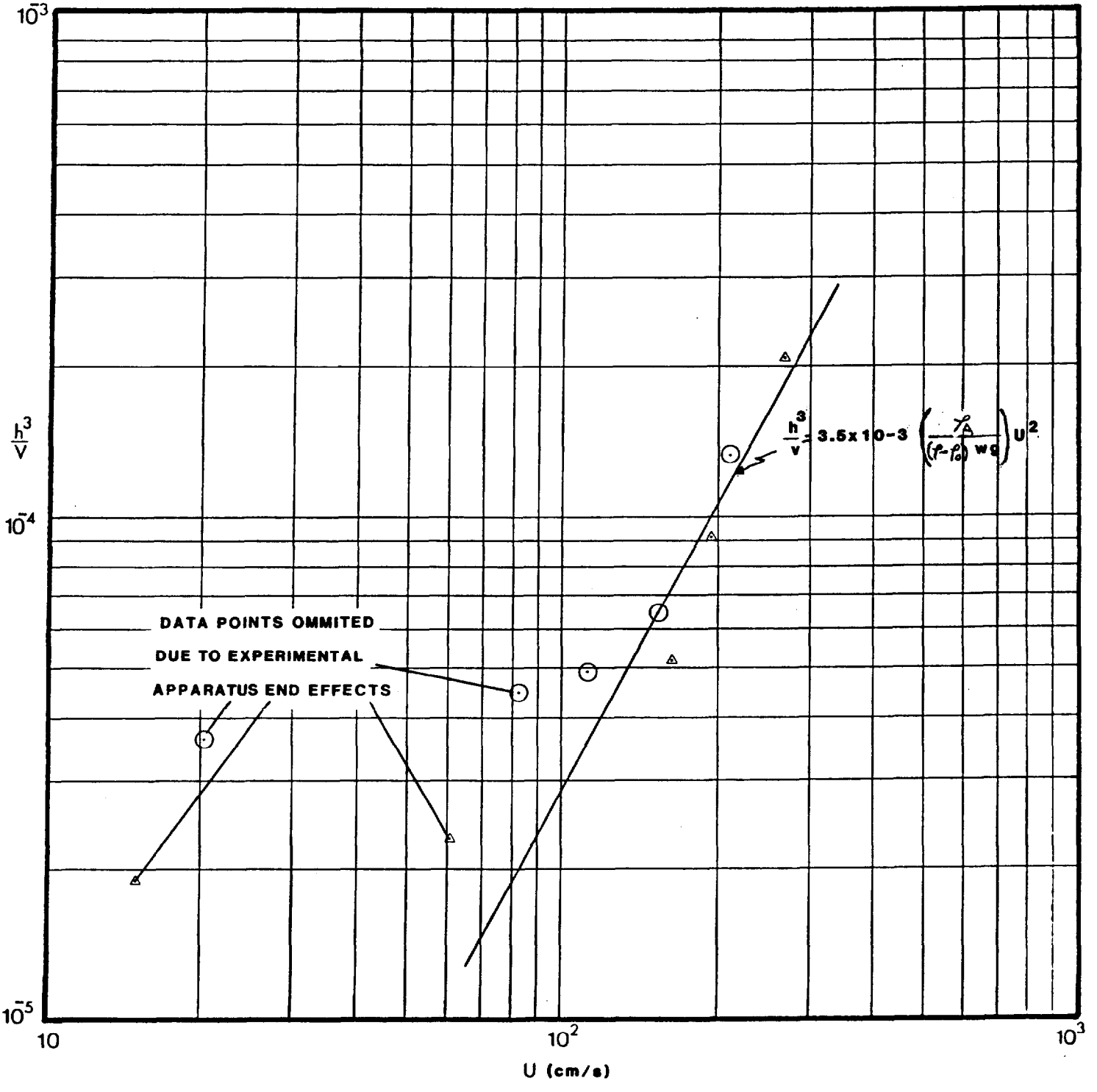

FIGURE 4.7

EQUILIBRIUM OIL THICKNESS
VS
OPPOSING WIND SPEED

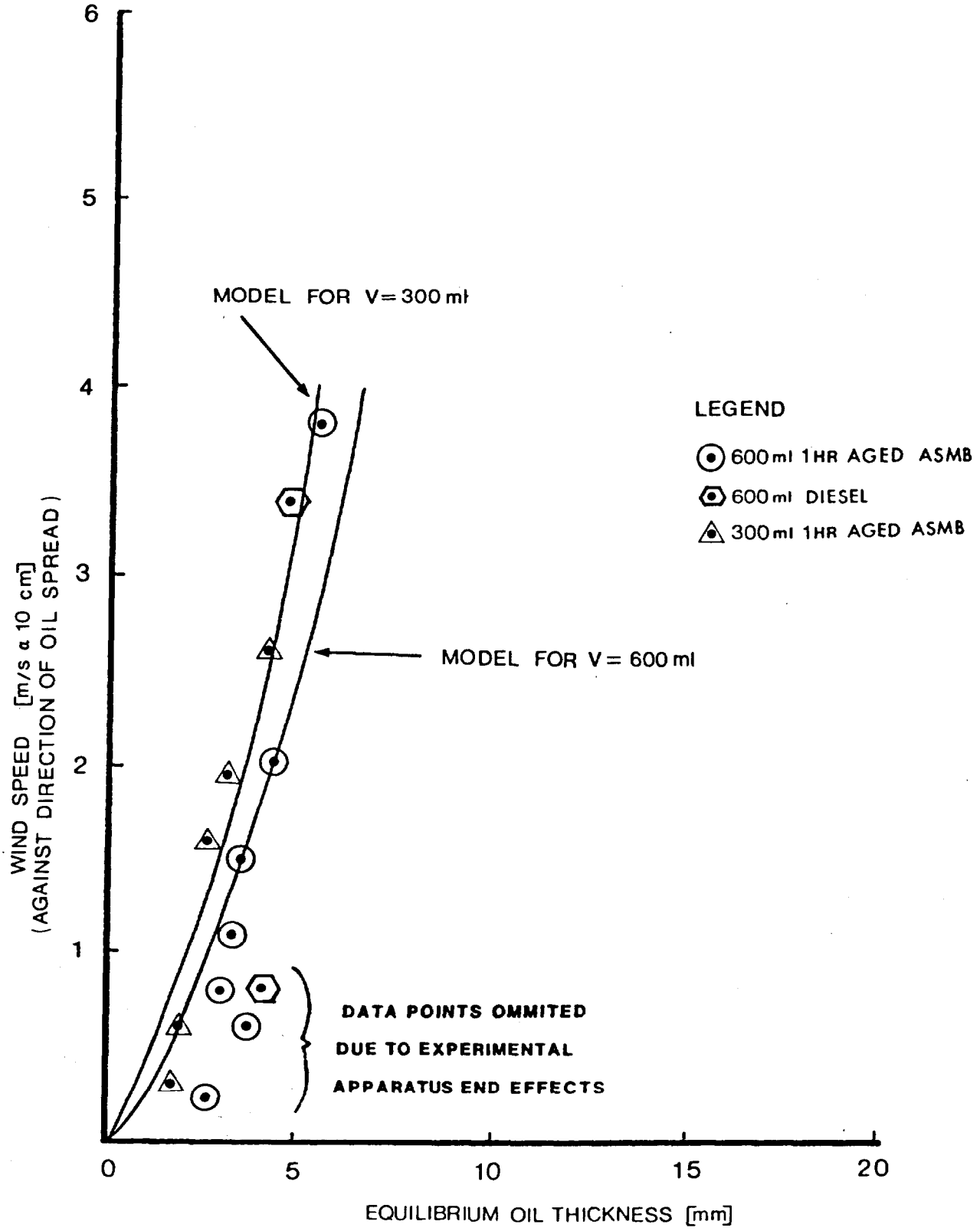

FIGURE 4.8 - FLAME SPREADING

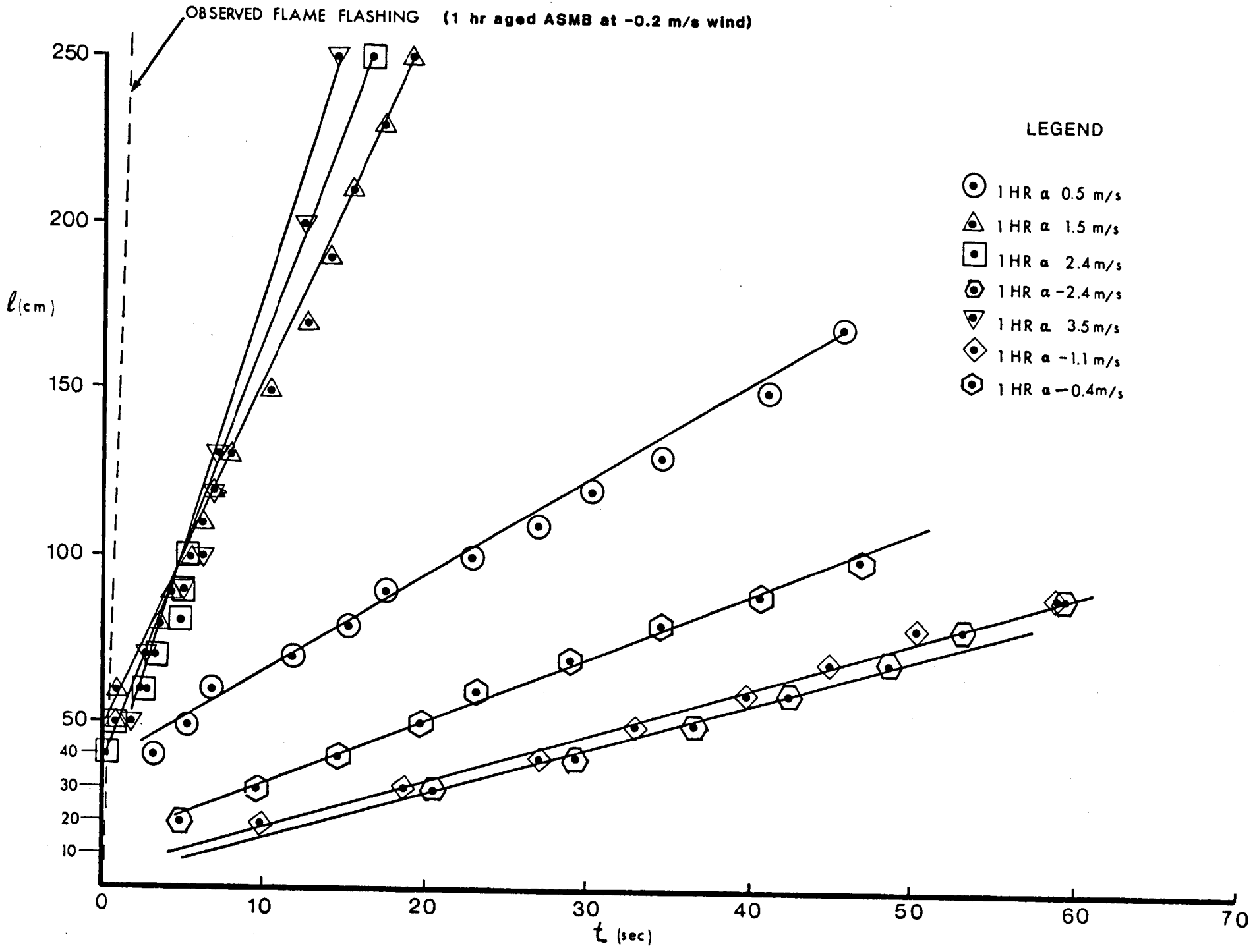

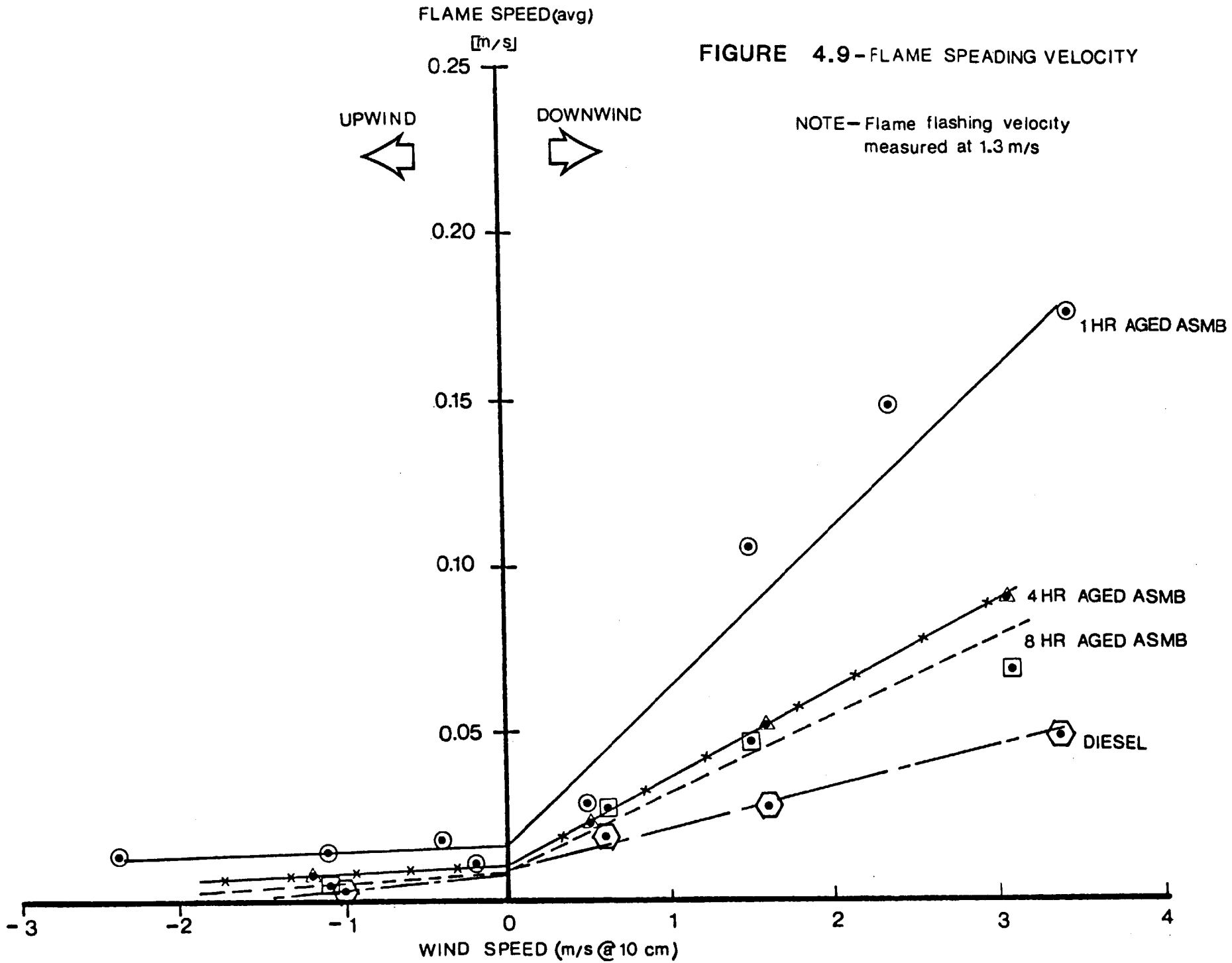

FIGURE 4.9 – FLAME SPEADING VELOCITY

The results of these tests indicate that the data can be approximated by an equation of the form.

(4.11) $U_F = mU + b$ [m/s]

where U_F = flame velocity
m, b = constants

As well, it appears that both m and b are functions of oil type. In order to quantify the effect of oil type, the Initial Boiling Point (T_B) was selected to represent the volatility of the oil. Figure 4.10 shows the relationships between the slope (m) and intercept (b) of the data on Figure 4.9 and the Initial Boiling Point of the oil.

In order to model the data, the parameter:

(4.12) $(T_B - T_A)/T_B$

where T_A = ambient temperature (^oK)
T_B = initial boiling point of oil (^oK)

was used. The model for b was determined to take the form:

(4.13) $b = 1.3 \exp(-c((T_B - T_A)/T_B)^d)$

where c,d = constants

This equation has the properties that, as T_B increases, b decreases exponentially and when $T_B = T_A$, b is constant at 1.3 m/s (the flame flashing velocity with no wind).

The model for m was determined to take the form:

(4.14) $m = \exp(-f((T_B - T_A)/T_B)^g)$

where f, g = constants

This equation also has the property that, as T_B increases, m decreases exponentially and when $T_B = T_A$, m is constant at 1 (the flame flashing velocity is equal to the wind speed plus 1.3 m/s).

FIGURE 4.10

Dependence of m and b on Initial Boiling Point

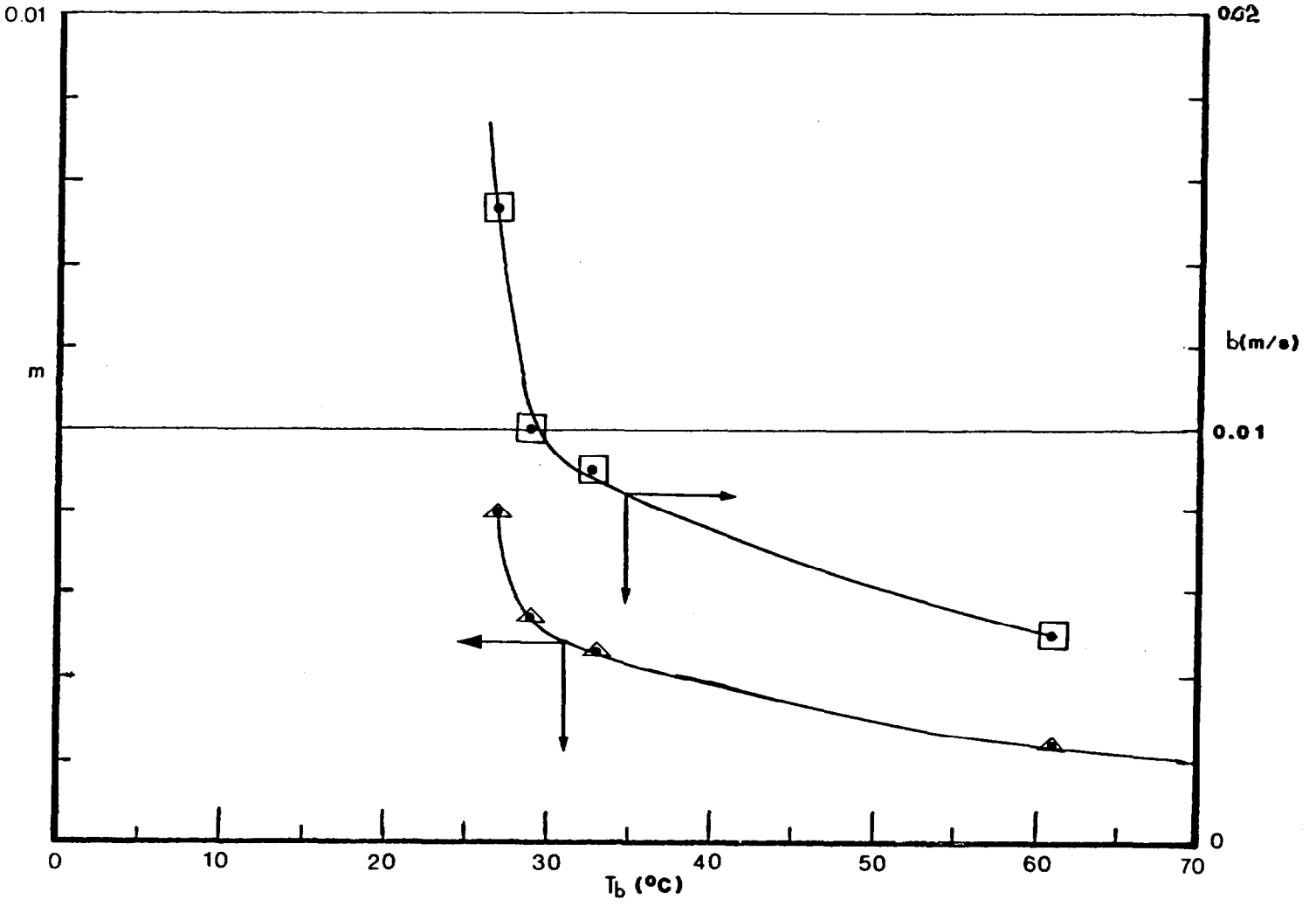

Both the models for m and b have the property that as T_A increases m and b increase slightly. This is consistent with the data shown in Figure 4.11.

Figure 4.12 shows the fit of the experimental data points to equations 4.13 and 4.14 with:

$c = 7.88$

$d = 0.1856$

$f = 6.52$

$g = 0.2302$

Combining equations 4.11, 4.13 and 4.14 to give the overall equation for downwind flame spreading velocity as a function of wind speed yields:

$$(4.15) \quad U_{F_d} = \exp(-6.52((T_B - T_A)/T_B)^{0.23})U + 1.3\exp(-7.88((T_B - T_A)/T_B)^{0.19})$$

Although upwind flame spreading velocity is a weak function of wind speed (see Figure 4.9) for the purposes of this work it can be asssumed to be independent of wind speed. Thus:

$$(16) \quad U_{F_u} = 1.3\exp(-7.88((T_B - T_A)/T_B)^{0.19})$$

4.2.4 Combined Oil and Flame Spreading

Several runs were performed to investigate oil and flame spreading combined. For these, burning oil was released at one end of the trough and the spread of both the oil and flame recorded.

FIGURE 4.11

Flame Spreading

vs

Temperature

8 Hr Aged ASMB With 1.4 m/s Wind

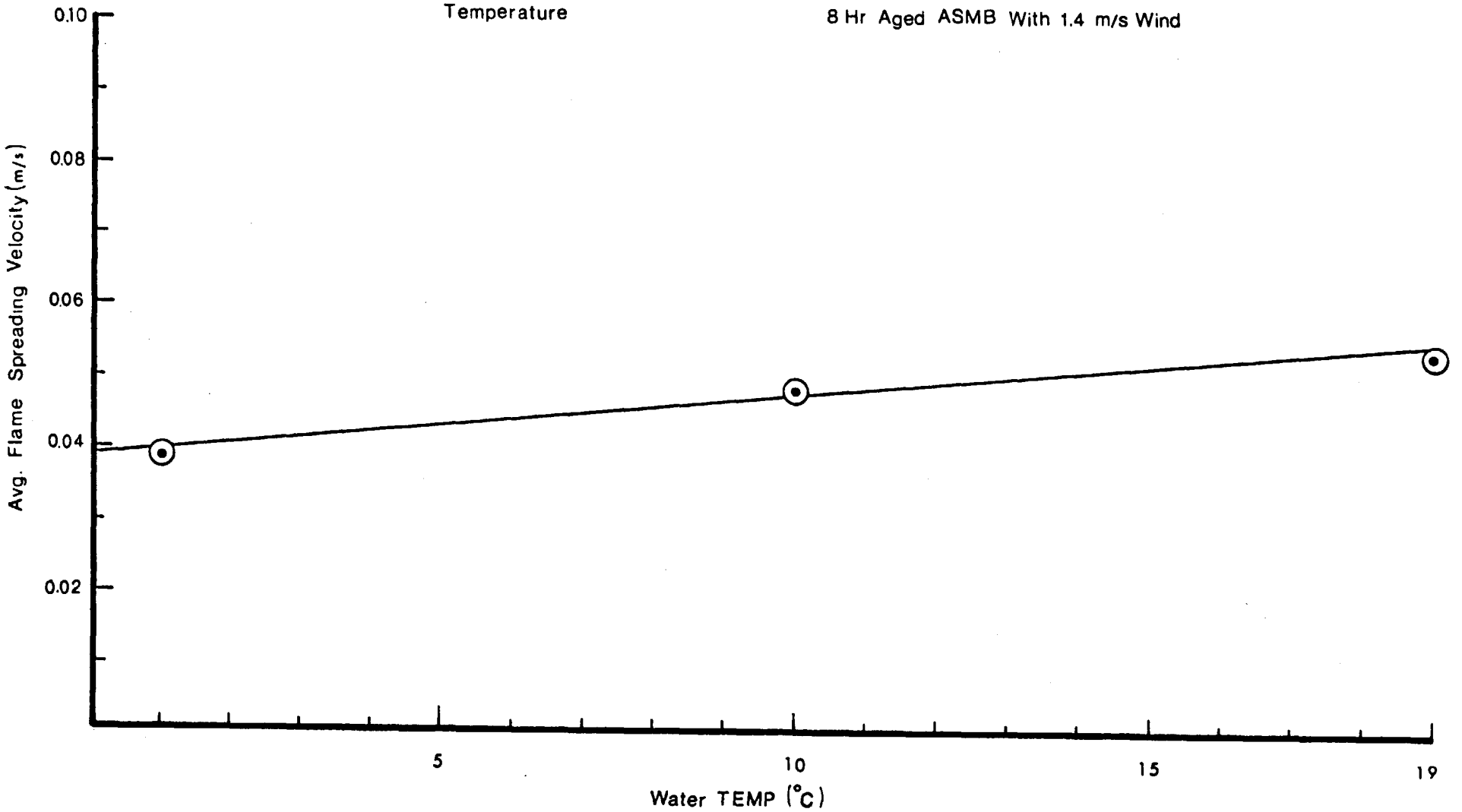

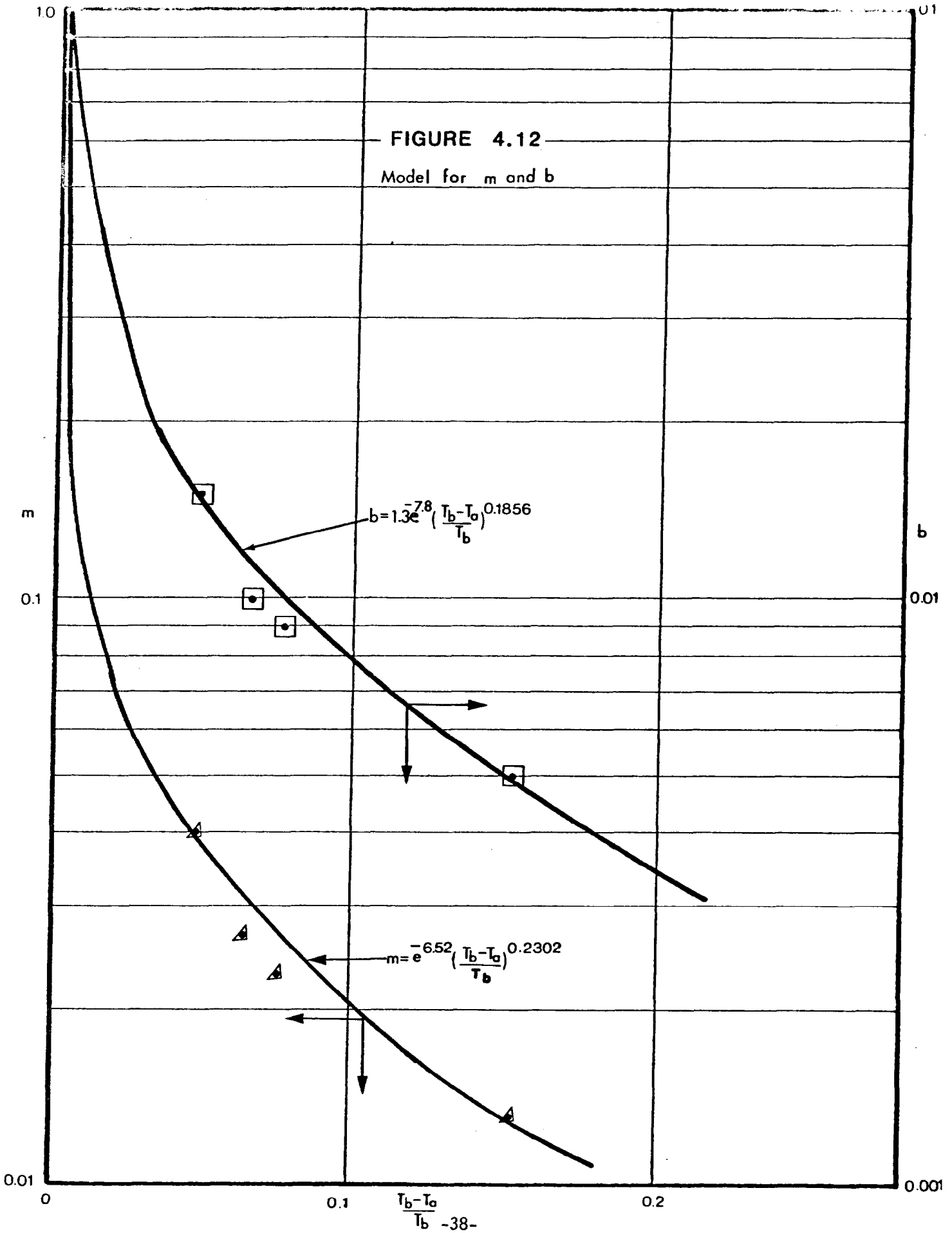

FIGURE 4.12

Model for m and b

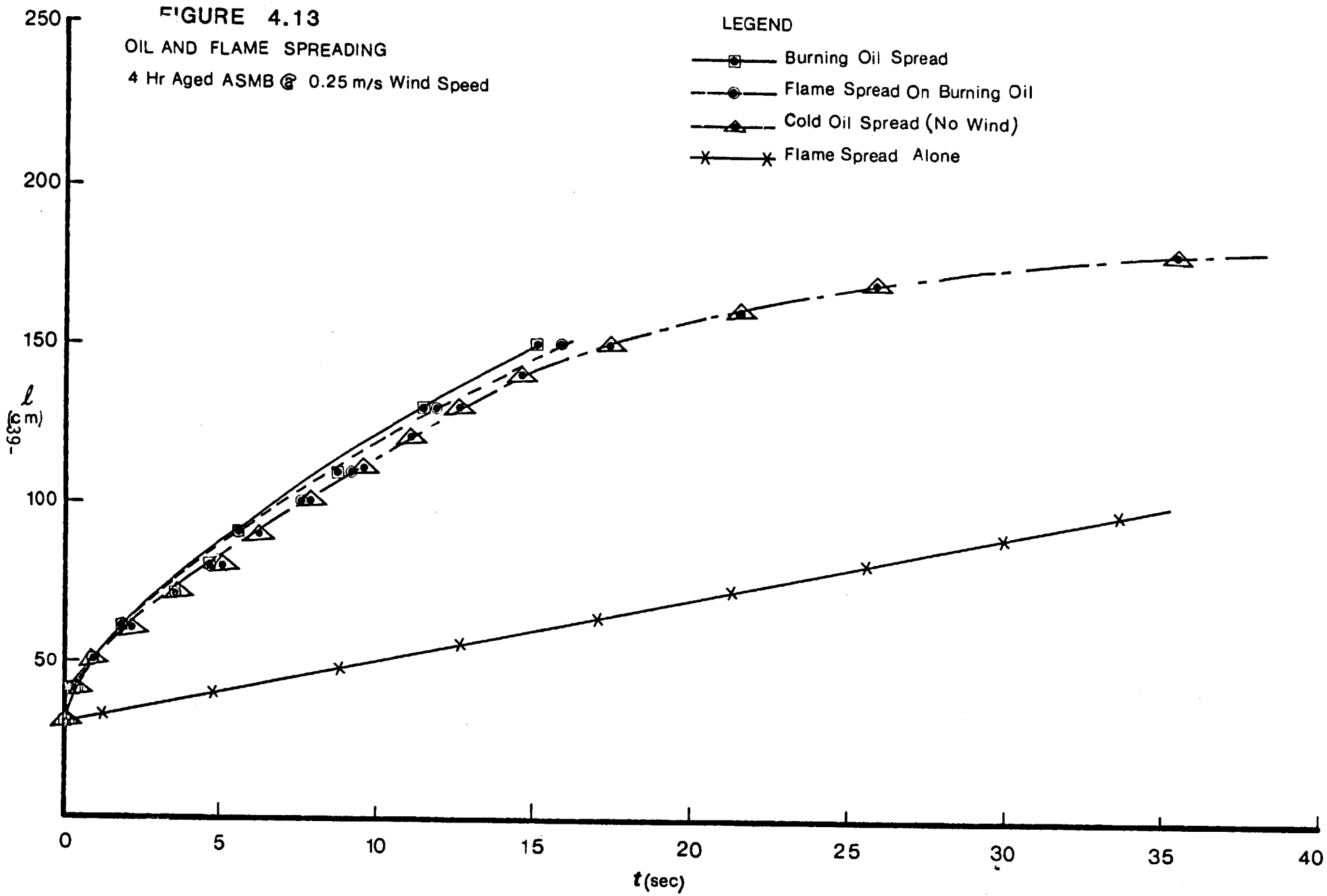
FIGURE 4.13
OIL AND FLAME SPREADING
4 Hr Aged ASMB @ 0.25 m/s Wind Speed
LEGEND
Burning Oil Spread
Flame Spread On Burning Oil
Cold Oil Spread (No Wind)
Flame Spread Alone
250
200
150
100
50
0
5
10
15
20
25
30
35
40
t (sec)
ℓ (cm)

With all the crude oils tested the flame kept up with the oil spreading over the entire range of wind speeds tested. Figure 4.13 shows the typical results obtained (4 HR ASMB at a wind speed of 0.25 m/s). It is interesting to note that the burning oil did not spread appreciably faster nor farther than did cold oil, possibly because of poor heat transfer in the oil. Some heat losses to the metallic trough may have occured.

Flames did not keep up with the burning diesel fuel except at wind speeds less than 1 m/s.

4.3 SUMMARY OF SMALL-SCALE TESTING

The important observations of this work were, for the types of oils tested:

- oil viscosity affects the spreading rate of oil. In the gravity-inertia phase the rate decreases with the -0.09 power of oil viscosity and in the gravity-viscous regime the rate decreases with the -0.15 power of oil viscosity. This phenomenon seems to be related to the oil viscosity at the oil/water interface as burning oil spreads at the same rate as cold oil.

- the flame spreading velocity can be related mathematically to wind speed, ambient temperature and oil volatility.

- once afire, crude oil remains burning as it spreads (until the slick thickness drops below about 1 mm.)

5.0 MID-SCALE TANK TESTS

The mid-scale testing was conducted in an outdoor test tank in Waterloo, Ontario. Its purpose was to investigate the removal efficiency of uncontained slicks, two-dimensional oil-and flame-spreading, and burning rate as a function of slick thickness.

5.1 METHODS

The removal efficiency and spreading tests involved a variety of fresh crude oils and diesel (see Table 5.1), initially contained in one and two metre diameter metal rings on the water surface of the tank (Plate 5.1). The oil was ignited, then released by lowering the ring below the water surface (Plate 5.2 and 5.3). Spreading was recorded on videotape and removal efficiency determined by recovering and measuring the volume of oil residue.

Burning rate as a function of slick thickness was determined by igniting and burning contained oil slicks of varying thickness (up to 2 cm) and recording the burn time and volume of residue.

5.2 RESULTS AND DISCUSSION

5.2.1 Slick Combustion Rate

Table 5.2 shows the results of the burning rate experiments. Figure 5.1 shows a plot of the measured average regression rate (total volume burned / time from ignition to extinction) against initial slick thickness. Also shown are the data from Wakamiya et al, 1982 for a variety of crude oils in 2m diameter pans and the results of McAllister and Buist, 1981 from a 2 hour test burn in a fireproof boom (2.6 m diameter). It can be seen that, firstly, slicks over about 5 mm thick burn at a rate independent of thickness; secondly 2 m diameter slicks burn slightly faster than 1 m diameter slicks, but above 2 m diameter burning rate does not seem to be a strong function of slick size; and thirdly (as shown by Wakamiya et al, 1982) slicks seem to burn faster at higher ambient temperatures (about 15% faster for an average 15^{o}C rise in temperature).

TABLE 5.1

PHYSICAL PROPERTIES OF OILS
USED IN MID-SCALE TESTS

PROPERTY	OIL TYPE			
	LLOYDMINISTER+ CRUDE	NORMAN WELLS+ CRUDE	ALBERTA SWEET MIXED BLEND	DIESEL
DENSITY @ 15°C (g/cm^3)	0.90	0.83	0.83	0.844
VISCOSITY @ 15°C (cSt)	7.7	8.8	7	4.0
INTERFACIAL TENSION* @ 15°C (dynes/cm)				
OIL/AIR	25	22.7	24	28.4
OIL/WATER	31.2	26.8	27	28.1
INITIAL BOILING POINT (°C)	40	48	20!	61!

* WATER/AIR = 70.6 dynes/cm

+ from Energetex, 1981b

! MODIFIED ASTM PROCEDURE; SEE APPENDIX 5

PLATE 5.1 - MID-SCALE TEST TANK SETUP

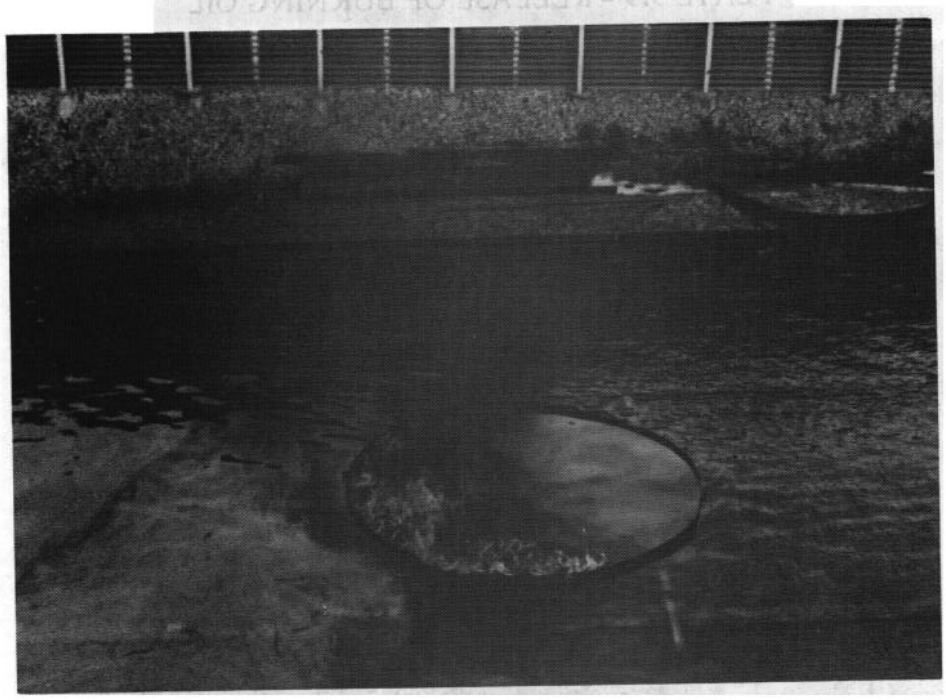

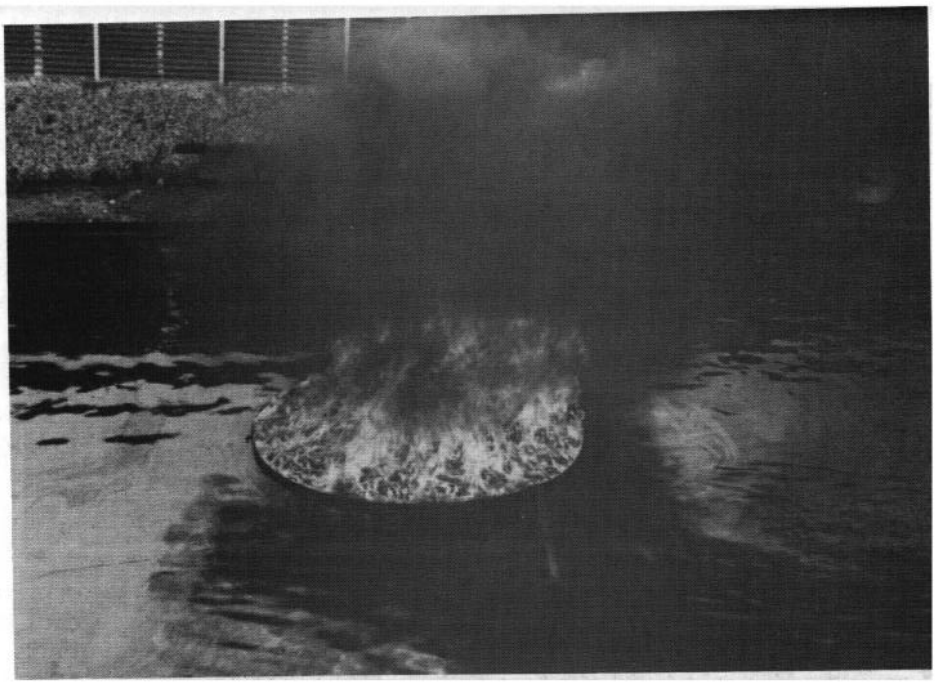

PLATE 5.2 - IGNITION OF CONTAINED OIL

PLATE 5.3 - RELEASE OF BURNING OIL

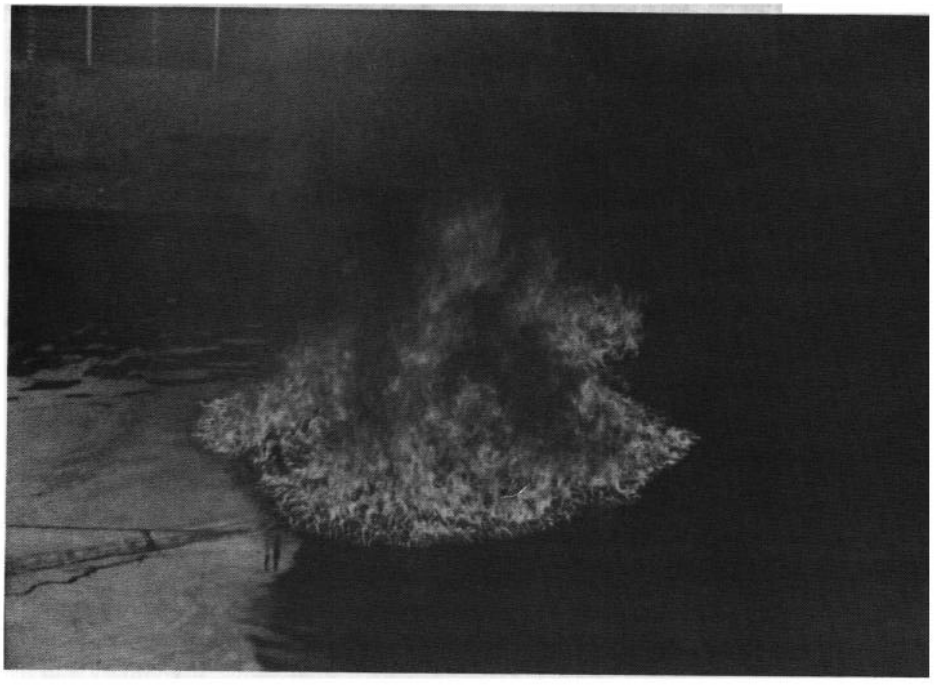

PLATE 5.4 - OIL AND FLAME SPREADING

TABLE 5.2

CONTAINED OIL SLICK - REGRESSION BURNING RESULTS

Test No.	Oil Type	Oil Volume (l)	Pool Dia. (m)	Initial Oil Thickness (mm)	Residue Volume (l)	Residue Thickness (mm)	Burning Time (min)	Regression Burning Rate (mm/min)	
1	ASMB	4	1	5.0	0.7	0.9	2:20	1.8	
2	ASMB	6	1	7.6	0.85	1.1	3:15	2.0	
3	ASMB	8	1	10.1	0.95	1.2	4:50	1.8	
4	ASMB	10	1	12.7	0.95	1.2	6:40	1.7	
5	ASMB	12	1	15.3	1.0	1.27	8:35	1.6	
6	ASMB	16	1	20.3	1.0	1.27	11:43	1.6	
7	ASMB	16	1	20.3	0.8	1.0	9:30	2.0	
8	ASMB	17	1	21.6	0.8	1.0	10:00	2.0	
9	ASMB	20	1	25.4	1.0	1.27	14:00	1.7	
10	ASMB	32	1	40.7	0.9	1.15	19:00	2.0	
11	Diesel	6	1	7.6	1.1	1.4	3:50	1.6	*
12	Diesel	12	1	15.3	1.6	2.0	7:15	1.8	*
13	Diesel	20	1	25.4	0.9	1.15	11:50	2.0	
14	Diesel	12	2	3.8	4.2	1.33	2:20	1.0	*
15	Diesel	20	2	6.3	4.1	1.3	3:00	1.6	*
16	ASMB	10	2	3.1	1.7	0.54	1:35	1.7	
17	ASMB	14.7	2	4.6	2.3	0.73	2:00	1.9	
18	ASMB	20	2	6.3	2.7	0.859	2:19	2.3	

* Residue emulsified

FIGURE 5.1 COMPARISON OF SLICK REGRESSION RATES
(CONTAINED BURNS)

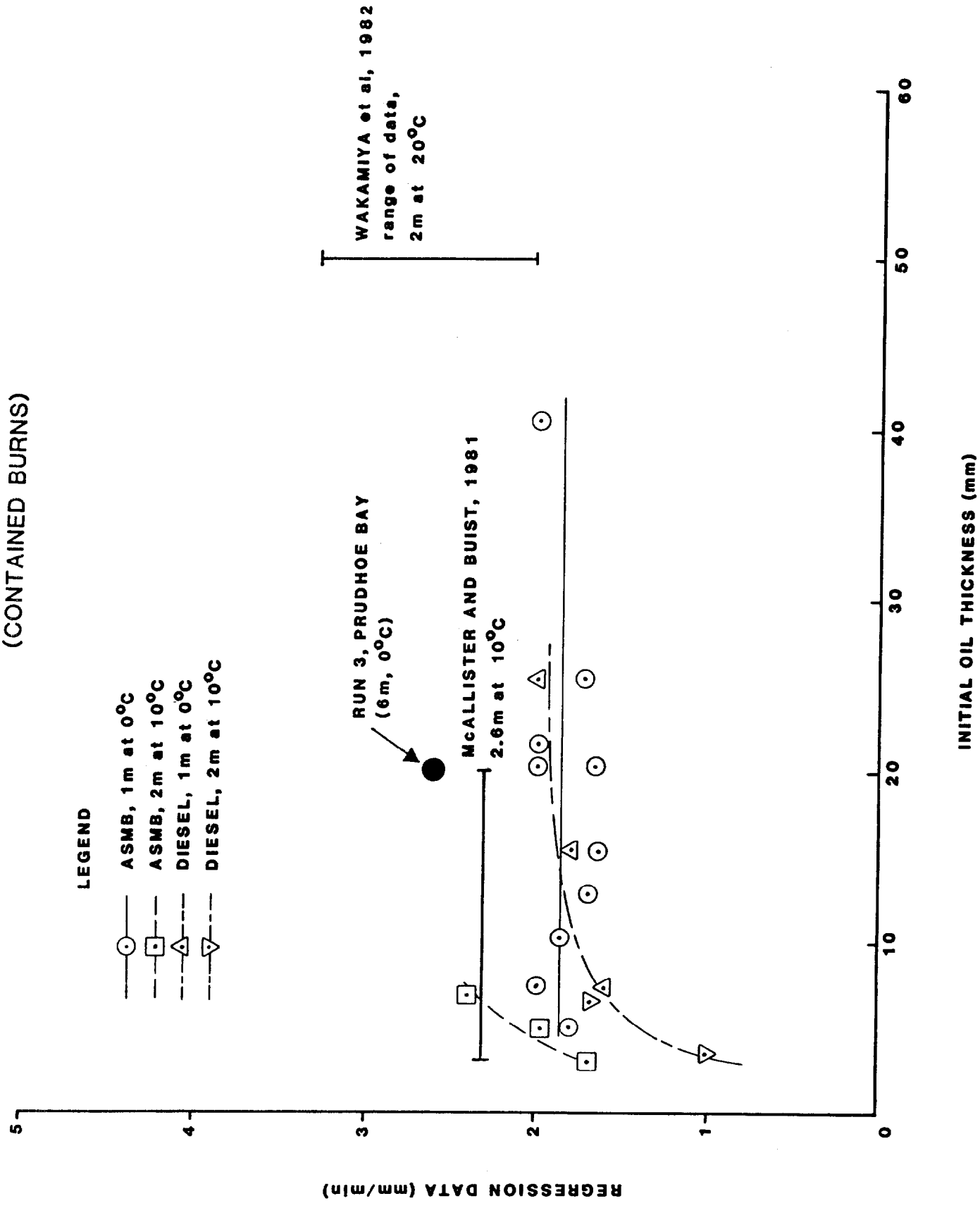

The rapid reduction in regression rate with decreasing thickness below about 5 mm is confirmed by the data of Wakamiya et al, 1982 and is likely due to increasing heat transfer to the underlying water. A good estimate for the regression rate for large ($\not\geq$ 2 m), thick ($\not\geq$ 5 mm) oil slicks on water would be about 2 to 2.5 mm/min.

5.2.2 Removal Efficiency

Table 5.3 shows the results of the tank tests of uncontained slick combustion. The residue of Run 11 was highly emulsified and no removal efficiency could be calculated. In all the tests, with the exception of those involving diesel, the flames kept up with the spreading oil until it reached a thickness of about 1 mm.

5.2.2.1 Modelling

In order to predict uncontained slick removal efficiencies for instantaneously ignited slicks the following model was developed.

From a mass balance, assuming that the oil density is relatively constant:

$$(5.1)\quad V(t) = V_o - V_B(t)$$

where $V(t)$ = volume of oil in slick at time t (m^3)

V_o = initial volume of oil spilled (m^3)

$V_B(t)$ = volume of oil burned to time t (m^3)

differentiating gives

$$(5.2)\quad \frac{dV}{dt} = \frac{-dV_B}{dt}$$

Now, it is known that the rate of combustion is given by

TABLE 5.3

UNCONTAINED OIL SLICK - COMBUSTION RESULTS

Test No.	Oil Type	Oil Volume (l)	Water Area (m^2)	Ring Dia. (m)	Oil Residue (l)	Combustion Efficiency (%)	Preheating* Time (min)	Burning Time (min)	Comments
1	Lloyd	4	24	1	3.8	0			
2	Lloyd	6	24	1	4.3	28.0	0:20	2:00	
3	Lloyd	10	24	1	4.5	55.0	0:30	1:00	
4	Lloyd	14	24	1	7.0	50.0	0:55	0:35	
5	Norman Wells	8	24	1	3.0	62.5	0:37	0:51	
6	Norman Wells	12	24	1	4.5	12.5	0:15	0:50	
7	Norman Wells	16	24	1	6.0	62.5	0:20	0:45	
8	Norman Wells	16	48	1	7.0	56.0	0:25	0:45	
9	Norman Wells	20	24	1	8.0	60.0	0:20	0:60	
10	Diesel	8	24	1	6.3	21.0	0:45	0:50	
11	Diesel	14	90	2	20.0	?	1:10	0:60	residue emulsified
12	Diesel	20	90	2	13.6	32.0	1:35	0:30	
13	ASMB	10	90	2	5.8	42.0	0:50	0:35	
14	ASMB	20	90	2	6.3	68.5	0:10	0:40	
15	ASMB	26	90	2	8.4	67.6	0:25	0:40	

* time from ignition to oil release

(5.3) $\frac{dV_B}{dt} = RA(t)$

where R = regression rate of slick (m/s)

$A(t)$ = area of slick at time t (m^2)

and since

(5.4) $A(t) = V(t)/h(t)$

(5.5) $\frac{dV_B}{dt} = RV(t)/h$

substituting into 5.2 and separating variables

(5.6) $\frac{dV}{V(t)} = -R/h \; dt$

assuming R/h is relatively constant and can be represented by an average value, then integrating

(5.7) $V = V_o \exp(-Rt/h)$

where t = time since start of spread (s)

following the derivation of Fay, 1969, substituting V(t) for V and using the appropriate constants (Fannelop & Waldman, 1971) for axisymmetric spreading, it can be shown that:

In the gravity-inertia regime,

(5.8) $r = 1.14 (\Delta\rho g V_o/\rho)^{1/4} \exp(-Rt/4h)\, t^{1/2}$

where r = slick radius at time t (m)
$\Delta\rho$ = density difference between water and oil (kg/m^3)
g = acceleration of gravity (9.8 m/s^2)
ρ = density of water (kg/m^3)

in the gravity-viscous regime,

(5.9) $r = 0.98 \left(\frac{\Delta\rho g V_o^2}{\rho \nu^{1/2}}\right)^{1/6} \exp(-Rt/3h) t^{1/4}$

where ν = kinematic viscosity of water (1×10^{-6} m^2/s)

and in the surface tension-viscous regime,

(5.10)

$r = 1.6 \left(\frac{\sigma}{\rho \nu^{1/2}}\right)^{1/2} t^{3/4}$

where σ = spreading coefficient (N/m)

the transition from gravity-driven to surface-tension driven spreading occurs when:

(5.11) $h_c = \frac{(\sigma/\rho)^{1/2}}{\Delta g}$

This spreading model (excluding the gravity-inertia regime because it plays no part for small spills) was run on a microcomputer. For each time interval an area, volume remaining and thickness was calculated. Each subsequent iteration used the preceeding value of h to determine the value of R/h (R assumed constant at 2 or 2.5 mm/min).

5.2.2.2 Comparison with Results

The results of the model are compared to the data on Figure 5.2. The two agree, except for the case of diesel oil when the flames did not keep up with the spreading oil. No other obvious effect of crude oil type (i.e. volatility or viscosity) on removal efficiency is apparent from the data. The model is not very sensitive; additional data points are required to make it so. It may be that the more volatile crudes burn somewhat faster but, being less viscous, spread somewhat faster; the two effects may cancel each other.

5.3 SUMMARY

Oil slicks of about 2 m in diameter and thicker than 5 mm burn at a constant rate of 2 to 2.5 mm/min independent of oil type, slick area or slick thickness. High removal efficiencies can be obtained with even very small slicks ignited and then released. A relatively simple model has been derived to predict burning efficiency as a function of initial spill volume assuming instantaneous ignition and a constant burning rate previously chosen. Further experimental data is needed to adjust the model.

FIGURE 5.2

COMPARISON OF UNCONTAINED BURN RESULTS WITH MODEL

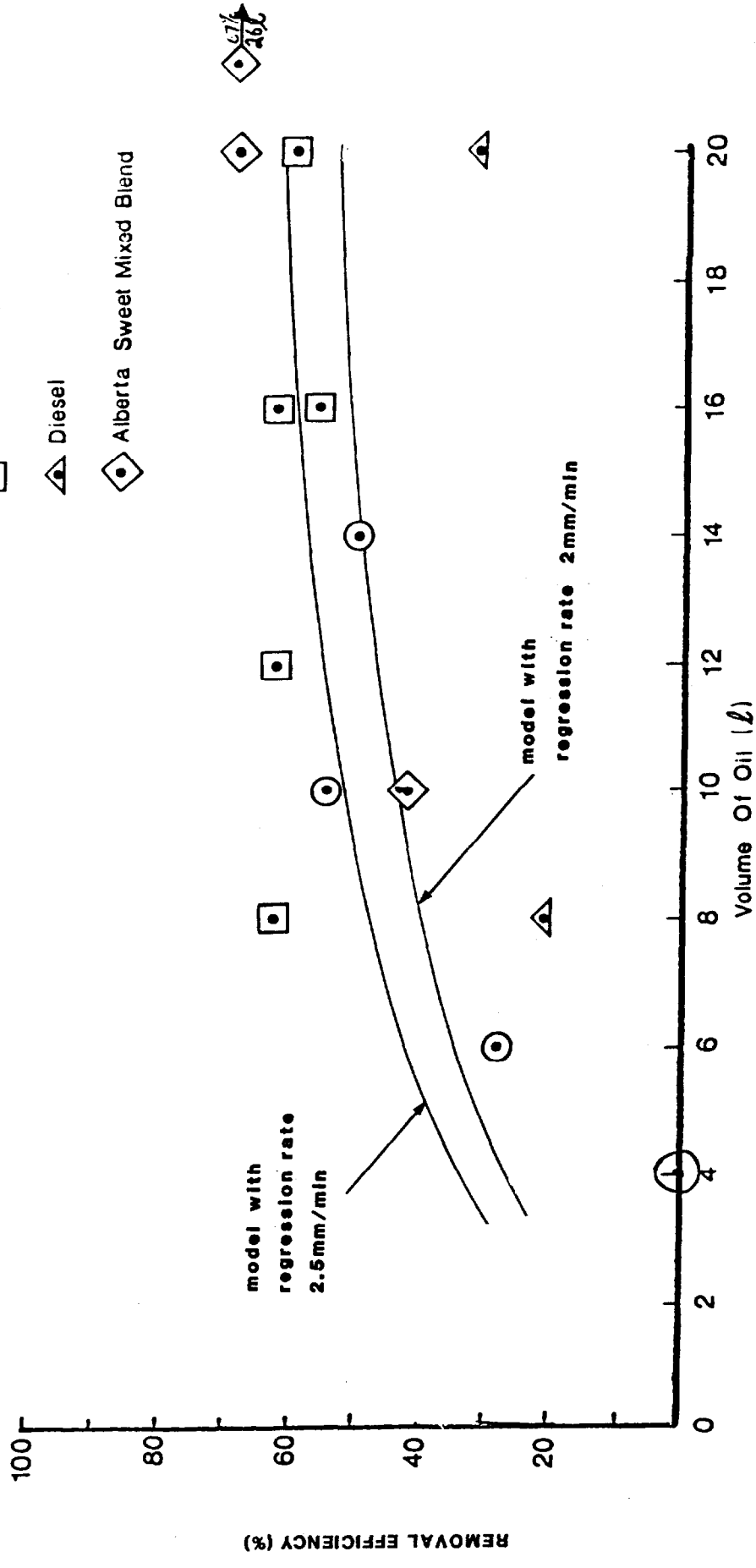

6.0 LARGE-SCALE TESTING

The goal of this phase of the testing was to determine the spreading of oil and flame and removal efficiency at a larger scale, measure induced airflows and evaluate the effect of delayed ignition.

6.1 METHODS

These tests were conducted in a 45 m x 67 m shallow test pit near Sohio Alaska Petroleum Company's East Dock facility in Prudhoe Bay, Alaska. The minimum water depth was 15 cm. At the centre of the pit (see Figure 6.1 and Plate 6.1) a 30 cm high, 6 m diameter sheet metal ring was balanced on four stakes and held in a circular shape by several stakes placed inside the ring around its circumference.

Stakes were also driven into the pit bottom, at 2 m intervals out from the geometric centre of the ring, in order to estimate the size of the oil slick. Each stake was colour-coded with surveyor's tape.

Prior to each test a specified volume of Prudhoe Bay Crude oil (measured by dipping the storage tank) was pumped into the ring through a submerged hose (Plate 6.2). The properties of the crude oils used for each test are given in Table 6.1. Gas chromatographs and further data may be found in Appendix 3. Tests 1 and 2 were designed to measure oil and flame spreading and removal efficiency for instantaneously ignited slicks. Test 3 was designed to measure combustion rate and air entrainment, and test 4 was designed to evaluate the effect of delayed ignition.

For tests 1, 2 and 3 the oil inside the ring was ignited using a propane weed burner (Plate 6.3). In tests 1 and 2 once the flames has spread (Plate 6.4) the ring was dropped, (Plate 6.5) by pulling out the supporting stakes using ropes from the sides of the pit. Each burn was recorded on videotape (see Figure 6.1 for placement) to document oil and flame spreading.

FIGURE 6.1 TEST PIT LAYOUT - PLAN VIEW

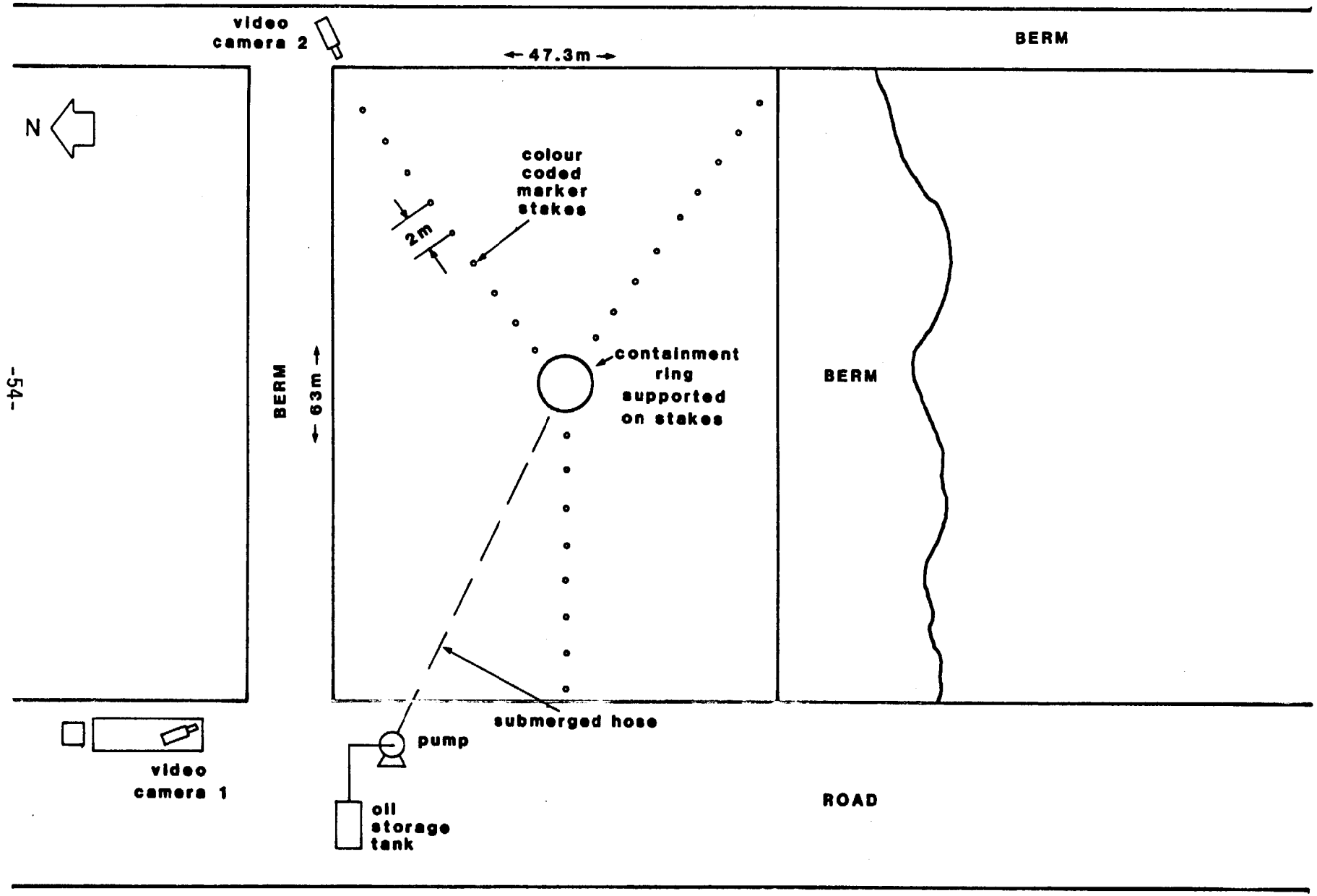

PLATE 6.1 - VIEW OF TEST PIT FROM SOUTH-WEST CORNER

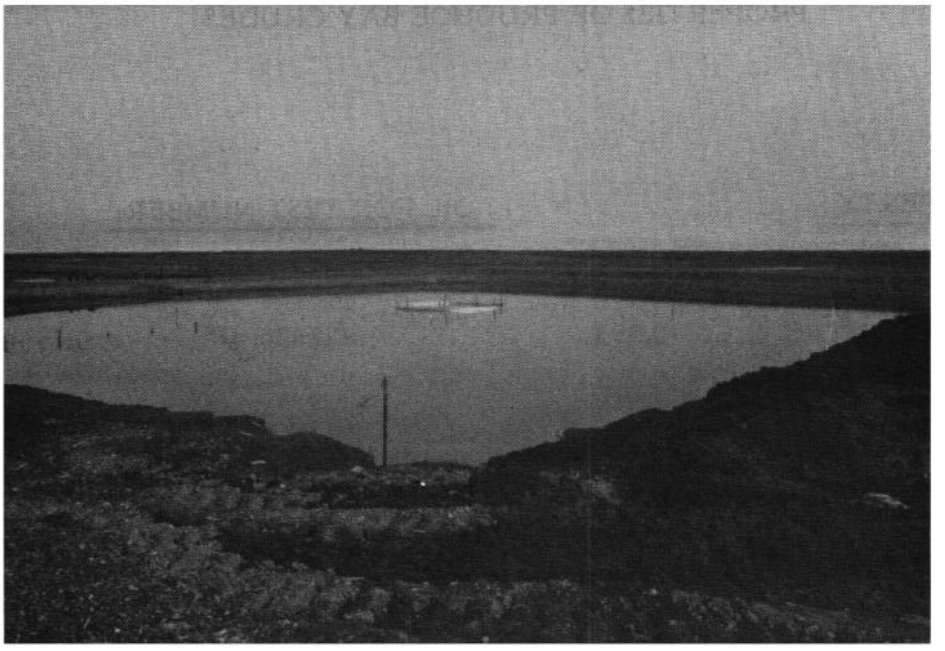

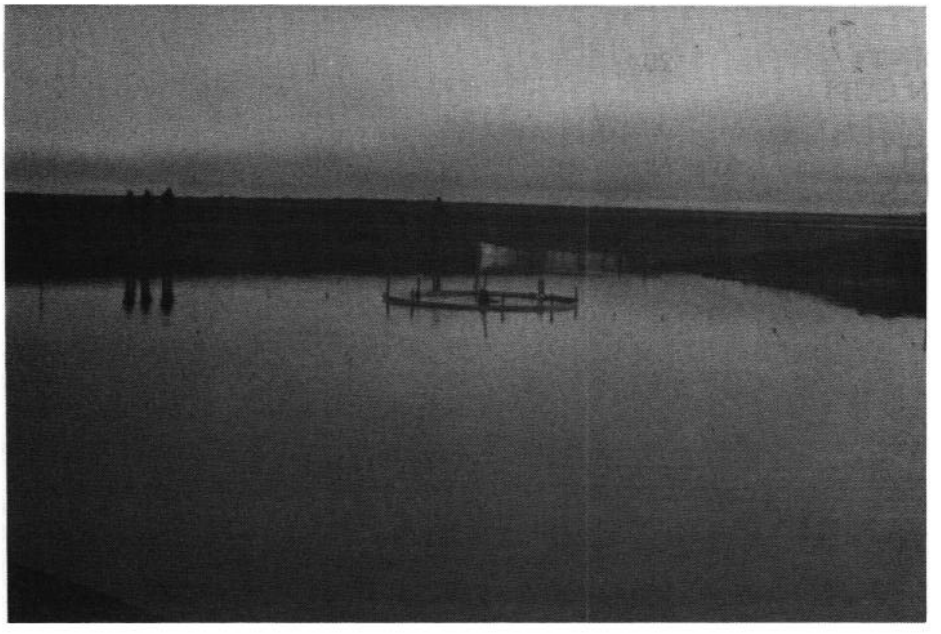

PLATE 6.2 - PUMPING OIL INTO RING (FROM NORTH-WEST CORNER)

TABLE 6.1

PROPERTIES OF PRUDHOE BAY CRUDES

PROPERTY	OIL FOR TEST NUMBER:		
	1	2 and 3	4
DENSITY @ 15°C (g/cm^3)	0.8951	0.8934	0.8956
VISCOSITY @ 15°C (cSt)	38	46	45
INTERFACIAL TENSION @ 25°C (dynes/cm)			
OIL/AIR	26.8	26.6	25.7
OIL/WATER	23.4	23.4	24.3
WATER/AIR	62.1	65	65.6
FLASH POINT* (°C - OPEN CUP)	20	1	11
FIRE POINT (°C - OPEN CUP)	74	60	63

* SOHIO PRODUCTION LAB. DATA

PLATE 6.3 - IGNITING OIL IN RING

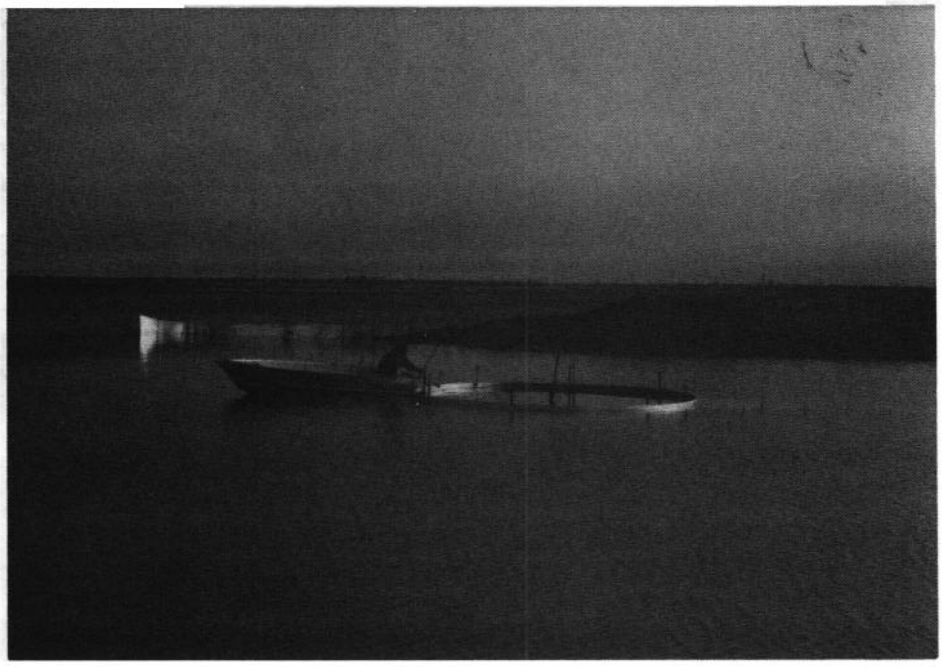

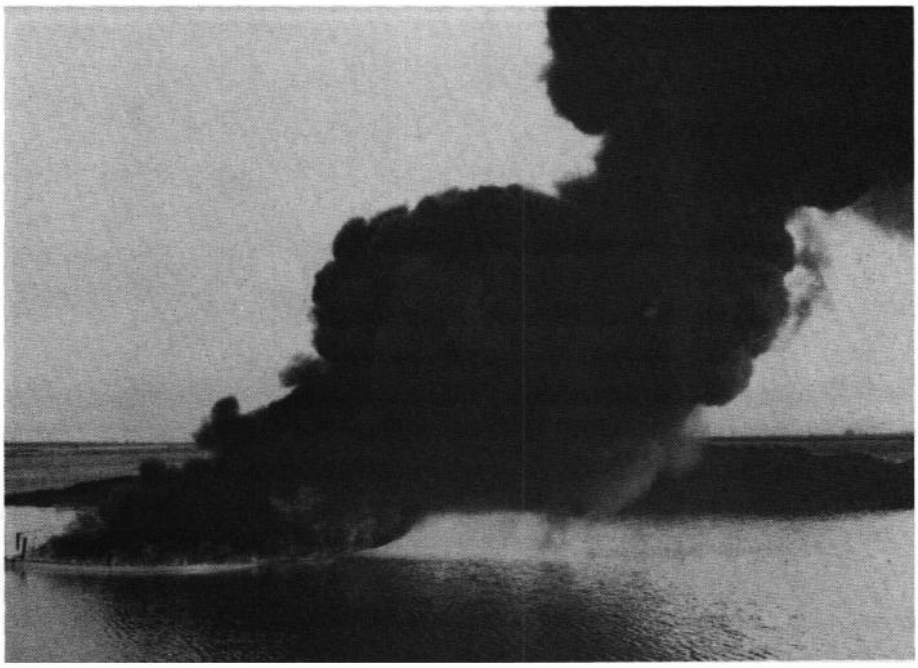

PLATE 6.4 - OIL SURFACE COMPLETELY ON FIRE

PLATE 6.5 - RING DROPPED

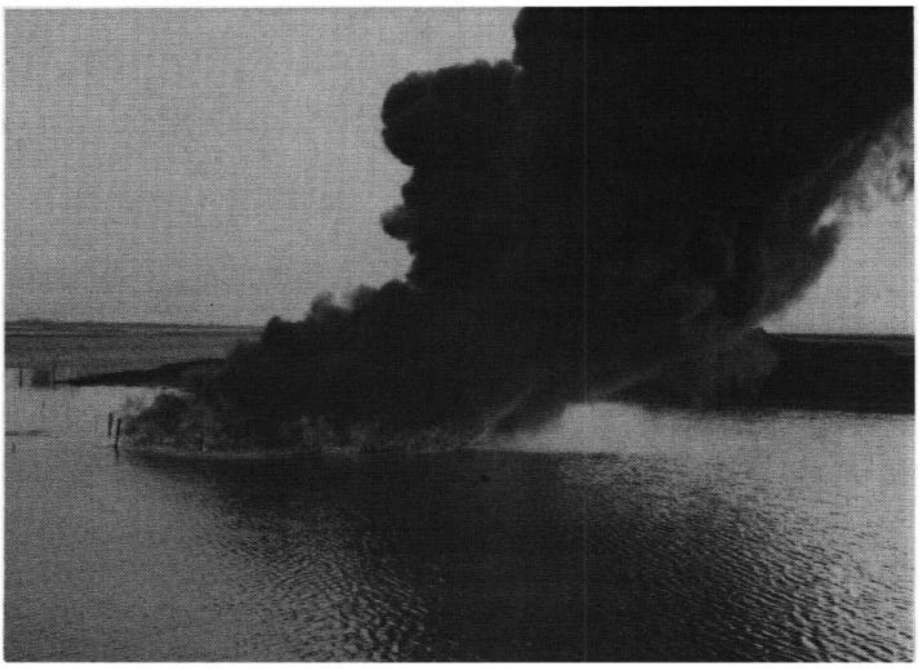

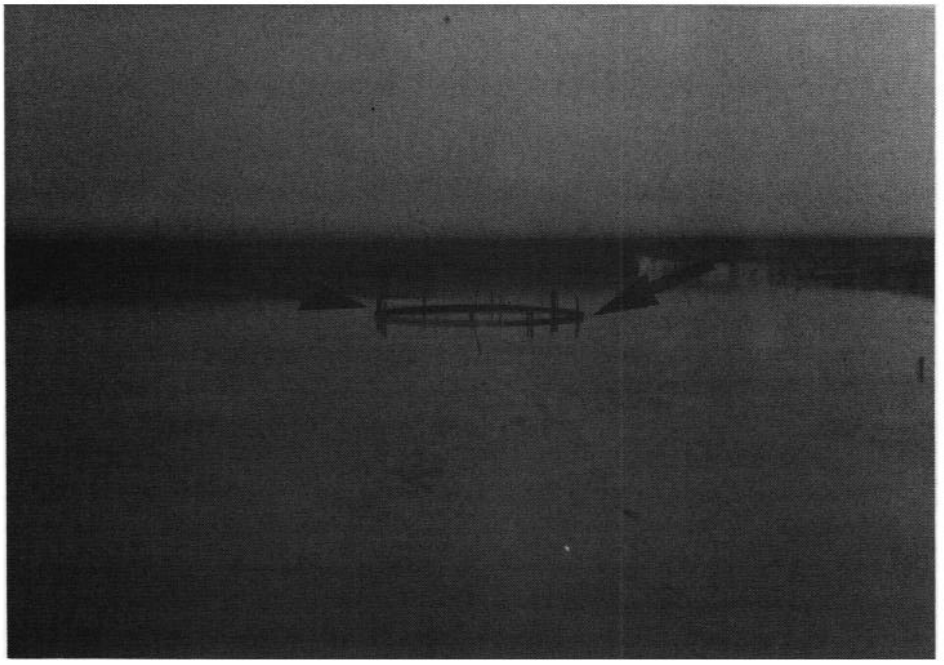

PLATE 6.6 - PITOT TUBE PLACEMENT FOR TEST 3
(ARROWS SHOW LOCATION)

For test 3 two bi-directional pitot tubes (see McCaffrey, 1976) were placed about 50 cm from the outside of the ring 20 cm above the water surface, one on the upwind side and one on the downwind side to measure entrained air velocities (Plate 6.6). These were connected to individual electronic manometers and strip chart recorders (Plate 6.7).

The burning oil was contained within the ring for the duration of test 3.

For test 4, eight baking trays, each supported on two stakes, were placed about 1 cm above the water, approximately 1 m from the outer edge of the ring, spaced evenly around the ring's circumference (about 3 m apart). An oil soaked sorbent pad was placed in each tray, the tray was filled with oil and ignited (Plate 6.8). Once all the trays were burning vigourously the ring was dropped and the oil released (Plate 6.9).

After each test the oil residue was collected and weighed. After test 1 sorbents were used (Plate 6.10) but after tests 2, 3 and 4 the residue was concentrated using shovels, picked up off the water and placed in buckets and garbage bags.

After the tests were complete, the videotapes were analyzed to determine oil and flame widths from the two cameras at right angles. It was assumed that each slick was elliptical in shape, thus its area as a function of time could be calculated from:

$$(6.1)\quad A = \pi ab$$

where A = area of slick (m^2)

a = width of slick from camera 1 (m)

b = width of slick from camera 2 (m)

PLATE 6.7 - ELECTRONIC MANOMETERS AND CHART RECORDERS

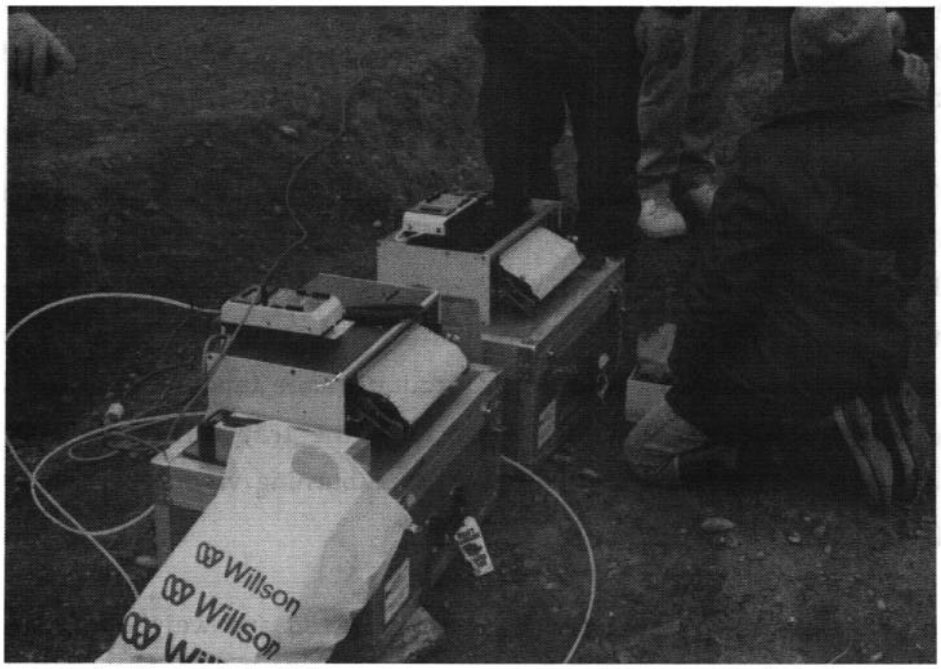

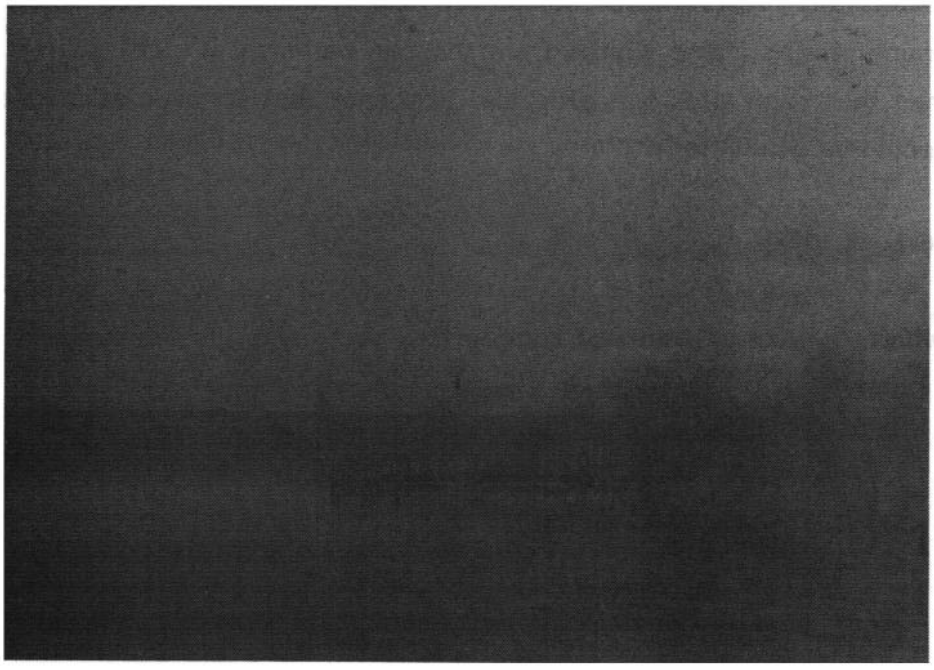

PLATE 6.8 - PLACEMENT OF BURNING OIL TRAYS FOR TEST 4

PLATE 6.9 - DROPPING RING, TEST 4

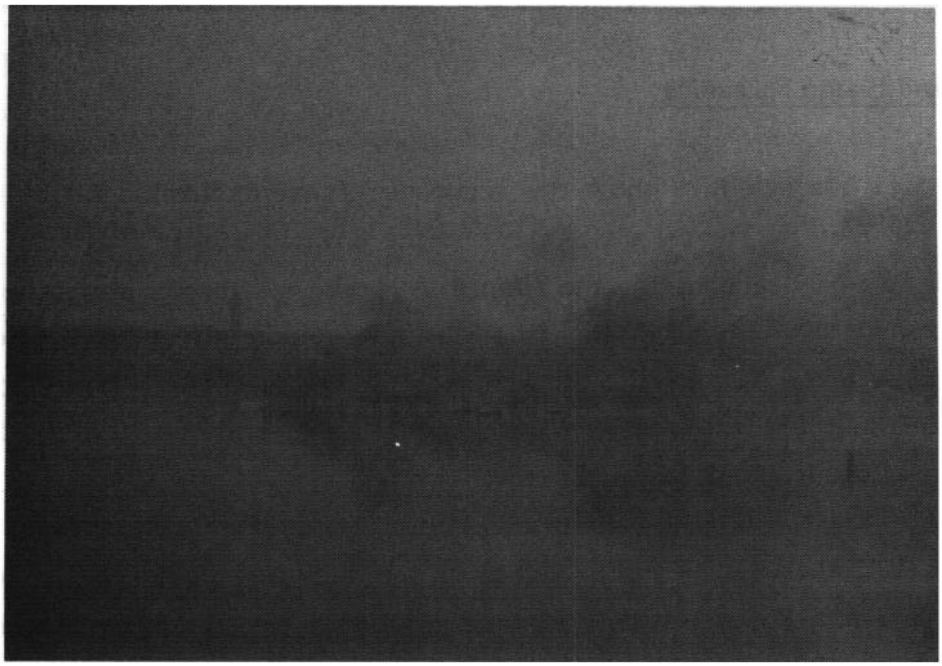

PLATE 6.10 - RESIDUE RECOVERY, TEST 1

6.2 RESULTS AND DISCUSSION

Table 6.2 summarizes the conditions and results of each of the tests.

6.2.1 Oil and Flame Spreading

Plate 6.11 through 6.16 show the sequence of events from ignition to extinction for Test 1. The oil was ignited on the downwind edge (Plate 6.11) and it took some 90 seconds for the flames to spread. After the test it was determined that the oil within the ring was not completely on fire when released. Only about 75% of the surface area was covered (see Plate 6.15). Between the time of release and extinction the slick drifted some 10 m in 150 sec (7 cm/s) at about 3% of the wind speed.

Figure 6.2 shows the measured values of the slick and flame widths for Test 1. Figure 6.3 shows the calculated oil and flame areas. Also shown are the predicted oil slick area (Fay, 1969) if no combustion were occuring and the predicted area of combustion using equations 5.9 and 5.10.

The difference between actual and predicted slick spreading may be because the inflow of air to supply the combustion slowed the oil spreading or due to viscosity or edge effects. The predicted flame area differs from the actual perhaps because the model is based on instantaneous ignition of the slick area. In Test 1 only 75% of the slick was on fire when it was released.

Figure 6.4 shows the slick and flame widths calculated for Test 2 (same procedure as Test 1 with 30% more oil). Figure 6.5 shows the predicted and calculated oil and flame areas as a function of time. In this case Fays model only slightly overestimates the initial oil spreading; however, it can be seen that once the flames reached an area of about 300 m^2 the oil spreading was retarded for some 30 seconds, possibly due to the effects of the induced flow of air into the fire. The predicted flame area does agree fairly well with the

TABLE 6.2

RESULTS OF LARGE-SCALE TEST BURNS

	TEST NO.			
	1	2	3	4
Initial Oil Volume (l)	958	1343	575	1273
Initial Oil Weight (kg)	857	1200	342	1140
Initial Oil Thickness (mm)	33	47	20	44
Ignition & Release	ignited & released	ignited & released	ignited, not released	released then ignited
Wind Speed (m/s)	2	2.5	0-2	2.5
Air Temperature (°C)	-1	2	0	1
Water Temperature (°C)	0	0	0	0
Residue Oil Volume (l)	N.M.*	≈120	N.M.	N.M.
Residue Oil Weight (kg)	240	109	62	133
Removal Efficiency (wt. %)				
TOTAL	72	90.9	87.9	88.3!
CORRECTED+	70.9	90.6	-	-

* N.M. - not measured

+ initial oil volume reduced by estimated amount burnt (at 2.5 mm/min) prior to dropping ring.

! burning oil reached edge of pit 200 s after release; small fire burned for about 150 s.

PLATE 6.11 - IGNITION OF OIL IN RING

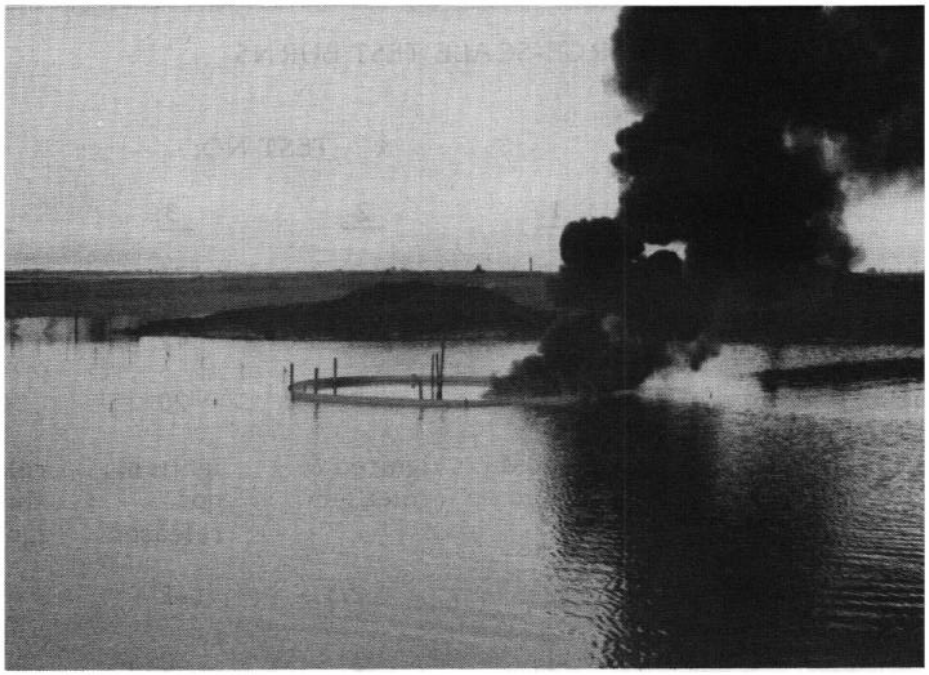

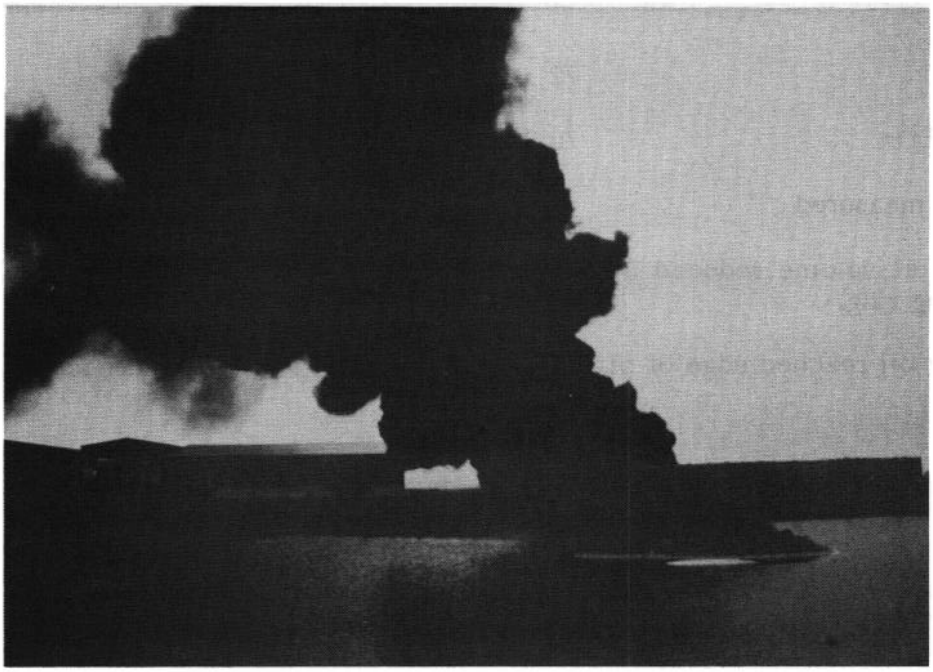

PLATE 6.12 - OIL RELEASE

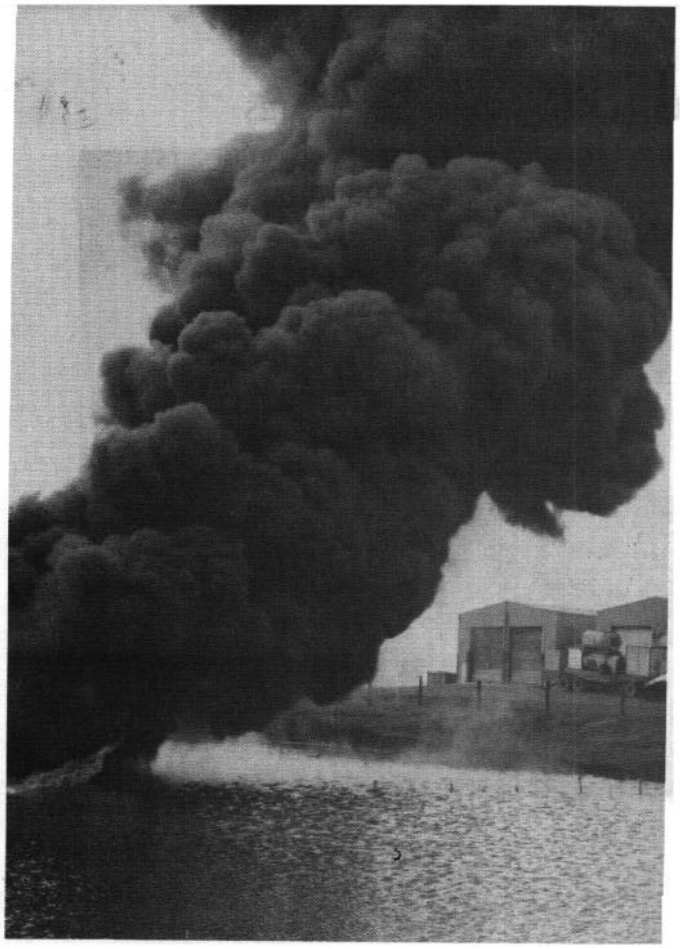

PLATE 6.13 -
FLAME HEIGHT

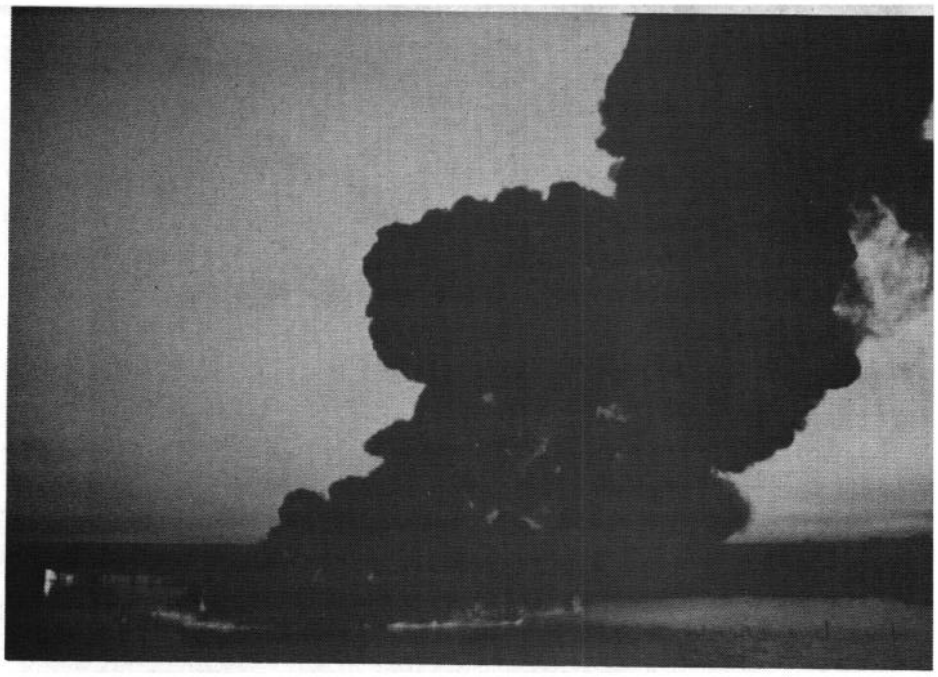

PLATE 6.14 - UNCONTAINED SLICK BURNING

PLATE 6.15 - EXTINCTION OF FLAMES

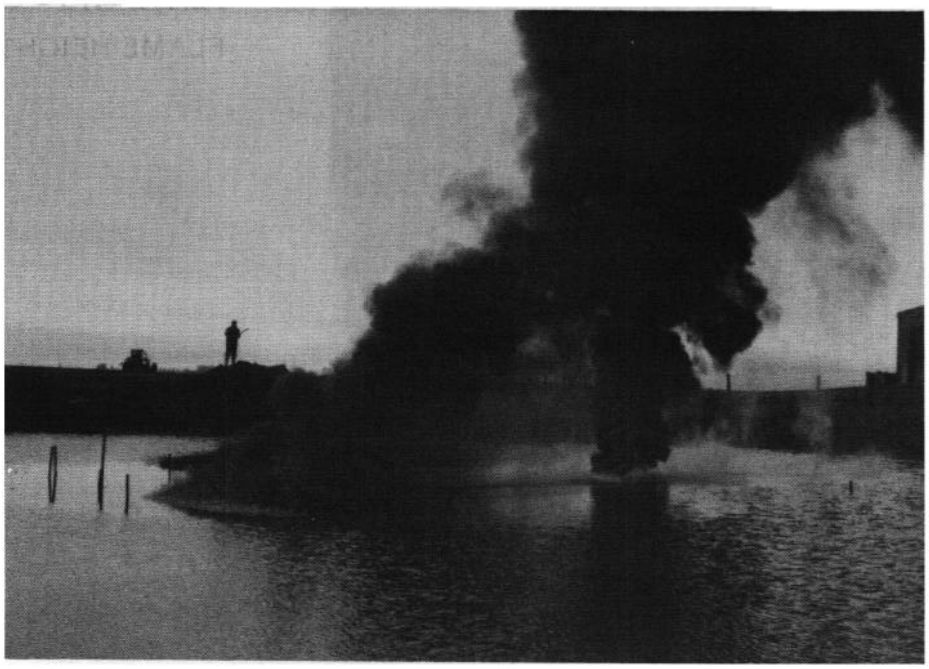

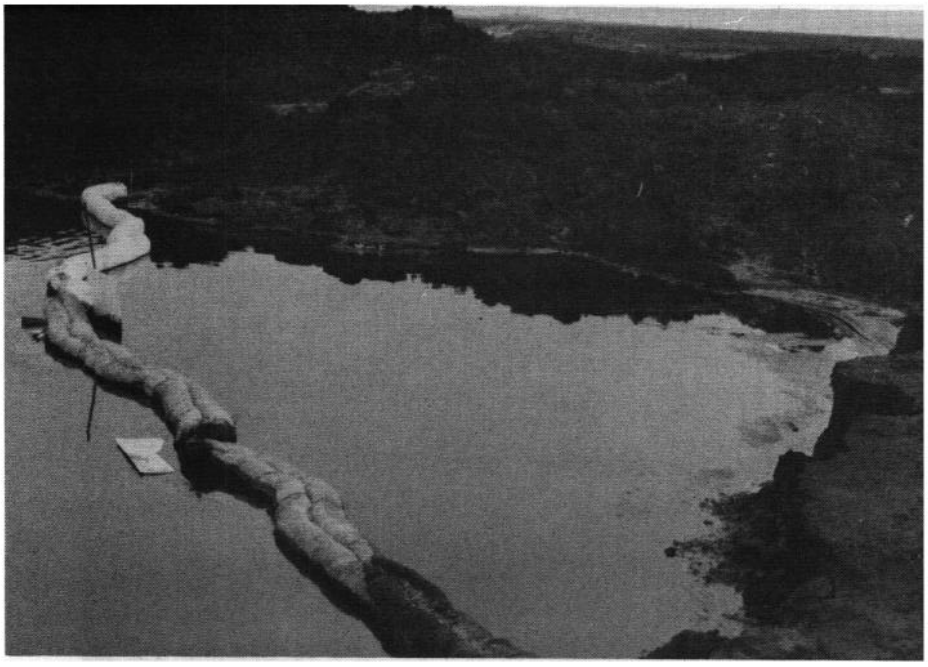

PLATE 6.16 - BURN RESIDUE

FIGURE 6.2 OIL AND FLAME WIDTH - TEST 1

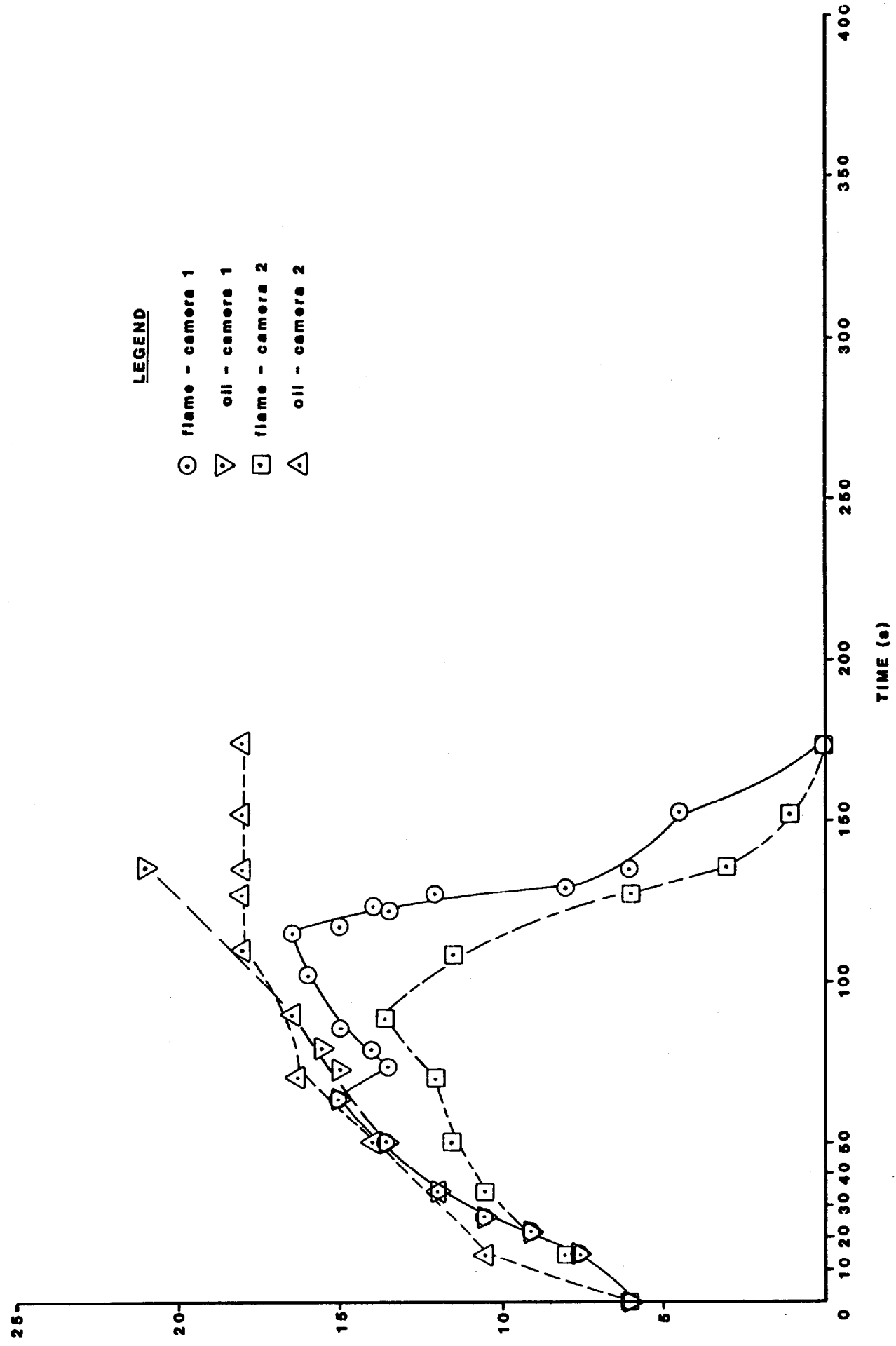

FIGURE 6.3 CALCULATED OIL AND FLAME AREA - RUN 1

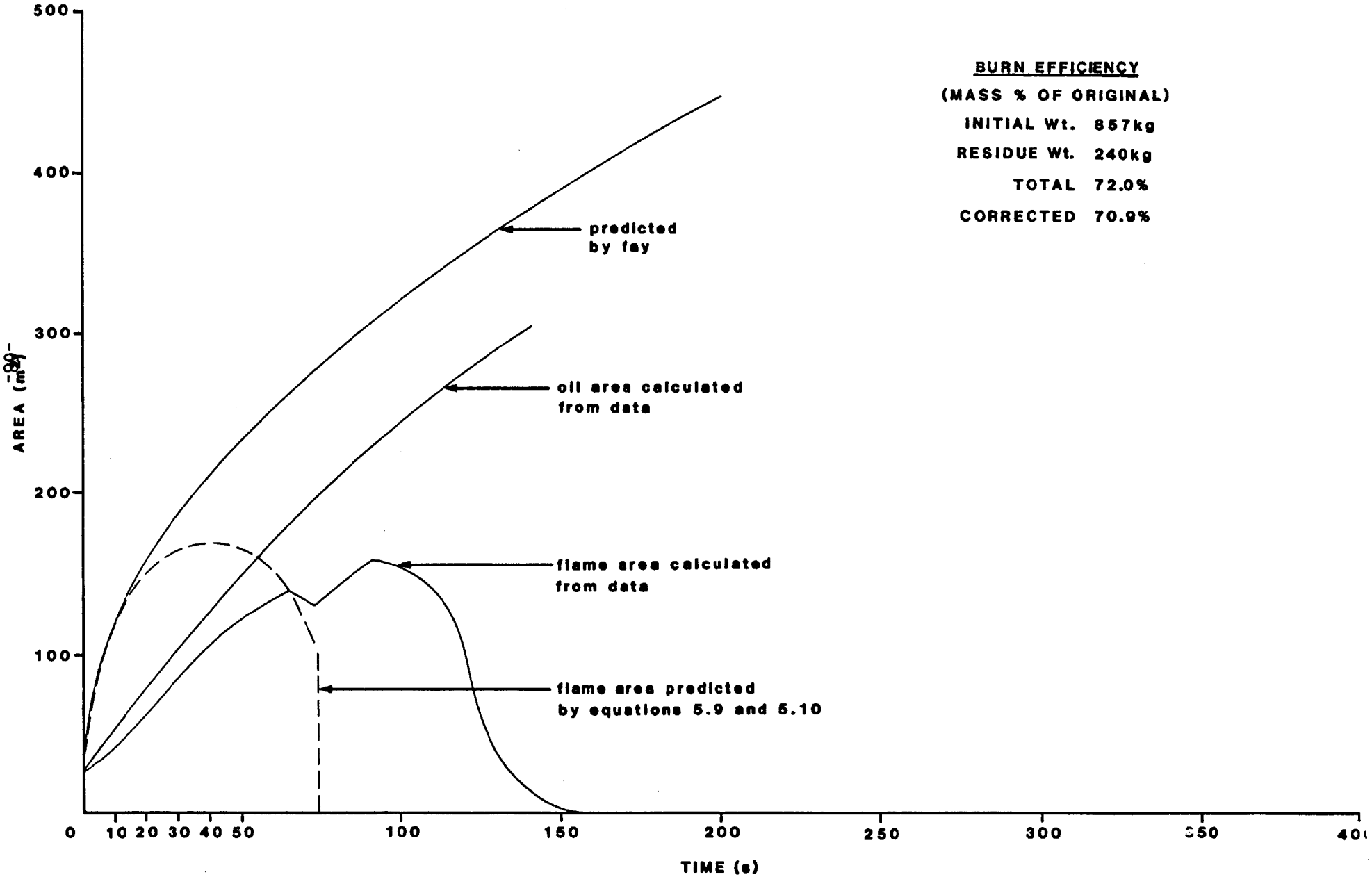

FIGURE 6.4 OIL AND FLAME WIDTH - RUN 2

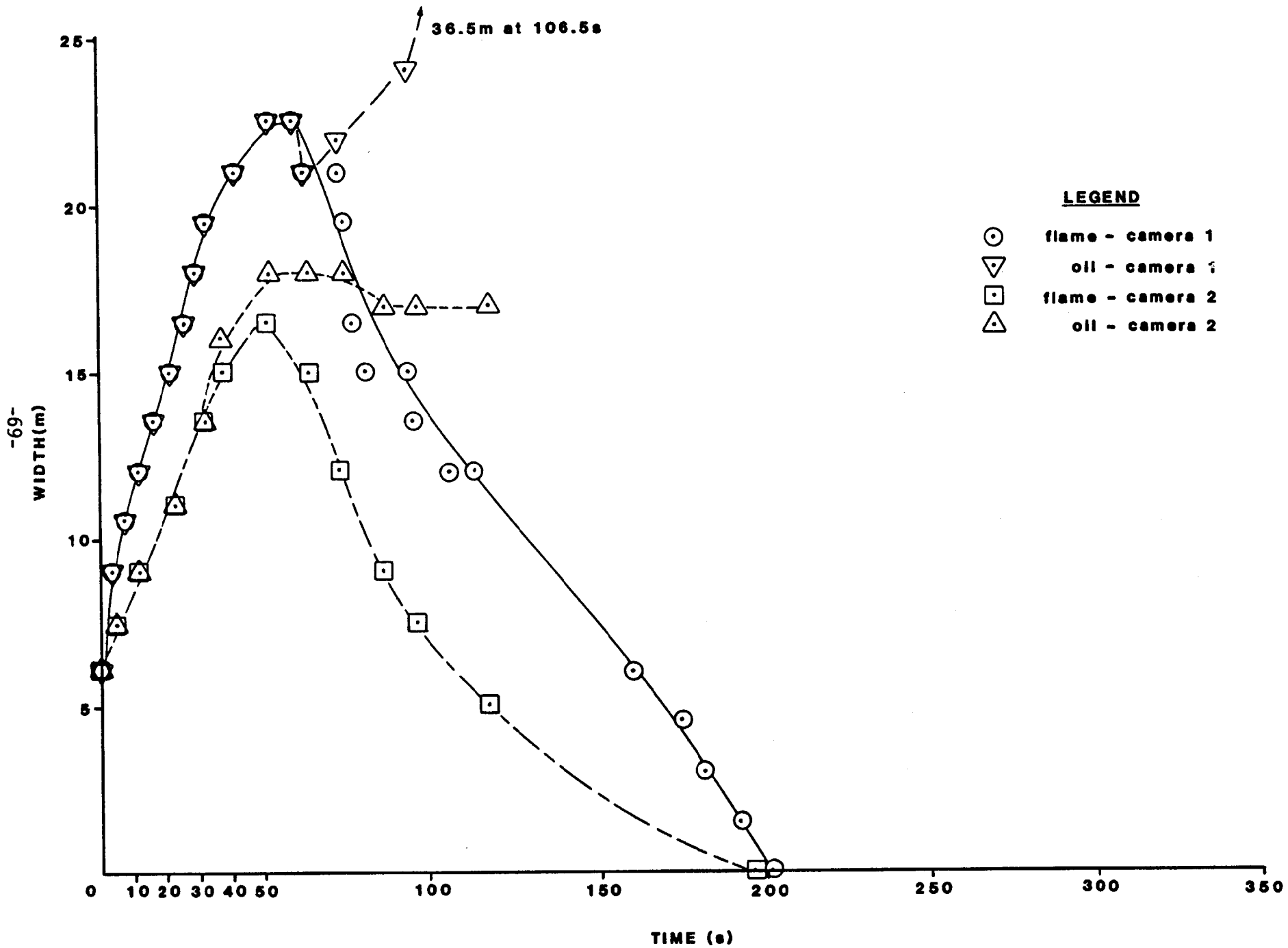

FIGURE 6.5 CALCULATED OIL AND FLAME AREA - RUN 2

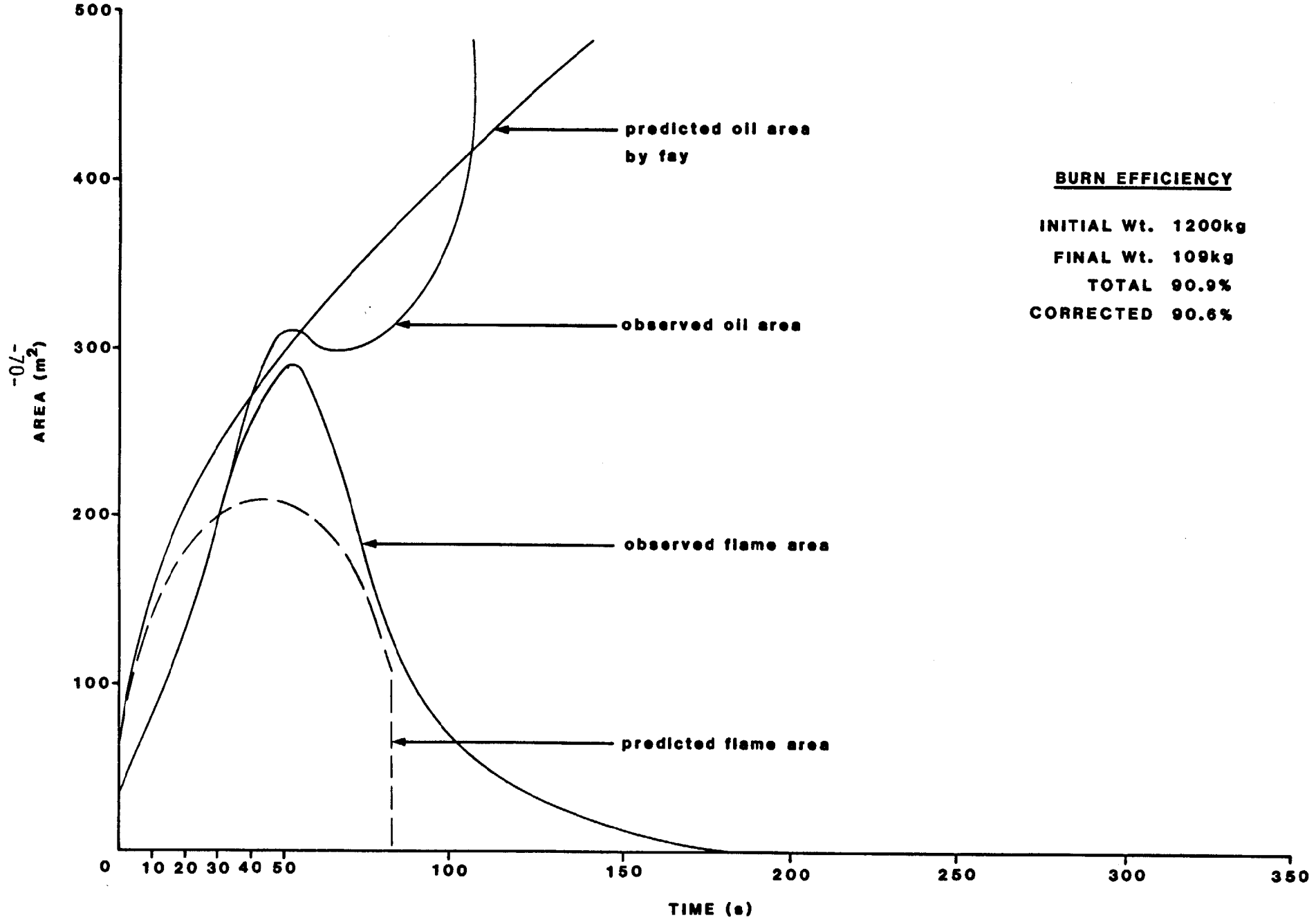

observed flame area. The predicted combustion efficiency of 92% (based on a 2.5 mm/min regression rate) agrees well with the results. The discrepancy between observed and actual flame spreading is likely due to the inaccuracy of the assumption that the term R/h is constant in integrating equation 5.6. The regression rate is likely a complex function of slick thickness, perhaps of the form:

(6.2) $R=R_o (1 - e^{-ch})$ - see Figure 5.1

where c = a constant unique for each oil type and slick size

Plates 6.17 through 6.29 show the progress of Test number 2. Plate 6.22 illustrates the consistency of the burn residue.

Plates 6.23 through 6.29 show test 4, in which the oil was released then ignited around its periphery by a circle of burning pans.

Plate 6.23 shows the ring just dropping below the waters surface and Plate 6.24 shows the "fingers" of flame developing as the oil spreads out beneath the burning pans. Plate 6.25 shows the "fingers" of flame spreading and beginning to merge. Plate 6.26 shows the fire at its peak when the central slick is completely ablaze, though flame "fingers" are still evident at the upwind edge. Plate 6.27 shows the slick, some time later as it drifts towards the edge of the pit and Plate 6.28 shows it as it just reaches the edge. Plate 6.29 shows the residue.

Figure 6.6 shows the measured flame widths for Test 4 (the oil slick could not be distinguished from the water because of the foggy, flat calm conditions). Figure 6.7 compares the calculated flame area with that predicted by the burning model and Fay's oil spreading model. Taking into account the delay in ignition the predicted and actual flame spreading is quite close. The predicted removal efficiency of 91% agrees well with the measured value at 88.3%.

PLATE 6.17 - TEST 2 JUST PRIOR TO OIL RELEASE

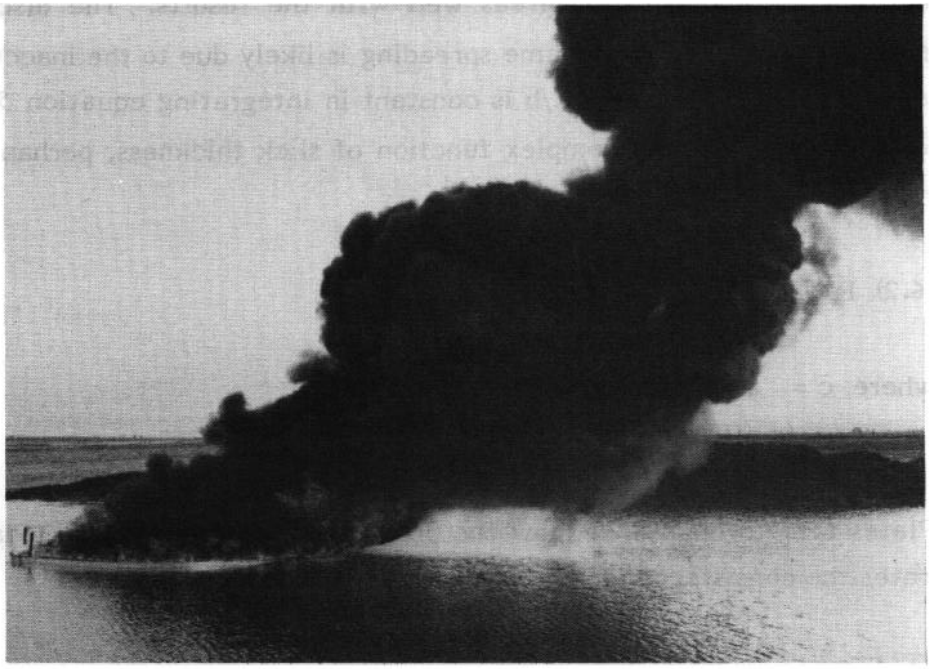

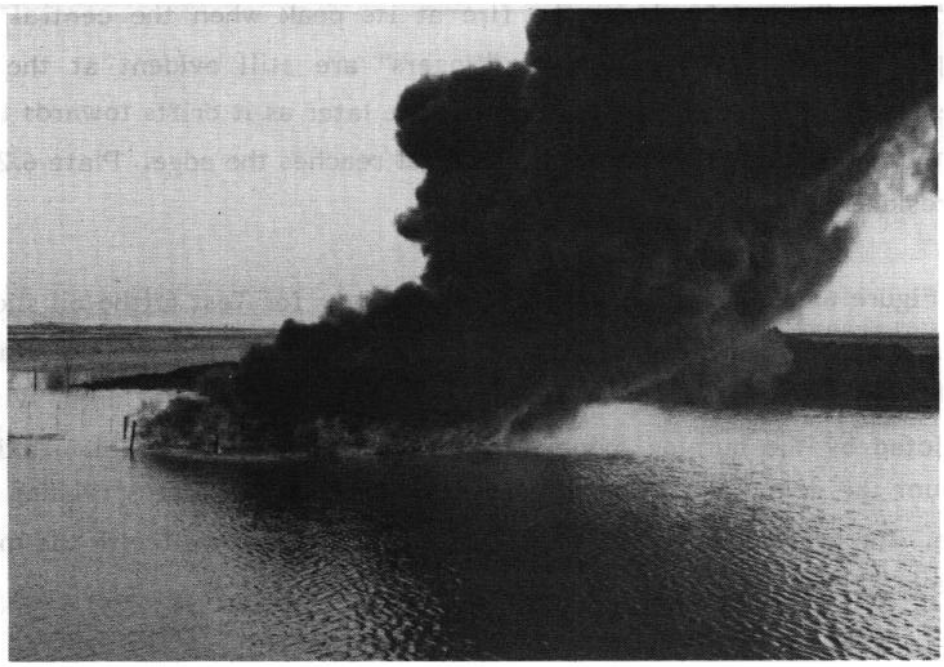

PLATE 6.18 - IMMEDIATELY AFTER DROPPING RING

PLATE 6.19 - OIL AND FLAME SPREADING AFTER RELEASE

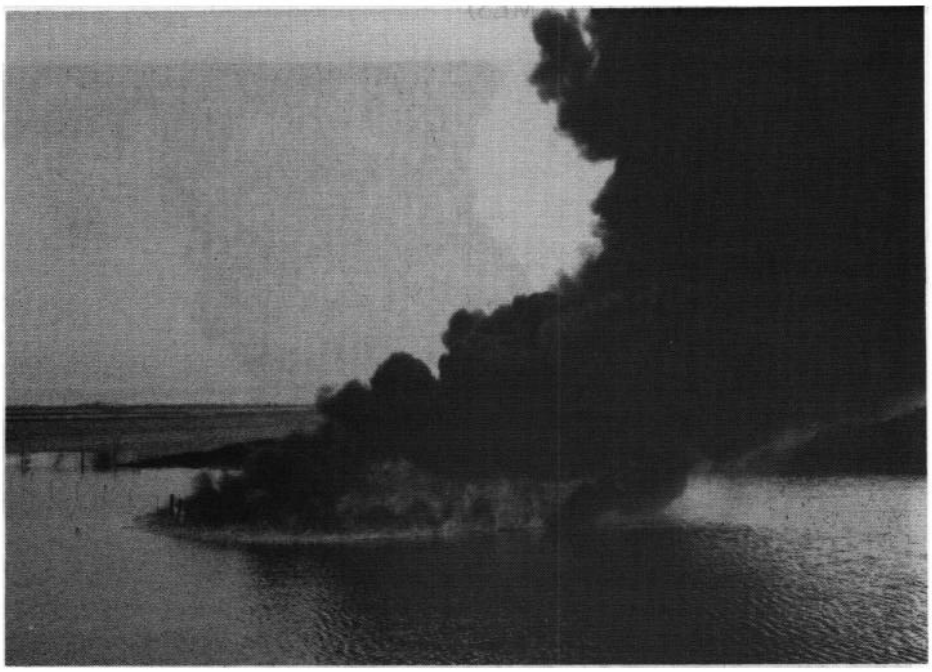

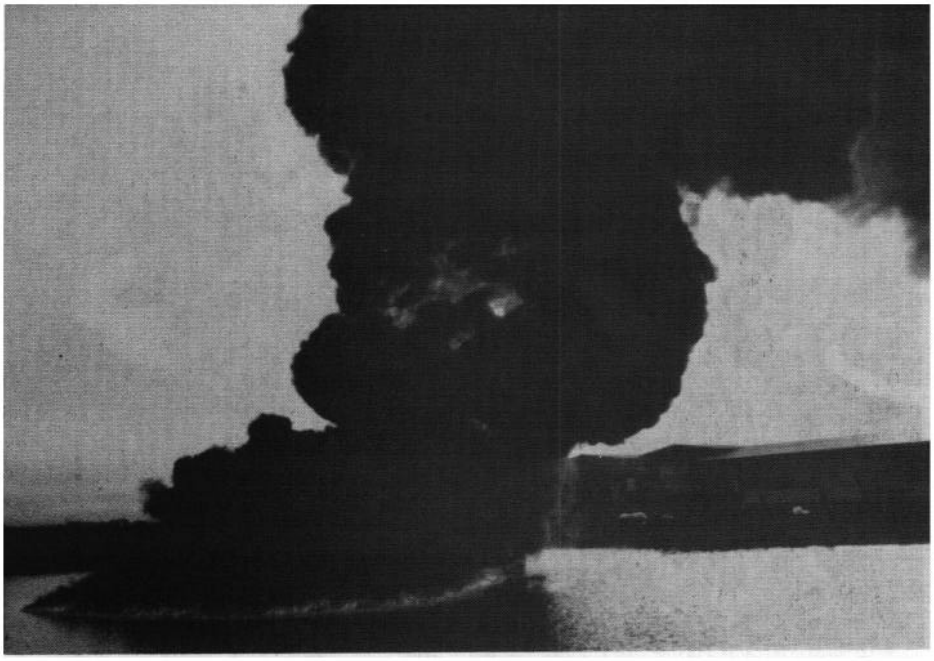

PLATE 6.20 - MAXIMUM FLAME AREA

PLATE 6.21 - FLAME AREA DECREASING (NOTE BAND OF THIN OIL AROUND FLAMES)

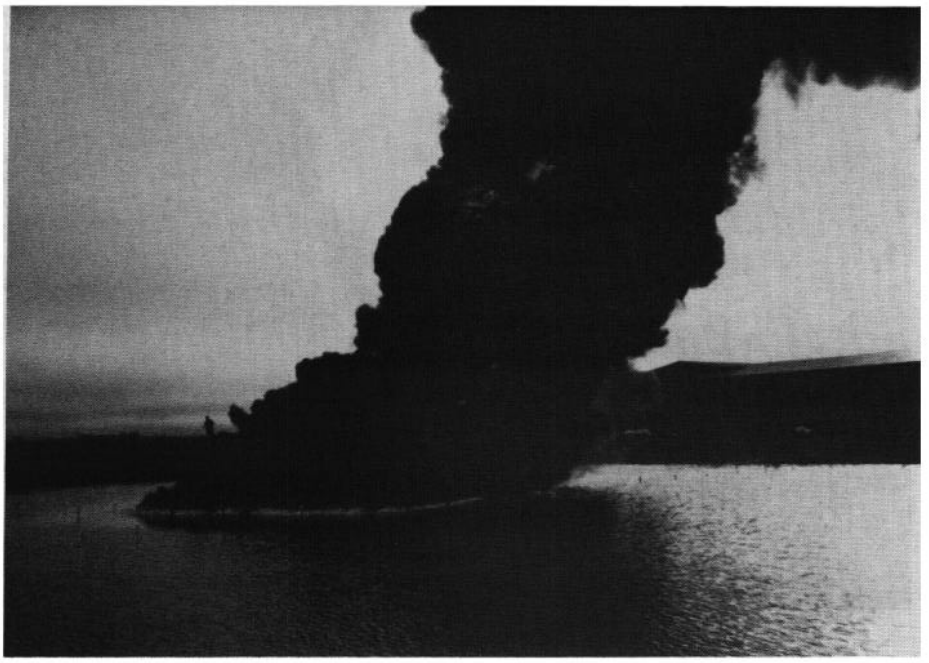

PLATE 6.22 - RESIDUE FROM TEST 2

PLATE 6.23 - TEST 4 JUST AFTER OIL RELEASE

PLATE 6.24 - FLAME "FINGERS" APPEARING

PLATE 6.25 - FLAME "FINGERS" MERGING

PLATE 6.26 - PEAK FLAME AREA

PLATE 6.27 - SLICK DRIFTING TOWARDS EDGE OF PIT

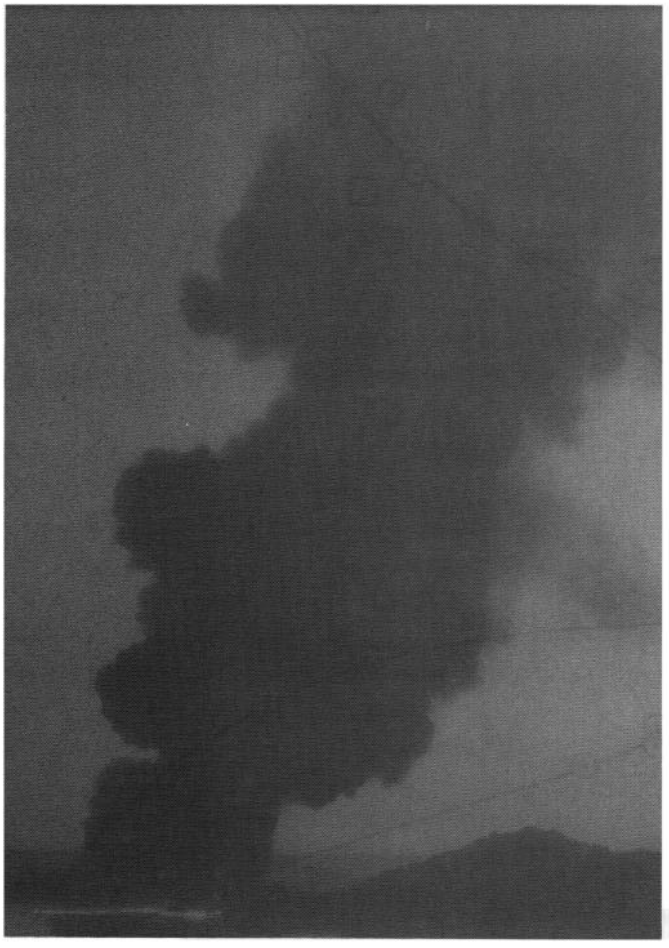

PLATE 6.28 - SLICK BURNING AGAINST EDGE

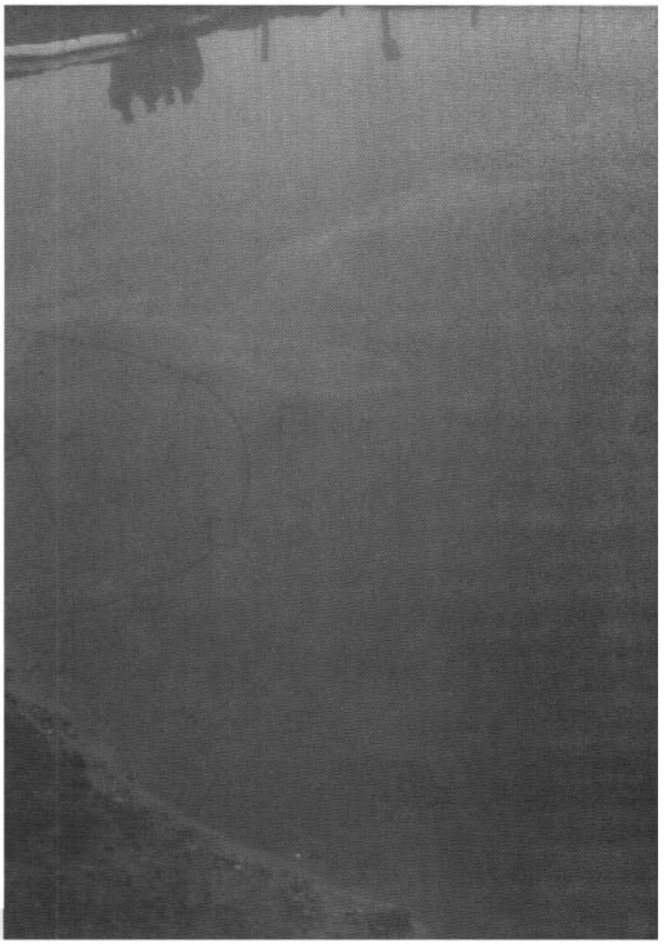

PLATE 6.29 - BURN RESIDUE

FIGURE 6.6 FLAME WIDTH - RUN 4

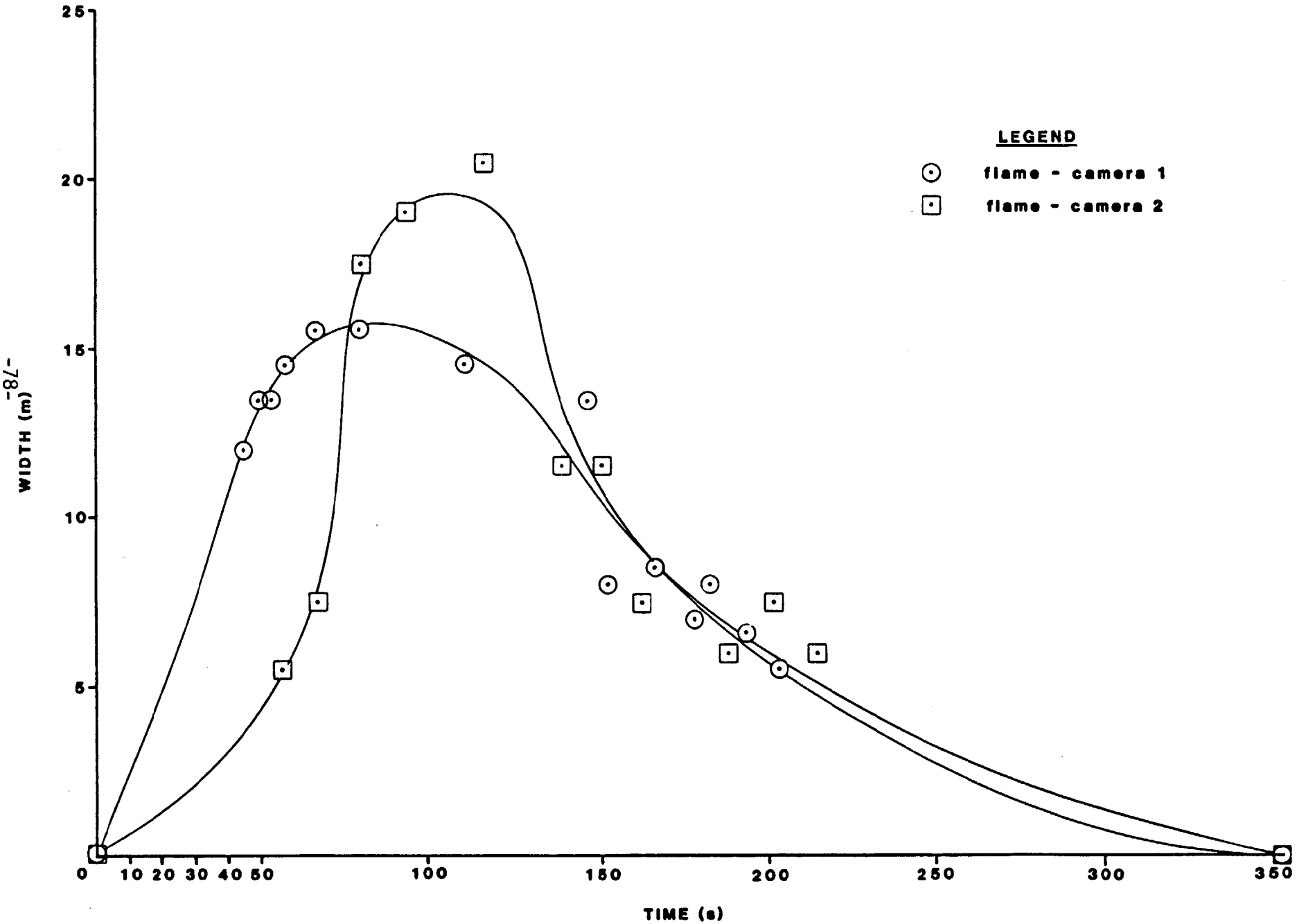

FIGURE 6.7 CALCULATED FLAME AREA - RUN 4

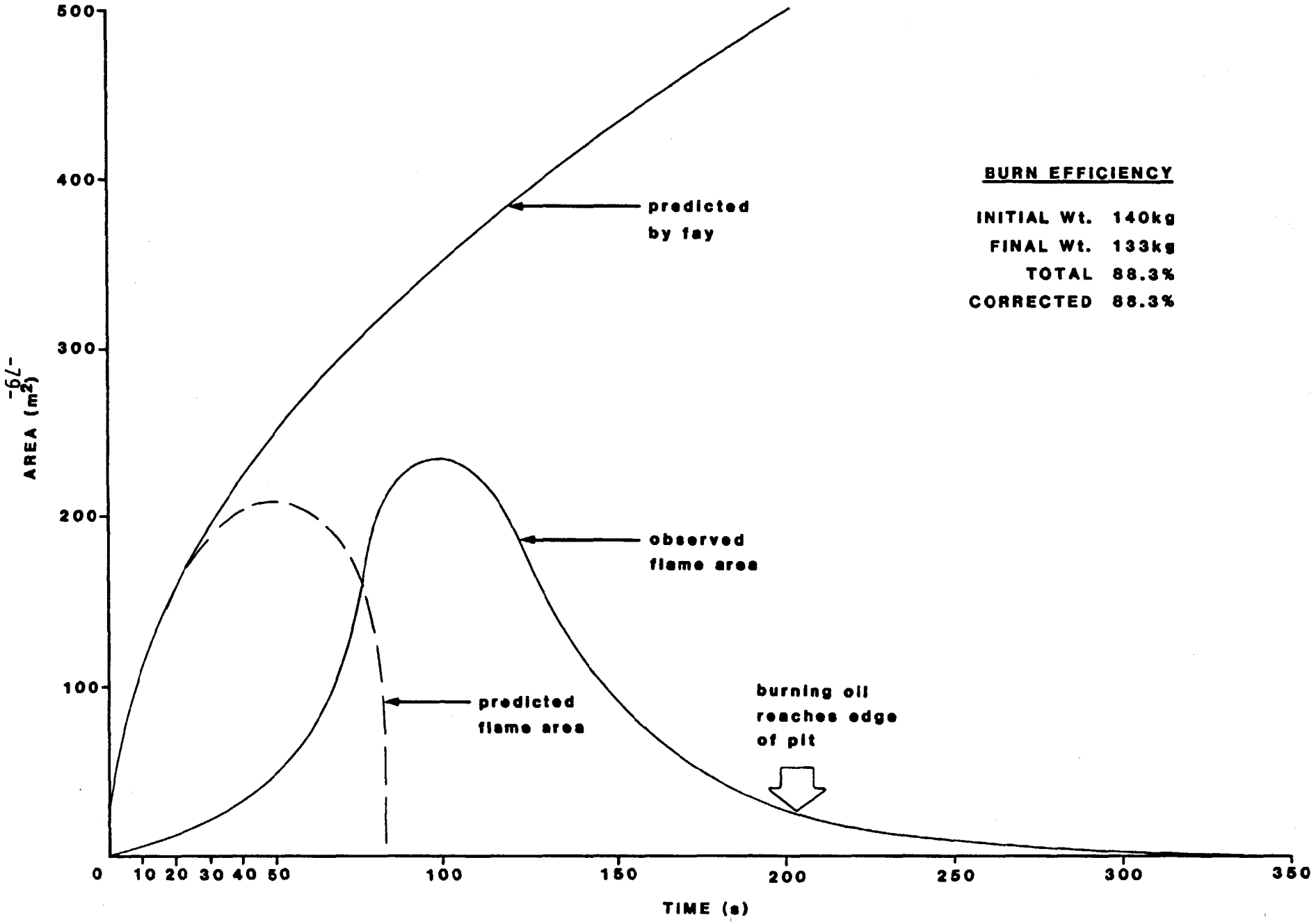

6.2.2 Air Entrainment and Self-Induced Wind-Herding

Figure 6.8 shows the results of the airflow measurements, (20 cm above the water surface at the height of the ring) upwind and downwind of the fire in test 3. The upwind pitot tube measured a definite induced airflow, with a velocity of about 15 cm/s above the ambient wind. The difference in ambient wind speed measured before and after the test may be a result of the light variable winds at the time of the test combined with zero-drift in the electronic manometer and/or chart recorder.

The downwind pitot tube (read visually) recorded highly turbulent airflows. This fact was confirmed visually by the prescence of "dust-devils" downwind of the fire (Plate 6.30). In fact the downwind pitot tube may have been immersed in flame for much of the burn and the apparent increase in downwind velocity may in fact be a component of the buoyant rise velocity of the diffusion flame being bent over by atmospheric winds.

The average of the upwind and downwind measurements is a net inflow of air at about 0.14 m/s. This agrees with the data of Thomas et al, 1965 for air entrainment into gas burners (about 11 and 17 cm/s, 0.53 and 0.38 m from the edge and 0.20 m above the base of the flame) and with the theory of McCaffrey, 1983 which predicts velocities of 20-25 cm/s at the same heights and radii out from the fire.

6.2.2.1 Modelling Self-Induced Wind-Herding

In order to model the effects of self-induced wind-herding of a burning oil slick the spreading force of the slick (assumed to be by gravity for the slicks of interest) is balanced by the drag force on the slick of the radially inward surface current induced by the entrained airflow, i.e.:

FIGURE 6.8 AIRFLOW MEASUREMENTS - RUN 3

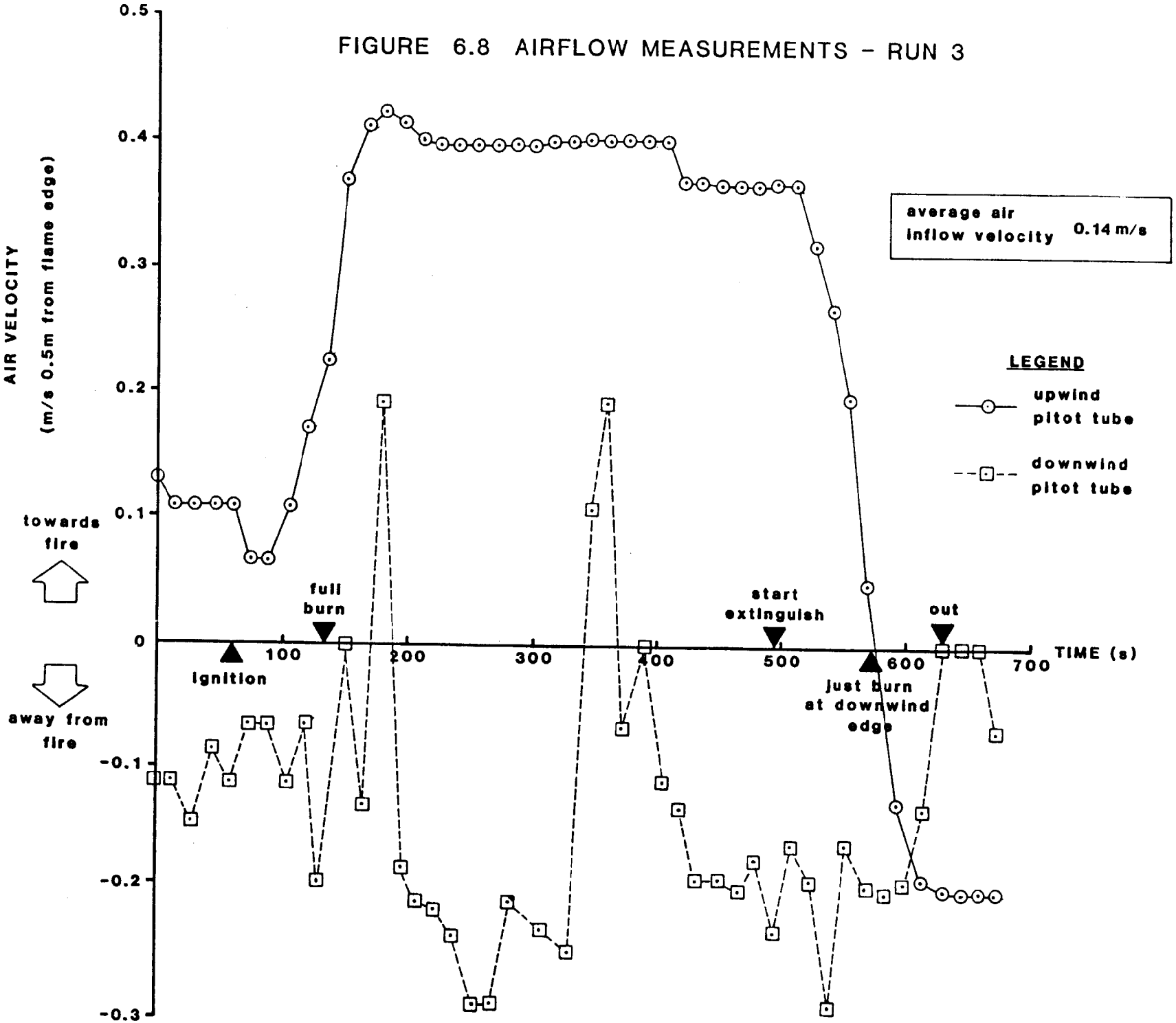

PLATE 6.30 - TURBULENCE DOWNWIND OF FIRE

Gravity force per unit volume = drag force per unit volume, or

$$(6.3)\quad \Delta\rho g h / \pi^{1/2} r = C_D \rho_A A U^2 / V$$

where $\Delta\rho$ = density difference between oil and water (kg/m^3)
g = acceleration due to gravity (9.81 m/s^2)
h = slick thickness (m)
r = slick radius (m)
C_D = drag coefficient
ρ_A = density of air (1.28 kg/m^3)
A = area of slick (m^2)
U = air velocity (m/s)
V = oil volume (m^3)

substituting $V = Ah$, and rearranging equation 6.3 yields

$$(6.4)\quad h = (\pi^{1/2} C_D \rho_A / \Delta\rho g)^{1/2} U r^{1/2}$$

From Chapter 7 it can be shown that, for large fires, U is a constant equal to about 0.25 m/s. Thus, substituting the value for C_D from the wind tunnel tests (3.5×10^{-3} - Chapter 4) and $\Delta\rho = 105$ kg/m^3 yields

$$(6.5)\quad h = 7 \times 10^{-4} r^{1/2}$$

This equation predicts a self-induced wind-herded slick thickness of 2.2 mm for a 10 m radius (300 m^2 area) slick, which agrees with the data for test 2 (see Figure 6.5) which indicates a cessation of oil spreading at 300 m^2 with an estimated thickness (including oil losses to combustion) of 3 mm.

6.2.3 Removal Efficiency

Figure 6.9 shows the removal efficiency as a function of oil volume for both the large and mid-scale testing. In general, as oil volume increases so does removal efficiency. Comparison of the large-scale data points indicates that:

- ignition of the entire slick area results in a higher removal efficiency than ignition of the periphery (90.6% vs 88.3%)

- ignition of the entire surface area or of the full circumference of the spreading oil is more efficient than ignition of a portion of the downwind slick.

This last point is important for oil spill burning operations. It seems that, unlike burning oil contained in a melt pool, unlit oil is not fed into the area on fire by the wind. In the case of test 1 about 25% of the upwind area of the slick in the containment ring was not on fire upon its release; the burn efficiency for test 1 was about 75% of that of test 2 when the entire slick area was on fire upon release. It seems that a thick, free floating slick, in the absence of large scale eddies, is advected en masse by the wind driven surface currents and unignited oil is not pushed into the fire-zone. Since the upwind flame spreading rates are low (1-2 cm/s) it is unlikely that oil, upwind of a floating ignition source drifting with the slick, would be ignited. Thus it is important to ignite the upwind extremeties of a thick slick with conventional igniters or develop an igniter that drifts more slowly than the oil and ignites a long strip of oil from the middle out to the upwind edge.

Also shown on Figure 6.9 is the prediction of the model developed in Chapter 5 and the prediction of the model developed in the next chapter, which neglects volume loss to combustion but includes the self-induced wind-herding phenomenon, and an ignition delay term. Due to a lack of data points in the region of 100 L oil volume no conclusion can be made in terms of the most descriptive model, though both models show the same trend.

FIGURE 6.9 COMBUSTION EFFICIENCY - INSTANTANEOUS IGNITION

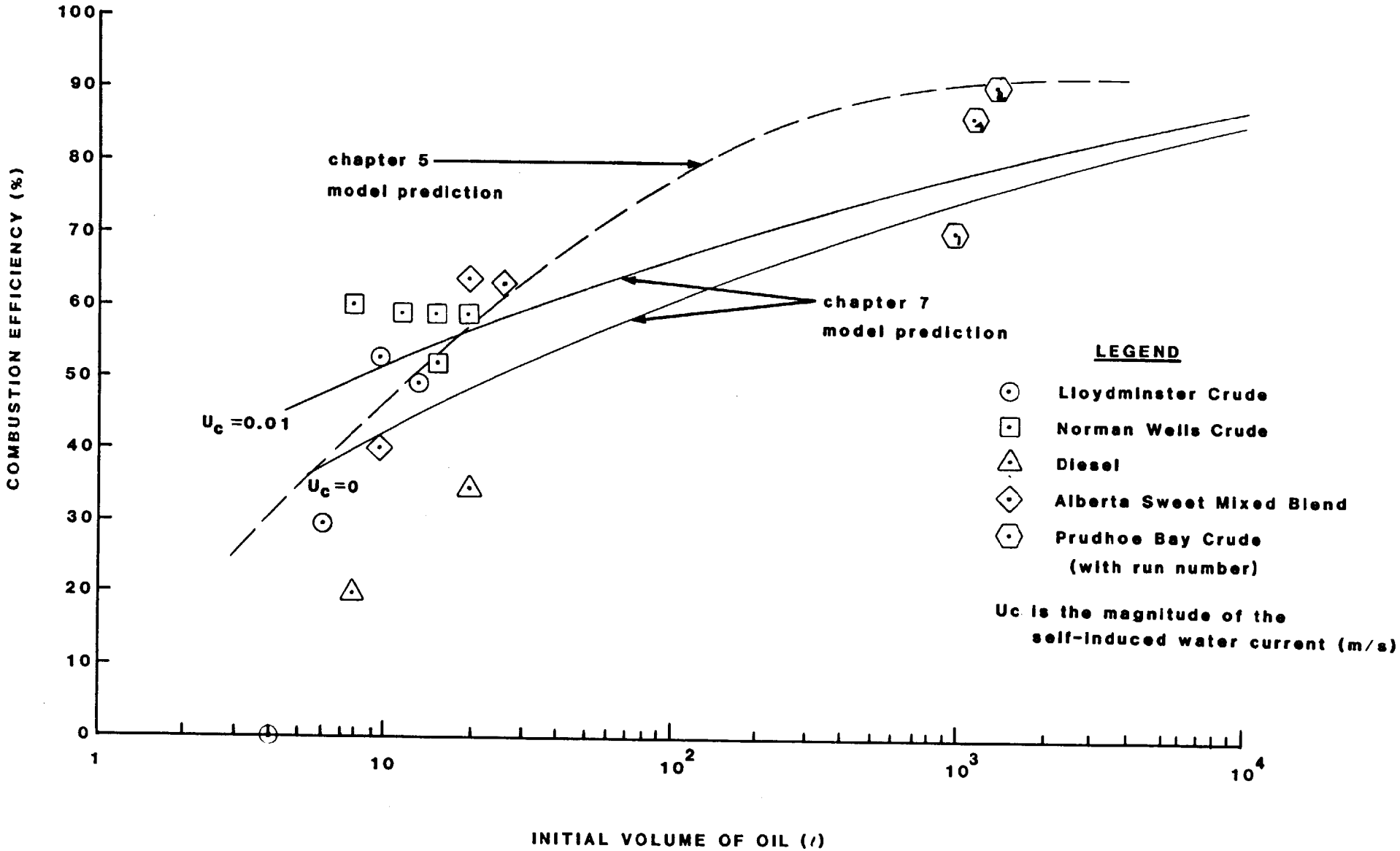

6.3 SUMMARY

The major findings of this phase of the study were:

* as the oil volumes increase the instantaneous ! ignition removal efficiency increases

* ignition around the slick's periphery immediately after release results in almost as high removal efficiencies as ignition of the entire surface area of the slick prior to release.

* the flames do not spread significantly upwind to ignite unburnt areas; this points out the importance of igniting the entire upwind area or circumference to maximize removal efficiency.

* entrained air velocities were measured at an overall average of 0.14 m/s; air upwind of the fire is drawn in smoothly while downwind of the fire the air is extremely turbulent.

* self-induced wind-herding was observed and measured in one test; the value of the equilibrium thickness is 3 mm for a 300 m^2 slick, which agrees reasonably well with theory and the wind-tunnel tests.

! (entire slick area on fire upon release)

7.0 MODELLING THE BURNING OF UNCONFINED OIL SLICKS

7.1 INTRODUCTION

In Chapter 5 it was shown that the well-known description of a spreading non-burning slick (Fay, 1969) could be combined in a simple way with the equation of conservation of mass of the spilled oil to produce a model which agreed well with the data obtained for burning slicks. This model described the burning of the slick in terms of a constant volume rate of burning per unit of slick, or in other words a regression rate of the slick thickness.

In this chapter the same approach is used in a more complicated model to include the effect of wind-herding, and to predict the effect of a delay in igniting the slick.

The spilled oil is assumed to spread according to the well-known laws formulated by Fay: initially a gravity-inertial spread with slick radius proportional to $t^{1/2}$, followed by a gravity-viscous spread with slick radius proportional to $t^{1/4}$. The subsequent surface tension-viscous spread is not dealt with because the transition to that regime is uncertain and may occur when the slick is too thin to burn.

It is assumed that the combustion process affects the spread of the slick in only one way, namely that the air flowing into the flame induces a water surface current which opposes the spreading of the slick. This is a self-generated "wind herding" phenomenon.

The slick continues to burn until its thickness reaches some minimum value at which point the heat loss to the water under the slick uses up all the heat feedback to the slick from the flame above it. The experimental value for this minimum thickness is 0.8 mm (Energetex, 1981b).

The removal efficiency of the slick is the difference between the volume of the oil spilled and the volume of the remaining layer of unburned residue which has that thickness, all divided by the volume of oil spilled. For any given spill volume, the removal efficiency is maximum when the slick is ignited immediately. Delaying the ignition decreases the efficiency. If ignition is delayed until the slick thickness is less than the minimum ignitable, none of the oil can burn, and the removal efficiency is zero.

The equations of the spreading burning slick were solved for four spill volumes: 0.01, 1.0, 10^2 and 10^4 m^3. The calculations were performed with two values of the induced water current: zero and 0.01 m/s, over a wide range of ignition delay times.

7.2 THE SPREAD OF AN OIL SLICK ON WATER

7.2.1 The Three-Regime Model

Fay, 1969 described the spread of an oil slick on water in terms of three regimes distinguished by a balance between different pairs of forces: gravity-inertial, gravity-viscous, and surface tension-viscous. He identified the important physical variables and used simple physical reasoning as well as dimensional analysis to derive appropriate equations describing each regime. Fannelop and Waldmann, 1971 carried out a detailed analysis of the process, confirming Fay's description and evaluating the constants of proportionality. Their governing equations for the spread of a circular slick in the first two regimes are:

(7.1) Gravity-inertial (GI): $$\frac{r_s(t)}{L} = 1.14 \left(\frac{g \Delta \rho}{\rho_w L}\right)^{1/4} t^{1/2}$$

(7.2) Gravity-viscous (GV): $$\frac{r_s(t)}{L} = 0.98 \left(\frac{g^2 \Delta \rho^2}{\rho_w \mu_w}\right)^{1/12} t^{1/4}$$

where
- $r_s(t)$ = radius of slick at time t(m)
- L = $V_s^{1/3}$ (m)
- V_s = volume of spill (m^3)
- g = acceleration of gravity (9.8 m/s^2)
- $\Delta\rho$ = $\rho_w - \rho_{oil}$ (200 kg/m^3 - typically)
- ρ_w = density of water (1,000 kg/m^3)
- ρ_{oil} = density of oil (800 kg/m^3)
- μ_w = dynamic viscosity of water (kg/ms)
- t = time (s)

The constants in equations (7.1) and (7.2) are dimensionless. All the units are in the algebraic terms.

Equations (7.1) and (7.2) describe the spread of a slick which is not burning. They are modified later to take combustion into account.

The third regime of spreading, surface tension-viscous, is not included in this work. It probably occurs when the slick is already too thin to burn.

7.2.2 Transition from GI to GV

It is important to know how long the spreading slick can be described by the gravity-inertial regime.

Following Fay, 1969, the transition from the GI regime to the GV regime is identified by the condition that the slick thickness $h = V_s/\pi r^2$ equals the water-side boundary-layer thickness $= (\nu_w t)^{1/2}$.

Therefore, at the transition from GI to GV

$$r^*_s = (V_s/\pi)^{1/2} (\nu_w t^*)^{-1/4} \tag{7.3}$$

where * denotes the values of r_s and t at transition from GI to GV, and $\nu_w = \mu_w/\rho_w$ is the kinematic viscosity of water; (10^{-6} m^2/s).

7.2.3 The Spreading Equation

There are several effects of the burning of the slick on its spread. First, V_s is not constant. It decreases with time as the slick burns. Secondly, both the oil and the water underneath it become heated and their viscosity decreases. In the gravity-viscous regime these two effects would oppose one another. It will be assumed that they cancel each other completely and that V_s is constant.

That leaves the third effect, which is less obvious. As the slick burns, the flame and buoyant plume above it entrain ambient air. This sets up a wind directed toward the slick from its surroundings. In turn, the entrained wind exerts a drag on the water and induces a surface current directed toward the slick. This current opposes the spreading of the slick. The overall effect can be though of as a self-generated wind-herding of the burning slick.

The mathematical model of this process will be the spreading equation

$$\frac{dr_s}{dt} = \frac{dr_{s,u}}{dt} - U_c \tag{7.4}$$

where $\frac{dr_s}{dt}$ = rate of growth of the radius of a burning slick

$\frac{dr_{s,u}}{dt}$ = rate of growth of the radius of a slick which is not burning, to be calculted from equ. (7.1) and (7.2)

U_c = surface current induced by the air flow into the fire.

All terms in equation (7.4) have the units of m/s.

7.2.4 The Induced Surface Current

The induced surface current is assumed to be proportional to the speed of the air flowing into the fire. This air speed, in turn, can be evaluated from what is known about turbulent diffusion flames and pool fires.

Fig. 7.1 Diagram of the flame illustrating the calculation of the air inflow velocity u_a and surface current u_c.

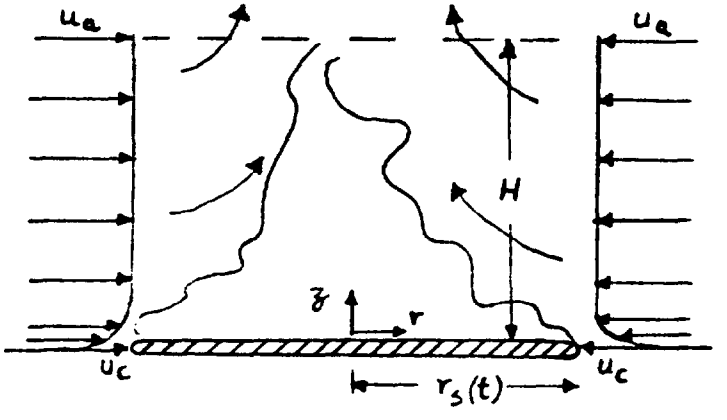

Assuming a flame of height H, a mass balance on the air alone gives

(7.5) $\dot{m}_{a,in} = \dot{m}_{a,out}$

but

(7.6) $\dot{m}_{a,in} = 2\pi r_s \int_a^H U(z)dz$

$= 2\pi r_s \int_a^H u_a$

if the displacement thickness of the air boundary layer is ignored. The air outflow can be related to the burning rate of the slick $\dot{m}_s$.

$$\dot{m}_{a,out} = (a/f)\,\Psi\,\dot{m}_s$$

where
- $\dot{m}_a$ = the mass flow of air (kg/s)
- H = the flame height (m)
- ρ_a = the density of air (1.28 kg/m^3)
- (a/f) = the stoichiometric air/fuel ratio by weight, about 15 for hydrocarbons
- Ψ = the dilution factor = actual air entrained up to the end of the flame divided by the stoichiometric amount of air required.
  - Ψ = 5 for diffusion flames of hydrocarbons (Steward, 1970).
- $\dot{m}_s$ = the total burning rate of the slick (kg/s).

Given the values of (a/f) and Ψ,

(7.7) $m_{a,out} \doteq 75\, m_s$

The flame height H is proportional to the slick radius

(7.8) $H = \alpha r_s$

The proportionality factor α can be found in the literature (Becker and Liang, 1978). Combining equations (7.5), (7.6), (7.7) and (7.8) gives

(7.9) $2\pi r^2 \rho_a u_a = 75\, \dot{m}_s$

The burning rate of the slick $\dot{m}_s$ is related to the slick area. Babrauskas, 1983 indicates that for crude oil pools greater than 1 m in radius that relationship is a simple proportionality

(7.10) $m_s = \pi r_s^2 \dot{m}_s''$

where $\dot{m}_s''$ for crude oil is 0.022 to 0.045 kg/m^{2}s.

Brzustowski and Twardus, 1982 have shown that a slick burns more slowly than a pool because of the heat loss from the oil to the water underneath. This effect is particularly pronounced for slicks only slightly thicker than the minimum thickness which can burn (typically, about 1 mm). Since the present model deals with slicks which start out thick and approach the minimum thickness only when thay are about to be extinguished, the value 0.033 kg/m^2s is taken for $\dot{m}''_s$.

When equation (7.10) is plugged into (7.9) and the values for $_a$ and m_s are used, it turns ot that

$$u_a = 1/\alpha$$

With α typically of order 4 (Becker and Liang, 1978), $u_a = 0.25$ m/s.

It is thought that induced surface currents are 3 or 4% of the wind speed (Mackay, 1984). This makes the surface current u_c of order .01 m/s. Consequently, this value will be used in the calculations as an upper bound on u_s. Calculations will also be performed with $u_c = 0$, so that the effect of surface current on removal efficiency might become evident.

7.3 WORKING EQUATIONS FOR THE BURNING AND SPREADING SLICK

7.3.1 Dimensionless Spreading Equation in the GI Regime

Evaluating $\frac{dr_{s,u}}{dt}$ from equ. (7.1) and substituting in equation (7.4) gives the following equation for the spreading rate of a burning slick in the GI regime.

$$(7.11) \qquad \frac{dr_s}{dt} = 0.57\, V_s^{1/4} \left(\frac{g\Delta\rho}{\rho_w}\right)^{1/4} t^{-1/2} - u_c$$

Now define a dimensionless slick radius x by

$$(7.12) \quad r_s = V^{1/3} x$$

and a dimensionless time τ by

$$(7.13) \quad t = V^{1/6} \left(\frac{\rho_w}{g\Delta\rho}\right)^{1/2} \tau$$

In terms of these new variables, equation (7.11) reduces to

$$(7.14) \qquad \frac{dx}{d\tau} = 0.57\, \tau^{-1/2} - b$$

where $b = u_c V_s^{-1/6} \left(\frac{\rho_w}{g\Delta\rho}\right)^{1/2}$

Equation (7.14) holds only in the gravity-inertial (GI) regime. It can be integrated directly with the initial conditions $x = 0$ at $\tau = 0$ to give the result

$$(7.15) \qquad x = 1.14\, \tau^{1/2} - b\tau$$

a simple modification of equation (7.1).

The values of b depend on V_s and u_c. They are listed in Table 7.1; b is dimensionless.

TABLE 7.1

VALUES OF THE PARAMETER b

V_s, m^3	u_c, m/s: 0	u_c, m/s: 0.01
10^{-2}	0	0.01539
1	0	0.007143
10^2	0	0.003315
10^4	0	0.001539

7.3.2 Dimensionless Transition Equation

Equation (7.3) relating the time and slick radius at transition to the gravity-viscous regime of spread can also be expressed in terms of the dimensionless variables x and τ. It becomes

$$(7.16)\quad x^* = 19.41\, V^{1/8} \tau^{*\,-1/4}$$

7.3.3 Dimensionless Spreading Equation in the GV Regime

Evaluating $\frac{dr_{s,u}}{dt}$ from equation (7.2) and substituting in equation (7.4) gives the following equation for the spreading rate of a burning slick in the GV regime.

$$(7.17)\quad \frac{dr_s}{dt} = 0.245\, Vs^{1/3} \left(\frac{g^2 \Delta \rho}{\rho_w^2 \nu_w}\right)^{1/12} t^{-3/4} - u_c$$

and in terms of x and τ

$$(7.18)\quad \frac{dx}{d\tau} = 0.245\, c\tau^{-3/4} - b$$

where $c = (V_s \Delta\rho g / \rho_w \nu_w^2)^{1/24}$

With initial conditions $x = x^*$ at $\tau = \tau^*$, this can be integrated directly to

$$(7.19)\quad x = x^* + 0.980\, c\, (\tau^{1/4} - \tau^{*1/4}) - b\,(\tau - \tau^*)$$

It is convenient to define

$$(7.20)\quad A = x^* - 0.980\, c\, \tau^{*1/4} + b\tau^*$$

The values of c depend on V_s. They are listed in Table 7.2; c is dimensionless.

TABLE 7.2

VALUES OF THE PARAMETER C

V_s, m^3	c
10^{-2}	2.6844
1	3.2522
10^2	3.9401
10^4	4.7736

7.3.4 Combustion Efficiency

The basic definition of combustion efficiency is the ratio of the mass of oil burned to the mass spilled. The mass spilled is $V_s \rho_o$.

The mass burned follows from equation (7.10), i.e.:

$$\int_0^t \dot{m}_s'' \pi r_s^2 (t)\, dt$$

The removal efficiency η_{comb} is given by

$$(7.21)\quad \eta_{comb} = \frac{\pi \dot{m}_s''}{V_s \rho_o} \int_0^{t_q} r^2(t)\,dt$$

and in terms of x and τ

$$\eta_{comb} = \frac{\pi \dot{m}_s''}{\rho_o} V_s^{-1/6} \left(\frac{\rho_w}{g \Delta \rho}\right)^{1/3} \int_0^{\tau_q} x^3\,d\tau$$

With $\dot{m}_s'' = 0.033$ kg/m^{2}s, $\rho_o = 800$ kg/m^3 this reduces to

$$(7.22)\quad \eta_{comb} = 9.263 \times 10^{-5}\, V_s^{-1/6}\, I_q$$

where

$$(7.23)\quad I_q = \int_0^{\tau_q} x^2\,d\tau$$

7.3.5 Thickness of Oil Slick Remaining

The criterion for the quenching of the burning oil slick is that the thickness of the slick reaches some minimum value at which all of the heat feedback from the flame is lost to the water under the slick. The experimental value for this mininum thickness is about 0.8 mm (Energetex, 1981b).

If is the thickness of slick remaining at any time t'

$$(7.24)\quad V_s - \frac{\pi \dot{m}_s''}{\rho_o} \int_0^{t'} r^2(t)\,dt = \pi r_s^2(t')\,\delta$$

Proceeding as in 7.3.4 this can be put in the form

$$(7.25)\quad \delta = \frac{1}{\pi x^2} (V_s^{1/3} - 9.263 \times 10^{-5}\, V_s^{-1/6}\, I_q)$$

7.3.6 The Integral I

It is evident in sections 7.3.4 and 7.3.5 that the integral of x^2 over τ is an essential quantity in the calculations. Fortunately, this integral is easy to evaluate explicitly.

In the GI regime x (τ) is given by equ. (7.19). This leads to

$$(7.27)\quad {}_{GI}I(\tau) = \int_0^{\tau} x^2 d\tau = 0.6498\tau^2 - 0.9120\, b\tau^{5/2} + 0.3333\, b^2\tau^3$$

In the GV regime x (τ) is given by equ. (4.9). This leads to

$$(7.28)\quad {}_{GV}I(\tau) = \int_0^{\tau} x^2 d\tau = I^* + 0.3333\, b^2(\tau^3 - \tau^{*3}) - 0.8711\, c(\tau^{9/4} - \tau^{*9/4}) - Ab(\tau^2 - \tau^{*2}) + 0.64027\, c^2(\tau^{3/2} - \tau^{*3/2}) + 1.568\, Ac(\tau^{5/4} - \tau^{*5/4}) + A^2(\tau - \tau^*)$$

where $I^* = {}_{GI}I^*(\tau^*)$ and A is given by equation (7.20).

7.3.7 The Effect of Delayed Ignition

In practice it may not be possible to ignite the oil as soon as it is spilled. For this reason, calculations were performed with the ignition delay time τ_d as a parameter. In these calculations, $\dot{m}''_s$ and u_c were both taken to be zero until ignition occurred. This means that for $0 \leq \tau \leq \tau_d$, the slick spreads according to equation (7.1) and (7.2). All of the terms involving consumption of oil were kept at zero by defining I to be zero until τ reached τ_d. For example, if τ_d was large enough that the slick was in the GV regime where it was ignited, τ_d replaced τ^* in equ. (7.28) and I* was replaced by I_d which was zero. All the calculations to that point where made with

$u_c = 0$ (i.e.: b=0) in both the GI and GV regime. At τ_d, however, it was assumed that b took its value instantly. This implies that ignition and the establishment of the air flow and surface current (if any) was rapid.

7.4 RESULTS

7.4.1 Combustion Efficiency for Immediate Ignition

The computed values of combustion efficiency η_{comb}, as well as the burning time, t_b, and the radius of the slick at extinction, $r_{s,q}$, are listed in Table 7.3. The results are shown for two values of induced water surface current: 0 and 0.01 m/s.

TABLE 7.3

COMBUSTION EFFICIENCY, BURNING TIME AND RADIUS OF SLICK AT EXTINCTION

V_s, m^3	u_c, (m/s)	t_{burn}, (s)	$r_{s,q}$, (m)	η_{comb} (%)
10^{-2}	0	19.9	1.48	44.3
	0.01	25.9	1.35	54.0
1	0	80.7	9.78	76.2
	0.01	88.5	9.20	78.9
10^2	0	270	61.2	91.2
	0.01	277	58.8	91.2
10^4	0	860	375	95.8
	0.01	876	369	96.5

The effect of the induced current is to increase the burning time and the combustion efficiency and to decrease the size of the slick when burning ceases. The effect is minor in the case of all but the smallest spill studied.

Calculations were also attempted with a higher value of the induced surface current, u_c = 0.1 m/s. Solutions could be obtained only for the two largest spills with that value. The trend shown in Table7.3 continued in both cases.

7.4.2 Removal Efficiency with Ignition Delay

The computed values for removal efficiency are plotted in Fig. 7.2 as a function of the ignition delay τ_d. Four pairs of curves are shown, one pair for each of the following values of V_s: 10^{-2}, 1, 10^2 and 10^4 m^3.

One curve in each pair was calculated for zero surface current (u_c = 0). The other was calculated for u_c = 0.01 m/s. In each case the removal efficiency decreases from a maximum value at the smallest delay. The values shown for τ_d = 10 are for all intents and purposes the same as those for zero delay.

In the case of zero surface current, the curves of η_{comb} approach zero continuously. With u_c = 0.01 m/s, the curves were very similar to those for u_c = 0 but only up to a point. At a certain value of τ_d, the equations could no longer be solved. The slick thickness began to increase, the slick radius decreased, and the burning rate began to decrease drastically. This behaviour occurred for all higher values of τ_d.

We will identify the threshold value of τ_d as the maximum possible delay in igniting the slick. If ignition is delayed any longer, burning may be ineffective. The values of the maximum ignition delay are listed in Table 7.4. Also included are x_q and η_{comb} for the maximum delay.

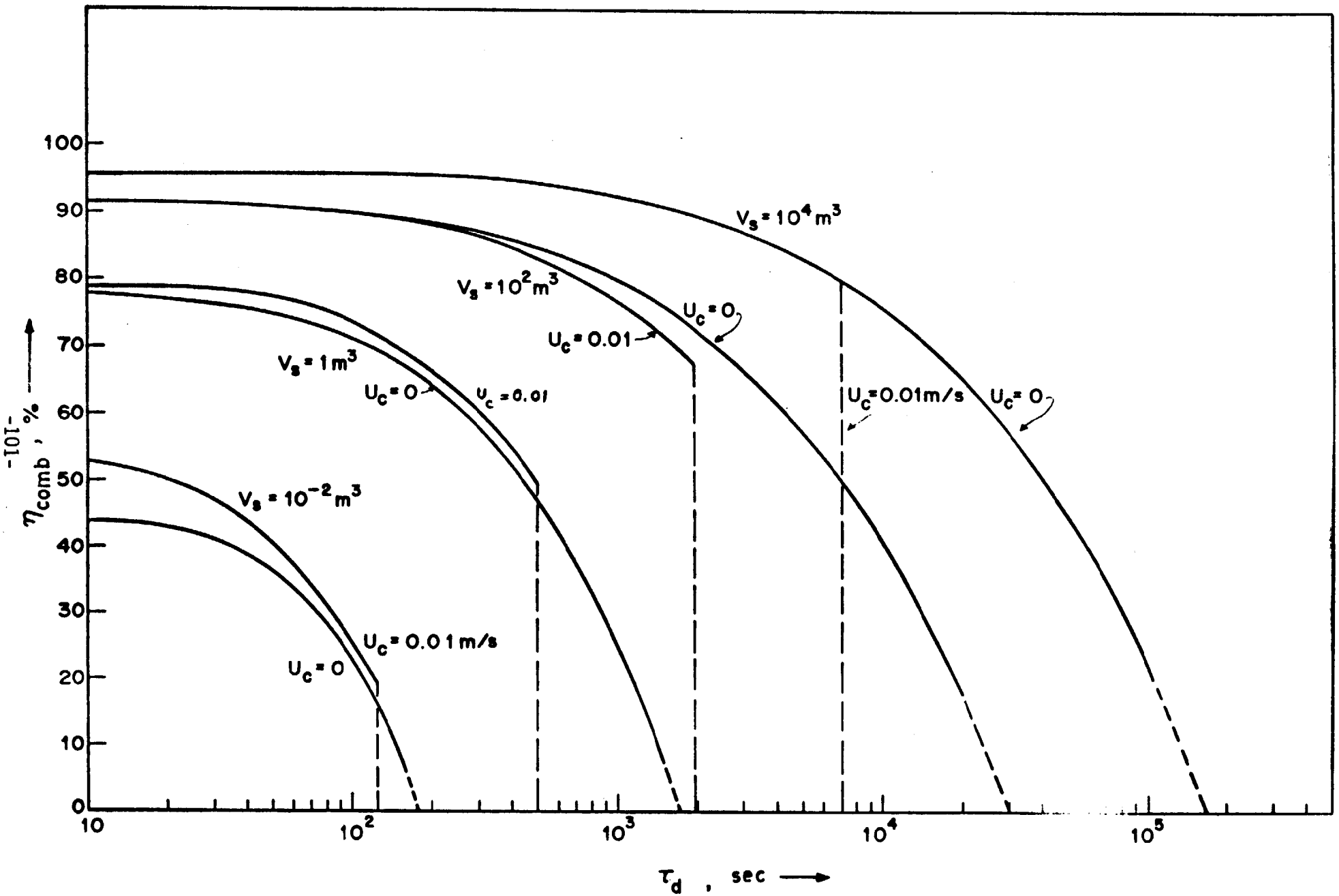

FIGURE 7.2 — COMBUSTION EFFICIENCY AS A FUNCTION OF IGNITION DELAY

TABLE 7.4

MAXIMUM IGNITION DELAY $\tau_{d,max}$
AND CORRESPONDING τ_q, X_q AND η_{comb}

V_s, m^3	$\tau_{d,max}$	τ_q	at $\tau_{d,max}$ X_q	η_{comb},(%)
10^{-2}	125	190	8.322	19.3
1	500	665	14.127	49.8
10^2	1,950	2,312	24.392	68.0
10^4	7,150	7,830	41.555	79.8

The maximum permissible ignition delay can be correlated with spill size. An excellent correlation is obtained in the form of a power law. In dimensional form it can be expressed as

(7.29) $$t_{d,max} = 0.0975\ V^{0.46}$$

where $t_{d,max}$ = maximum permissible delay time between the occurrence of the spill and its ignition; (hours)

V_s = spill volume; (m^3).

Equation (7.29) is plotted in Fig. 7.3.

A rough but useful approximation to equation (7.29) is

(7.30) $t_{d,max}$ (hours) = 1/10 $V_s^{1/2}$ (m^3)

which quickly gives the order of magnitude of the maximum delay.

The delayed ignition of a spreading slick is accomplished by placing igniters around its perimeter. The flame spreads outwards with the burning oil. The flame's inward spread is aided by the inward wind induced by the flames at the periphery.

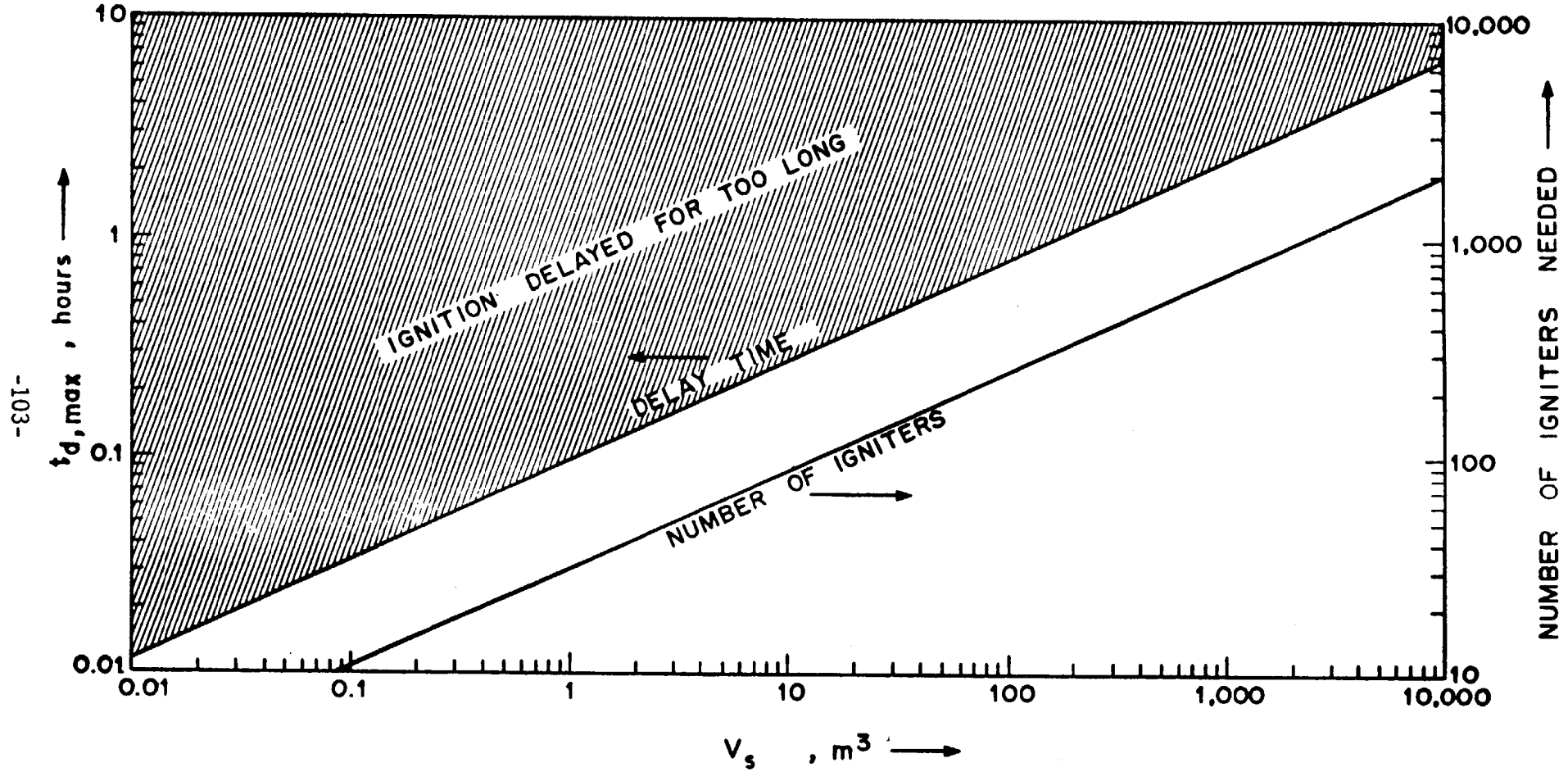

FIGURE 7.3 — MAXIMUM PERMISSIBLE IGNITION DELAY TIME AND THE NUMBER OF IGNITERS REQUIRED AT THAT TIME AS A FUNCTION OF SPILL VOLUME

As an example, igniters can be placed 3 m apart around the perimeter of the slick. The slick radius at $t_{d,max}$ is one of the results of the calculations. Therefore, the number of igniters needed to achieve ignition with the maximum permissible delay can be calculated. The results are presented in Table 7.5.

TABLE 7.5

EXAMPLE NUMBER OF IGNITERS NEEDED AT THE MAXIMUM IGNITION DELAY

V_s, (m^3)	Number Needed
10^{-2}	4
1	30
10^2	238
10^4	1,875

These results are also well correlated by a power law.

(7.31) $N = 31\ V^{0.45}$

Equation (7.31) is also shown in Fig. 7.3. The difference between the power of V_s in equation (7.29) and (7.31) cannot be significant. On that basis, the number of igniters needed to burn the slick after the maximum delay is proportional to that delay. The proportionality is about 320 igniters per hour. However to avoid confusion and keep the dependence on spill size in mind, it is preferable to use Fig. 7.3 to calculate both the maximum permissible delay and the number of igniters then required.

Additional results are presented in Appendix 4. They include the scaling factors for time and slick radius, as well as the parameters of the slicks whose behaviour was calculated.

7.5. SUMMARY

The calculations show clearly that the removal efficiency, for low viscosity, volatile crude oil, increases with increasing spill volume. The maximum value is 96.5% for a spill of 10^4 m^3 ignited immediately. At a certain delay time, different for each size of spill, the removal efficiency of the spill decreases sharply, and the possibility of burning any significant fraction of the spilled oil becomes uncertain.

These critical delay times can be approximated by a simple expression which can then be used to predict the critical ignition delay time for spills of any size. That expression is:

$$\text{delay time (hours)} = 0.1\ V_s^{1/2},\ V_s \text{ in } m^3$$

This means that a spill of 10^4 m^3 can still be ignited 10 hours after it occurs, but a spill of 1 m^3 must be ignited in 6 minutes.

Delayed ignition of a spill can be achieved by deploying igniters around the periphery. Experimental data indicate that there could be one igniter for every three metres of slick periphery. Combining this number with the radius of the slick at the critical ignition delay time gives an example of the number of igniters required to achieve ignition at the latest possible time: 30 are required for a spill of $1 m^3$, 238 for 10^2 m^3, and 1,875 for a spill of 10^4 m^3.

The model presented here gives an indication of the effects of scale, particularly of the spill volume, on the efficiency with which the spilled oil can be removed by combustion. The burning of a spreading oil slick is modelled sufficiently to predict major trends; however, the model is not likely to be accurate in its detailed predictions, and should be calibrated against experimental data from further experiments to elucidate the relationships between several parameters in pool fires.

It is evident that large spills can be burned more efficiently than small ones. It is also clear that one can delay ignition only for a limited time. When that time is exceeded, ignition is pointless because the slick is so thin that little of it can burn in any case. The model predicts the relationship between spill volume and maximum permissible ignition delay. The trend is probably accurate, but one should use the numbers with caution.

The proportionality between the maximum permissible ignition delay and the number of igniters required at that time seems reasonable, as does the proportionality constant which comes from experience.

There is no doubt that a model of this sort adds to the understanding of what is a very complicated process. It also provides an aid to its own calibration, since its major results can be tested. Such a calibration should be undertaken, both to test the basic assumptions of the model and to determine the importance of effects such as wind and waves which are too complex to have been included.

8.0 CONCLUSIONS AND RECOMMENDATIONS

8.1 CONCLUSIONS

* The ignition and burning of uncontained batch oil spills seems to be a feasible countermeasure for certain open water spills in remote areas.

* Combustion efficiency is primarily a function of spill volume; the larger the spill the higher the removal efficiency (about 90% for spills greater than 1 m^3 ignited instantaneously).

* The sooner a slick is ignited the higher the combution efficiency. The maximum permissible ignition delay for low viscosity, volatile crude oils can be estimated by:

  $t_{d,max} = 0.1\ V_s^{1/2}$, $t_{d,\ max}$ in hours, V_s in m^3.

* Ignition of the periphery of the slick results in almost as high removal efficiencies as ignition of the entire surface area. The required number of conventional igniters, spaced 3 m apart, at the maximum ignition delay can be estimated by:

  $N = 31\ V_s^{0.45}$, V_s in m^3

* Air, entrained by the combustion of the oil slick at a velocity of about 0.2 m/s, induces an inward surface current which inhibits and finally stops the oil's spread. The slick thickness at which this occurs is related to the size of the slick and can be estimated by:

  $h\ (m) = 7 \times 10^{-4}\ r^{1/2}$, h and r in m

* Flames spread downwind over oil at a rate proportional to the wind speed and controlled by the volatility of the oil at ambient temperature. The maximum measured flame velocity was 17 cm/s for a slightly aged crude oil in a 3.5 m/s wind. Upwind flame spreading is only a weak function of wind speed and is generally 1-3 cm/s.

* For the crude oils tested, the flames spread as rapidly as the oil spread. Only in the case of diesel fuel at low (less than 1m/s) wind speeds did the flames not keep up with the oil.

* Oil slick combustion rates are independent of slick thickness and area for slicks greater than 5 mm thick and 2 m in diameter. Below these critical values, combustion rate decreases with both thickness and area. Above these critical values, the slick regression rate is 2 to 2.5 mm/min.

* The higher the oil viscosity, the slower the slick spreads. This effect seems to be related to oil viscosity at the oil/water interface since a burning oil spreads at the same rate as does the cold oil. Poor heat transfer through the oil and heat losses to the metal trough may explain this phenomenon.

8.2 RECOMMENDATIONS

* Further small and mid-scale pool burning tests are required to more fully understand the relationships between oil type, regression rate, slick size and air entrainment.

* Field trials involving larger oil volumes (10 to 100 m^3) are required to:

    - assess the effect of longer ignition delay times than are possible with smaller spills,

- determine the effects of waves and ocean turbulence on the burning, and
- further calibrate the mathematical models.

* The use of spills of opportunity should also be considered to assess the above effects.

* A technique should be developed for effectively deploying commercially-available igniters around a slick; also the development should be undertaken of a new igniter that moves relatively from the centre to the periphery of a slick.

9.0 REFERENCES

Babrauskas, V. 1983. Estimating Large Pool Fire Burning Rates. Fire Technology. 19. No. 4. pp. 251-261. Nov.

Becker, H.A. and D. Liang. 1978. Visible Length of Verticle Free Turbulent Diffusion Flames, Combustion and Flame. 32. No. 2. pp. 115-137.

Brzustowski, T.A. and E.M. Twardus. 1982. A Study of the Burning of a Slick of Crude Oil on Water. Nineteenth Symposium (International) on Combustion, The Combustion Institute. pp. 847-854.

Buist, I.A., W.M. Pistruzak, S.G. Potter, N. Vanderkooy and I.R. McAllister. 1983. The Development and Testing of a Fireproof Boom. Proceedings of the 1983 Oil Spill Conference. San Antonio, Texas. pp. 43-52.

Butler, J.N. 1978. Marine Pollution. How Big a Problem? Conference on Oil Tanker Transportation. U.S. Department of Transportation Report No. PS-806000-DOT.

DNV (Det Norske Veritas, Ship Division). 1979. Tanker Oil Spill Analysis Study. Report to Canadian Marine Drilling Limited. Calgary.

Dickins, D.F. and I.A. Buist. 1981. Oil and Gas Under Sea Ice Study. Report to the Canadian Offshore Oil Spill Research Association (COOSRA). Calgary.

Energetex Engineering. 1981a. Burning of Crude Oil Under Wind Herding Conditions. Report to the Canadian Offshore Oil Spill Research Associates (COOSRA). Calgary.

Energetex Engineering. 1981b. A Study to Evaluate the Combustibility and Other Physical and Chemical Properties of Aged Oils and Emulsions. Environment Canada Report EE-5. Ottawa.

Fay, J.A. 1969. The Spread of Oil Slicks on a Calm Sea. Massachusetts Institute of Technology. Boston.

Fannelop, T.K. and G.D. Waldman. 1971. Dynamics of Oil Slicks. AIAA Journal Vol. 10. No. 4.

Goodier, J.L. nd R.J. Siclari, 1981. Combustion: An Oil Spill Mitigation Tool. Phase II - The Burning of the MT Burmah Agate. U.S. Department of Energy Report DOE/TIC-11471. Washington, D.C.

Hidy, G.M. and E.J. Plate. 1966. Wind Action on Water Standing in a Laboratory Channel. J. Fluid Mech. 26 (4). pp 651-687.

Horn, S.A. and P. Neal. 1981. The Atlantic Empress Sinking - A Large Spill Without Environmental Disaster. Proceedings of the 1981 Oil Spill Conference. Atlanta, GA.

IMO (International Maritime Organization). 1981. IMO News Magazine. No. 4.

Mackay, D.M. 1984. The Fate and Behaviour of Oil in Cold Climates. Report to Environment Canada. Ottawa. EE - 74

MacKinven, R., J.G. Ansel and I. Glassman. 1969. Influence of Laboratory Parameters on Flame Spread Across Liquid Fuels. Combustion Science and Technology. Vol. 1.

McAllister, I.R. and I.A. Buist. 1981 Dome Petroleum's Fireproof Boom-Development and Testing to Date. Proceedings of the Fourth Arctic Marine Oilspill Program Technical Seminar. Edmonton. pp. 479-498.

McCaffrey, B.J. 1976. A Robust Bidirectional Low-Velocity Probe for Flame and Fire Application. Combustion and Flame. 25. pp. 125-127.

McCaffrey, B.J. 1983. Momentum Implications for Buoyant Diffusion Flames. Combustion and Flame. 52. pp. 149-167.

Meikle, K.M. 1983. An Effective Low Cost Fireproof Boom. Proceedings of the 1983 Oil Spill Conference. San Antonio, Texas. pp. 39-42.

NORCOR. 1975. The Interaction of Crude Oil with Arctic Sea Ice. Beaufort Sea Project Report No. 27. Institute of Ocean Sciences. Sidney, B.C.

OSIR (Oil Spill Intelligence Report). 1981. The Oil Spill Experts Guide to Prevention, Law, Research and Cleanup. Vol. IV. No. 40. Cahners Publishing Boston. pp. 26-31.

Sirigano, W.A. and I. Glassman. 1970. Flame Spreading Above Liquid Fuels: Surface-Tension Driven Flows. Combustion Science and Technology. 1. pp. 307-312.

S.L. Ross Environmental Research Limited. 1981. The Use of Aerially Deployed Igniters for an Oil Blowout in the Southern Beaufort Sea. Report to Dome Petroleum Limited. Calgary.

S.L. Ross Environmental Research Limited. 1982a. Oil Spill Countermeasures for a Major Spill from a Vessel in Arctic Waters. Environment Canada Report EPS 3-EC-83-2. Ottawa.

S.L. Ross Environmental Research Limited. 1982b. Potential Large Oil Spills Offshore Canada and Possible Response Strategies. Report to Environmental Canada. Ottawa.

S.L. Ross Environmental Research Limited. 1983. A Study of On-Board Self-Helf Oil Spill Countermeasures for Arctic Tankers. Report to Environment Canada. Ottawa.

Steward, F.R. 1970. Prediction of the Height of Turbulent Diffusion Buoyant Flames. Combustion Science and Technology. 2. No. 4. pp. 203-212.

Tebeau, P.A., T.M. Meehan and S.A. Saspoff. 1984. A Laboratory Study of Oil Spreading Under Arctic Conditions. Draft Report for the U.S. Coast Guard R&D Centre. Groton, Conn.

Thompson, C.H., G.W. Dawson and J.L. Goodier. 1979. Combustion: An Oil Spill Mitigation Tol. U.S. Department of Energy Report EV-1830-1. Washington, D.C.

Wakamiya, W., S.E. Petty, A.Boiarski and A. Putnam. 1982. Combustion of Oil on Water: An Experimental Program. U.S. Department of Energy. Washington, D.C.

APPENDICIES

APPENDIX I

WIND TUNNEL VELOCITY PROFILES

see Figures A.1.1 and A.1.2 for velocity contours.

From Hidy and Plate (1966)

$$V/V^* = (1/k) \ln (Z/Z_o)$$

where
- V = wind velocity (m/s)
- V^* = friction velocity (m/s)
- K = Karmen constant
- Z = height above water (cm or m)
- Z_o = roughness height (cm or m)

in wind tunnels, over water

$$V^* = (3.41 \times 10^{-4} V)^{1/2} V$$

V(m/s)	V*(m/s)
0.9	0.016
3.6	0.126
9.3	0.524

see Figure A.1.3 for experimental values of Z_o.

scaling to an equivalent 10m wind speed

wind tunnel $V_{0.1}$	V*	Z0	V10m
0.9	0.016	$8.2 \times 10^{-1-}$	1.1 m/s
3.6	0.126	1×10^{-4}	5.1 m/s
9.3	0.524	8.2×10^{-3}	15.3 m/s

see Figure A.1.4 for relationship between $V_{0.1}$ and V_{10}.

46 0780

FIGURE A.1.1 WIND TUNNEL DOWNWIND CENTRELINE VELOCITY CONTOURS

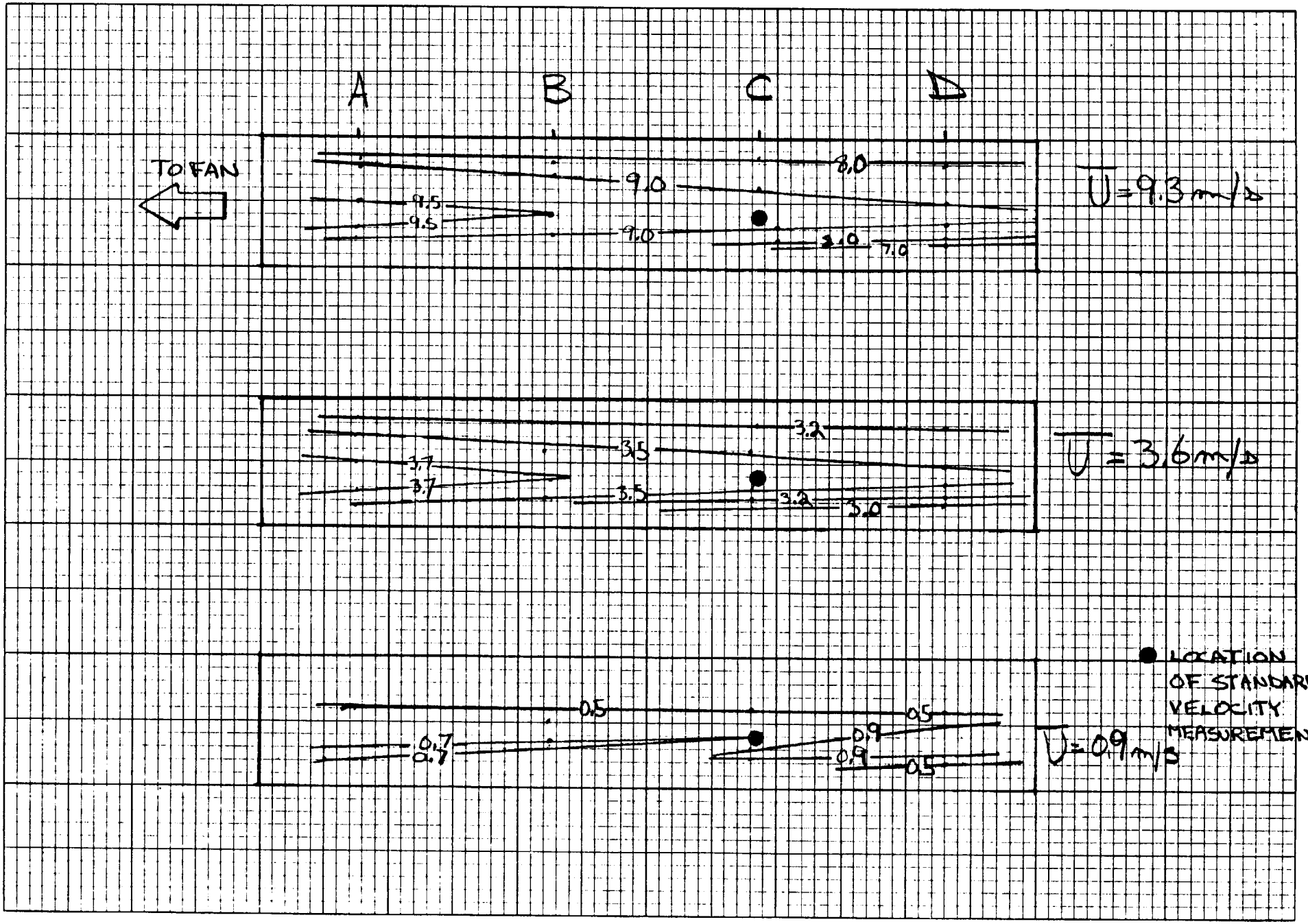

FIGURE A.1.2 WIND TUNNEL CROSSWIND VELOCITY CONTOURS

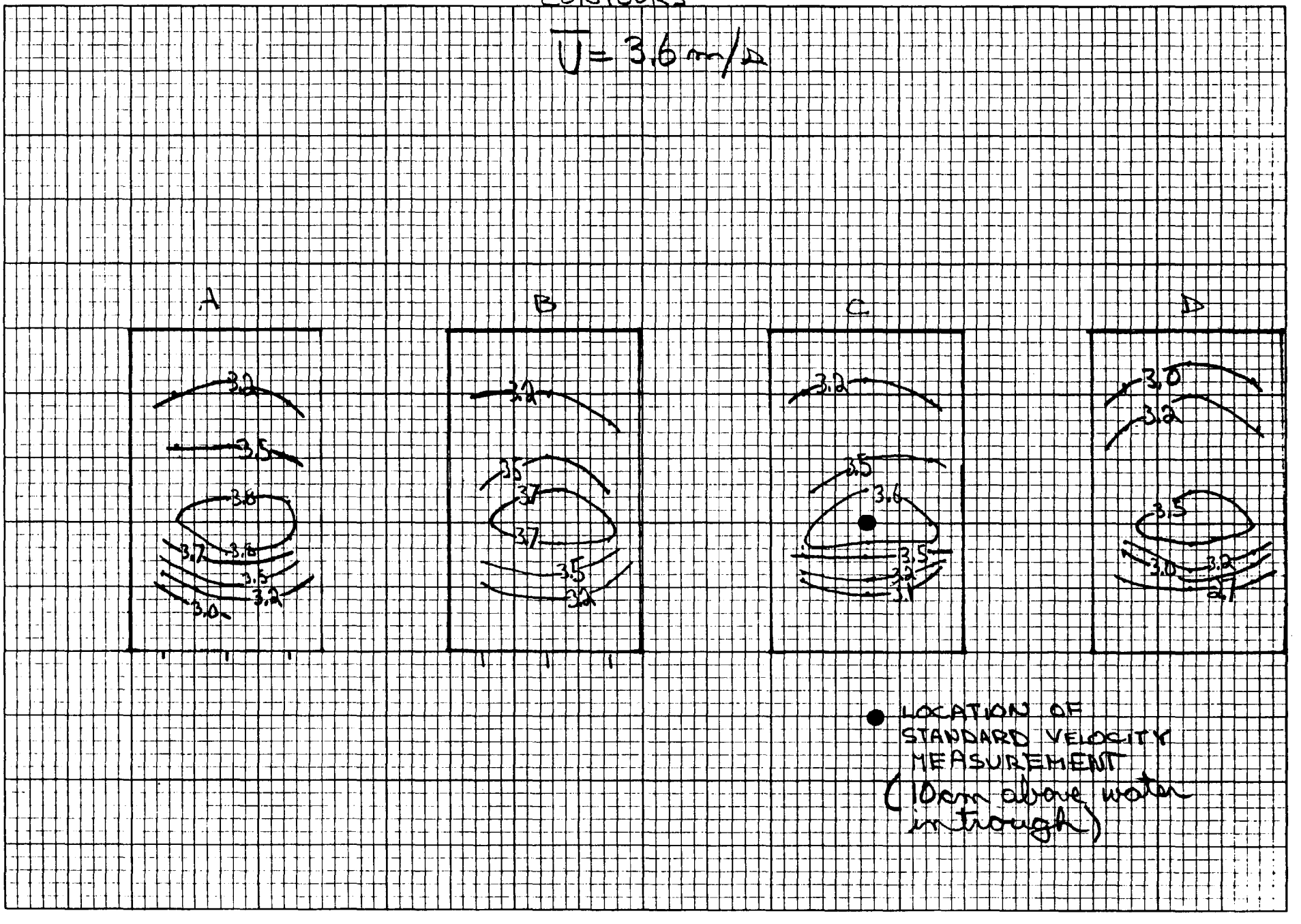

FIGURE A.13 - WIND TUNNEL VELOCITY PROFILES

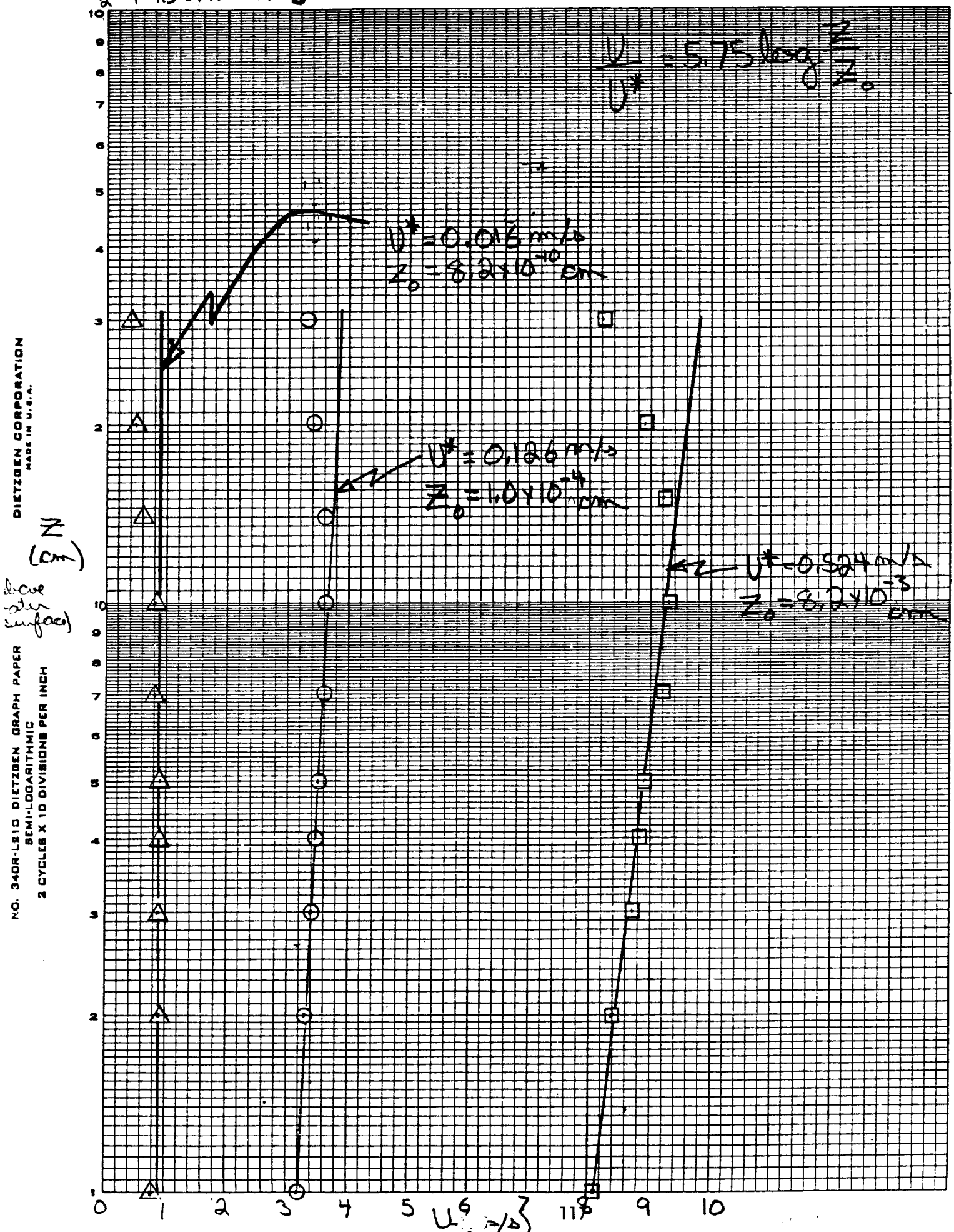

DIETZGEN CORPORATION MADE IN U.S.A.

NO. 340R-L21C DIETZGEN GRAPH PAPER SEMI-LOGARITHMIC 2 CYCLES X 10 DIVISIONS PER INCH

FIGURE A.1.4 - WIND TUNNEL VELOCITY SCALING

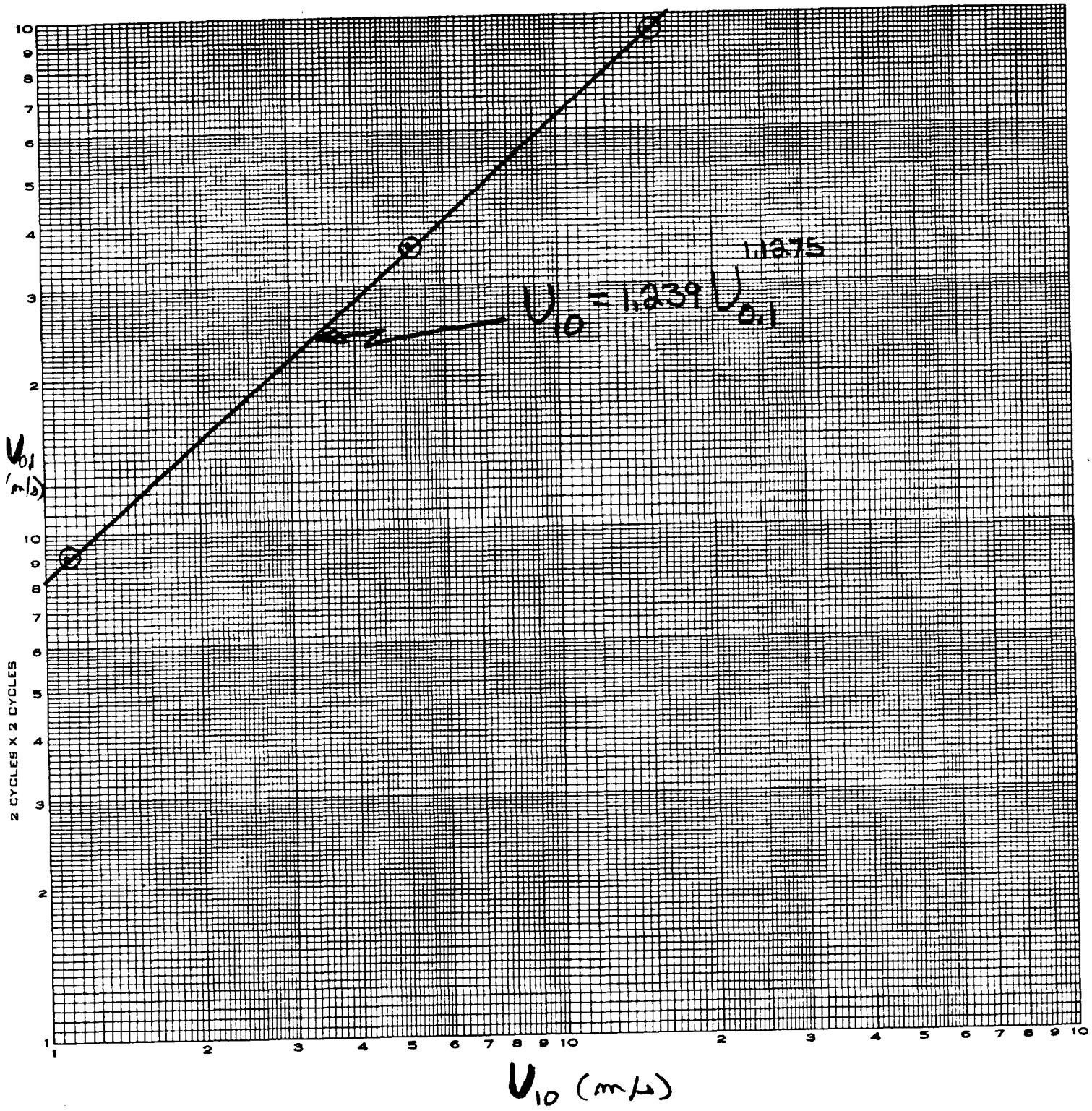

APPENDIX 2

SMALL-SCALE TESTING RAW DATA

TABLE A.2.1

TEST CONDITIONS

RUN NO.	OIL VOLUME(ml)	OIL TYPE	AIR TEMP(°C)	WATER TEMP(°C)	WIND SPEED(m/s)
Oil Spreading					
1	600	1 HR	12	12	0
2	"	"	13	13	0.6
3	"	"	14	14	3.8
4	"	"	14	14	8.0
5	"	"	14	12	-0.6
6	"	"	14	12	-3.8
7	"	4 HR	12	13	0
8	"	"	14	13	0.7
9	"	"	13	13	3.7
10	"	"	13	12	8.4
11	"	8 HR	15	12	0
12	"	"	15	13	0.7
13	"	"	13	12	3.4
14	"	"	14	13	8.4
15	"	DIESEL	14	12	0
16	"	"	14	12	8.4
17	"	"	15	11	3.4
18	"	"	15	12	0.6
19	"	"	15	12	-0.8
20	"	"	15	13	-3.4
21	"	1 HRin 35% saltwater	15	13	0
22	"	4 HR emulsion	15	13	0

RUN NO.	OIL VOLUME(ml)	OIL TYPE	AIR TEMP(°C)	WATER TEMP(°C)	WIND SPEED(m/s)
Flame Spreading					
23	1000	1 HR	15	13	0.5
24	"	"	13	13	2.4
26	"	"	14	13	1.5
27	"	"	12	12	3.5
27R	"	"	14	13	3.5
28	500	"	13	13	-0.2
28R	"	"	14	14	-0.2
29	"	"	14	13	-0.4
29R	"	"	14	13	-0.4
30	"	"	10	11	-1.1
31	"	"	13	12	-2.4
32	600	4 HR	11	10	3.1
33	"	"	10	10	1.6
34	"	"	10	10	0.53
35	"	"	13	11	-1.2
36	"	8 HR	12	10	3.1
37	"	"	12	10	1.45
38	"	"	10	10	0.6
39	"	"	14	10	-1.1
40	"	DIESEL	16	10	3.4
41	"	"	12	10	1.6
42	"	"	12	11	0.58
43	"	"	11	10	-1.0
Oil and Flame Spreading					
44	600	DIESEL	12	11	1.25
45	"	1 HR	11	11	1.2
46	"	4 HR	12	9	1.2
47	"	"	12	10	0.5
48	"	8 HR	12	9	1.25
49	"	"	11	9	0.6
50	"	1 HR	10	8	0.55
51	"	"	10	9	0.25
52	"	4 HR	11	9	0.25
53	"	8 HR	13	10	0.28
54	"	EMULSION	12	10	1.1
55	"	DIESEL	11	11	0.52
56	"	"	11	10	0.25
Flame Spreading					
57	600	8 HR	16	1	1.45
58	"	"	16	19	1.50
59	"	"	11	8	1.45

TABLE A.2.1
OIL SPREADING - RAW DATA

TIME TO REACH LENGTH (s)

RUN#	Length down trough (cm) 30	40	50	60	70	80	90	100	110	120	130	140	150	160	170	180	190	200	210	220
1	0.0	0.0	0.0	0.0	0.0	5.1	6.2	7.6	9.0	10.5	12.0	13.5	15.4	17.6	20.3	23.7	28.3	36.0	0.0	0.0
2	0.0	0.0	1.1	2.4	3.7	4.7	5.9	7.2	8.5	9.8	11.2	12.5	14.1	15.9	18.0	20.6	24.0	28.5	0.0	0.0
3	0.0	0.0	.9	1.5	2.3	2.9	3.6	4.4	5.1	5.9	6.6	7.3	8.1	8.8	9.8	10.9	12.5	13.9	15.0	16.7
4	0.0	0.0	.9	1.6	2.5	3.0	3.5	4.0	4.4	4.9	5.3	5.7	6.1	6.6	7.0	7.4	7.7	8.2	8.5	8.9
5	0.0	.8	1.9	3.2	4.4	5.9	7.5	9.0	10.8	12.8	14.9	18.0	23.1	0.0	0.0	0.0	0.0	0.0	0.0	0.0
6	0.0	0.0	2.0	3.9	6.1	8.3	10.6	13.7	18.8	0.0	0.0	0.0	0.0	0.0	0.0	0.0	0.0	0.0	0.0	0.0
7	0.0	0.0	.9	2.1	3.6	4.9	6.3	7.9	9.5	11.1	12.6	14.7	17.6	21.6	25.9	35.5	0.0	0.0	0.0	0.0
8	0.0	0.0	1.3	2.5	3.7	4.9	6.2	7.6	8.9	10.2	11.5	13.1	14.9	17.1	19.5	22.0	25.3	29.7	37.9	0.0
9	0.0	0.0	.6	1.3	2.2	2.9	3.9	5.0	6.1	7.3	8.4	9.6	10.7	11.8	13.1	14.1	15.2	16.4	17.6	18.9
10	0.0	0.0	.7	1.1	0.0	2.1	2.5	2.9	3.4	3.8	0.0	0.0	0.0	0.0	0.0	0.0	0.0	0.0	0.0	8.9
11	0.0	0.0	0.0	3.0	4.5	5.8	7.3	9.1	10.7	12.4	14.8	17.6	21.5	26.9	36.9	0.0	0.0	0.0	0.0	0.0
12	0.0	.4	1.3	2.8	4.2	5.5	7.2	8.8	10.6	12.3	14.8	18.0	23.2	34.9	0.0	0.0	0.0	0.0	0.0	0.0
13	0.0	0.0	.8	1.6	2.7	3.9	5.2	6.4	7.7	8.8	10.0	11.4	12.5	13.7	15.0	16.4	17.9	19.5	21.2	23.2
14	0.0	0.0	.6	.9	1.6	2.0	2.4	2.8	3.2	3.5	3.9	4.3	4.7	5.1	5.5	5.8	6.2	0.0	0.0	0.0
15	0.0	.3	.9	1.9	3.0	4.0	5.1	6.2	7.3	8.6	9.7	10.9	12.1	13.4	14.8	16.5	18.6	20.9	23.5	26.7
16	0.0	.2	.7	1.2	2.0	2.5	2.9	3.4	3.9	4.3	4.7	5.1	5.7	6.0	6.5	6.8	7.2	7.6	8.1	8.6
17	0.0	.3	.8	1.6	2.5	3.4	4.3	5.2	6.1	7.1	8.1	9.0	10.0	11.1	12.1	13.0	14.0	15.2	16.2	17.5
18	0.0	.4	.9	1.9	3.1	4.1	5.1	6.2	7.4	8.7	9.7	11.1	12.3	13.6	15.2	17.0	19.4	22.3	25.9	32.7
19	0.0	0.0	1.3	2.8	3.9	5.3	6.7	8.1	9.5	11.0	12.6	15.1	0.0	0.0	0.0	0.0	0.0	0.0	0.0	0.0
20	0.0	.6	1.6	3.0	4.2	5.7	7.2	8.7	10.3	12.0	15.3	0.0	0.0	0.0	0.0	0.0	0.0	0.0	0.0	0.0
21	0.0	0.0	.9	2.1	3.4	4.5	5.6	6.7	7.9	9.0	10.2	11.3	12.6	14.1	15.6	17.4	19.3	21.5	23.9	27.6
22	0.0	0.0	0.0	0.0	0.0	0.0	0.0	0.0	0.0	0.0	0.0	0.0	0.0	0.0	0.0	0.0	0.0	0.0	0.0	0.0

TABLE A.2.2 FLAME SPREADING

Time to Ignition Length (s)

Length down trough (cm)

Run #	10	20	30	40	50	60	70	80	90	100	110	120	130	150	170	190	210	230	250	270
23	0.0	0.0	0.0	3.3	5.2	6.7	12.0	15.6	17.7	23.1	27.1	30.2	34.5	41.3	46.0	0.0	0.0	0.0	0.0	0.0
24	0.0	0.0	0.0	.2	.6	2.5	3.4	4.8	4.9	5.2	0.0	0.0	0.0	0.0	0.0	0.0	0.0	0.0	16.6	0.0
26	0.0	0.0	0.0	0.0	.4	.9	2.8	3.8	4.4	5.4	6.2	6.9	8.0	10.6	12.8	14.1	15.8	17.9	19.6	0.0
27	0.0	0.0	0.0	0.0	0.0	0.0	0.0	0.0	0.0	0.0	0.0	0.0	0.0	0.0	0.0	0.0	0.0	0.0	0.0	0.0
27R	0.0	0.0	0.0	.5	2.0	2.7	3.3	4.3	5.3	6.1	6.4	7.1	7.4	0.0	0.0	0.0	12.8	0.0	0.0	14.5
28	0.0	.1	.2	.3	.3	.4	.5	0.0	0.0	0.0	0.0	0.0	0.0	0.0	0.0	0.0	0.0	0.0	0.0	0.0
28R	0.0	13.2	24.0	32.4	42.4	50.2	57.5	64.7	0.0	0.0	0.0	0.0	0.0	0.0	0.0	0.0	0.0	0.0	0.0	0.0
29	0.0	.2	.3	.4	.5	.6	.6	0.0	0.0	0.0	0.0	0.0	0.0	0.0	0.0	0.0	0.0	0.0	0.0	0.0
29R	0.0	4.6	9.8	14.6	19.9	23.6	29.0	34.5	40.6	47.0	0.0	0.0	0.0	0.0	0.0	0.0	0.0	0.0	0.0	0.0
30	0.0	9.9	18.7	27.0	33.3	39.6	45.1	50.7	59.4	0.0	0.0	0.0	0.0	0.0	0.0	0.0	0.0	0.0	0.0	0.0
31	0.0	4.7	20.5	29.6	36.4	42.4	48.8	53.6	59.5	0.0	0.0	0.0	0.0	0.0	0.0	0.0	0.0	0.0	0.0	0.0
32	0.0	0.0	.7	3.3	4.6	6.8	8.5	9.8	10.8	11.7	12.8	13.8	14.9	17.1	19.4	20.9	22.7	24.5	26.9	28.9
33	0.0	0.0	3.6	5.9	8.3	9.9	13.1	15.2	17.1	18.4	19.5	21.7	23.7	27.3	31.1	35.0	38.1	42.1	47.2	51.3
34	0.0	0.0	0.0	3.3	5.6	8.9	12.4	17.4	20.9	26.1	29.4	33.7	37.7	46.5	54.4	62.6	0.0	0.0	0.0	0.0
35	0.0	11.2	30.1	42.6	56.2	68.3	75.3	83.6	96.3	0.0	0.0	0.0	0.0	0.0	0.0	0.0	0.0	0.0	0.0	0.0
36	0.0	0.0	0.0	2.6	5.2	7.1	8.6	10.8	12.2	13.5	14.9	16.1	17.2	19.6	0.0	0.0	0.0	0.0	0.0	0.0
37	0.0	0.0	2.6	5.6	0.0	0.0	12.5	15.2	17.7	19.7	0.0	22.5	25.4	28.4	32.1	36.0	40.0	0.0	49.4	0.0
38	0.0	0.0	6.0	10.6	14.5	0.0	23.2	27.5	30.9	36.2	38.4	40.7	43.4	48.8	56.5	63.4	0.0	0.0	0.0	0.0
39	0.0	17.1	34.6	53.4	69.7	0.0	0.0	0.0	0.0	0.0	0.0	0.0	0.0	0.0	0.0	0.0	0.0	0.0	0.0	0.0
40	0.0	0.0	1.7	3.7	7.6	0.0	12.2	15.5	16.8	19.3	20.5	21.6	23.6	0.0	0.0	0.0	0.0	39.6	46.2	0.0
41	0.0	0.0	4.9	7.9	11.7	15.7	20.5	25.3	29.3	31.8	34.2	38.4	41.4	49.0	57.5	62.0	0.0	0.0	0.0	0.0

TABLE A.2.2 cont'd

42	0.0	19.8	22.9	28.9	31.1	0.0	39.4	48.4	56.7	60.8	65.1	0.0	72.6	0.0	0.0	0.0	0.0	0.0	0.0	0.0
43	0.0	16.8	30.1	46.8	66.3	0.0	0.0	0.0	0.0	0.0	0.0	0.0	0.0	0.0	0.0	0.0	0.0	0.0	0.0	0.0
57	0.0	0.0	1.9	6.8	9.2	10.7	13.7	16.3	18.8	21.9	24.8	26.3	30.0	36.4	0.0	45.4	0.0	0.0	0.0	0.0
58	0.0	0.0	2.8	5.3	8.5	0.0	12.4	14.3	16.9	19.7	20.9	22.1	23.5	27.0	0.0	32.4	36.7	0.0	0.0	0.0
59	0.0	0.0	5.3	8.2	10.7	13.0	16.5	0.0	21.2	23.4	26.1	28.6	30.3	36.7	0.0	45.4	52.0	0.0	0.0	0.0

TABLE A.3.3 — OIL & FLAME SPREADING

TIME TO REACH LENGTH (s) Top Row - Oil, Bottom Row - Flame

Length down trough (cm)

RUN #	10	20	30	40	50	60	70	80	90	100	110	120	130	150	170	190	210	230	250	270
44	0.0	0.0	0.0	0.0	0.0	0.0	0.0	0.0	0.0	0.0	0.0	0.0	0.0	0.0	0.0	0.0	0.0	0.0	0.0	0.0
	0.0	0.0	0.0	0.0	1.5	0.0	2.8	4.9	0.0	7.3	10.2	14.8	16.8	22.9	31.7	36.5	0.0	0.0	0.0	0.0
45	0.0	0.0	0.0	0.0	0.0	0.0	0.0	0.0	0.0	0.0	0.0	0.0	0.0	0.0	0.0	0.0	0.0	0.0	0.0	0.0
	0.0	0.0	0.0	0.0	0.0	0.0	1.1	2.7	4.1	0.0	0.0	5.8	0.0	9.3	12.6	0.0	0.0	0.0	0.0	0.0
46	0.0	0.0	0.0	0.0	0.0	0.0	0.0	0.0	0.0	0.0	0.0	0.0	0.0	0.0	0.0	0.0	0.0	0.0	0.0	0.0
	0.0	0.0	0.0	0.0	0.0	0.0	0.0	2.8	0.0	4.3	0.0	0.0	7.3	10.9	0.0	0.0	20.0	22.8	0.0	0.0
47	0.0	0.0	0.0	0.0	0.0	0.0	2.0	3.1	4.0	5.2	6.4	7.4	8.7	11.3	14.4	17.5	23.2	0.0	0.0	0.0
	0.0	0.0	0.0	0.0	0.0	0.0	2.6	3.3	4.5	5.7	6.9	8.0	9.2	11.7	14.7	18.5	24.2	0.0	0.0	0.0
48	0.0	0.0	0.0	0.0	0.0	0.0	0.0	0.0	0.0	0.0	0.0	0.0	0.0	0.0	0.0	0.0	0.0	0.0	0.0	0.0
	0.0	0.0	0.0	0.0	0.0	0.0	1.5	0.0	4.3	0.0	6.3	0.0	8.5	10.4	13.0	15.9	19.5	0.0	0.0	0.0
49	0.0	0.0	0.0	0.0	0.0	0.0	2.2	2.9	4.1	5.5	6.5	7.9	9.5	21.3	15.7	0.0	0.0	0.0	0.0	0.0
	0.0	0.0	0.0	0.0	0.0	1.6	2.4	3.4	4.9	6.1	7.2	8.6	9.9	13.2	0.0	0.0	0.0	0.0	0.0	0.0
50	0.0	0.0	0.0	0.0	0.0	0.0	0.0	0.0	4.2	5.5	6.5	7.7	9.0	11.6	14.2	18.1	0.0	0.0	0.0	0.0
	0.0	0.0	0.0	0.0	0.0	0.0	0.0	0.0	4.2	5.5	6.5	7.7	9.0	11.6	14.7	19.1	0.0	0.0	0.0	0.0
51	0.0	0.0	0.0	0.0	0.0	0.0	0.0	0.0	4.9	6.0	0.0	8.5	10.0	12.9	16.3	19.7	0.0	0.0	0.0	0.0
	0.0	0.0	0.0	0.0	0.0	0.0	0.0	0.0	4.9	6.0	0.0	8.5	10.0	12.9	17.2	22.9	0.0	0.0	0.0	0.0
52	0.0	0.0	0.0	.3	.9	1.9	3.5	4.6	5.8	0.0	8.9	0.0	11.5	15.2	21.0	0.0	0.0	0.0	0.0	0.0
	0.0	0.0	0.0	.3	.9	1.9	3.5	4.6	6.0	7.5	9.0	0.0	11.8	15.9	0.0	0.0	0.0	0.0	0.0	0.0
53	0.0	0.0	0.0	0.0	0.0	0.0	3.2	4.6	6.3	8.2	9.8	11.4	13.3	18.3	23.7	0.0	0.0	0.0	0.0	0.0
	0.0	0.0	0.0	0.0	0.0	0.0	5.8	8.0	9.3	11.4	14.8	17.0	18.8	23.3	30.6	0.0	0.0	0.0	0.0	0.0

TABLE A.2.3 cont'd.

54	0.0	0.0	0.0	0.0	0.0	0.0	0.0	0.0	0.0	0.0	0.0	0.0	0.0	0.0	0.0	0.0	0.0	0.0	0.0
___	0.0	0.0	0.0	0.0	0.0	0.0	0.0	0.0	0.0	0.0	0.0	0.0	0.0	0.0	0.0	0.0	0.0	0.0	0.0
___	0.0	0.0	0.0	.4	.9	1.7	2.7	3.0	4.7	5.0	7.0	8.1	9.2	11.9	14.9	19.1	0.0	0.0	0.0
___	0.0	0.0	0.0	0.0	1.0	1.7	3.1	4.1	5.1	6.4	7.6	8.9	10.3	13.4	16.4	23.5	0.0	0.0	0.0
56	0.0	0.0	0.0	0.0	0.0	1.7	2.8	3.7	4.7	5.9	7.1	8.4	9.7	13.0	17.8	0.0	0.0	0.0	0.0
___	0.0	0.0	0.0	0.0	0.0	3.0	4.0	5.2	6.7	7.9	9.4	11.0	12.1	19.7	0.0	0.0	0.0	0.0	0.0

APPENDIX 3

ANALYSIS OF PRUDHOE BAY CRUDES USED IN LARGE SCALE TESTS

CHEMICAL & GEOLOGICAL LABORATORIES OF ALASKA, INC.

P.O. BOX 4-1276
Anchorage, Alaska 99509

TELEPHONE (907) 562-2343

ANCHORAGE INDUSTRIAL CENTER
5633 B Street

ANALYTICAL REPORT

From Sohio Alaska Petroleum Company Product Insitu Burn Test

Address Anchorage, Alaska Date September 19, 1984

Other Pertinent Data

Analyzed by Staff Date October 16, 1984 Lab No. 6558

REPORT OF ANALYSIS
INSITU BURN TEST
EAST DOCK, ALASKA

DATE	INSITU BURN TEST NO.	SAMPLE	Dynes/cm @ 77 °F SURFACE TENSION	Dynes/cm @ 77 °F INTERFACIAL TENSION
9-12-84	1	Water	62.1	----
				23.4
9-12-84	1	Crude	26.8	----
9-12-84	2	Water	65.	----
				23.4
9-12-84	2	Crude	26.6	----
9-13-84	4	Water	65.6	----
				24.3
9-13-84	4	Crude	25.7	----

CHEMICAL & GEOLOGICAL LABORATORIES OF ALASKA, INC.

P.O. BOX 4-1276
Anchorage, Alaska 99509

TELEPHONE (907) 562-2343

ANCHORAGE INDUSTRIAL CENTER
5633 B Street

ANALYTICAL REPORT

From Sohio Alaska Petroleum Company Product Burn Test

Address Anchorage, Alaska Date September 19, 1984

Other Pertinent Data

Analyzed by Staff Date October 16, 1984 Lab No. 6558

REPORT OF ANALYSIS
INSITU BURN TEST
EAST DOCK, ALASKA

DATE	INSITU BURN TEST NO.	SAMPLE	TCC °F(*) FLASH PT.	COC °F(**) FIRE PT.	60/60 SPECIFIC GRAVITY	(VISCOSITY CURVE) DENSITY 15 °C
9-12-84	1	Crude	<25	165	0.8956	0.8951
9-12-84	2	Crude	<25	140	0.8939	0.8934
9-13-84	4	Crude	<25	145	0.8961	0.8956

(*) TCC = TAG CLOSED CUP
(**) COC = CLEVELAND OPEN CUP

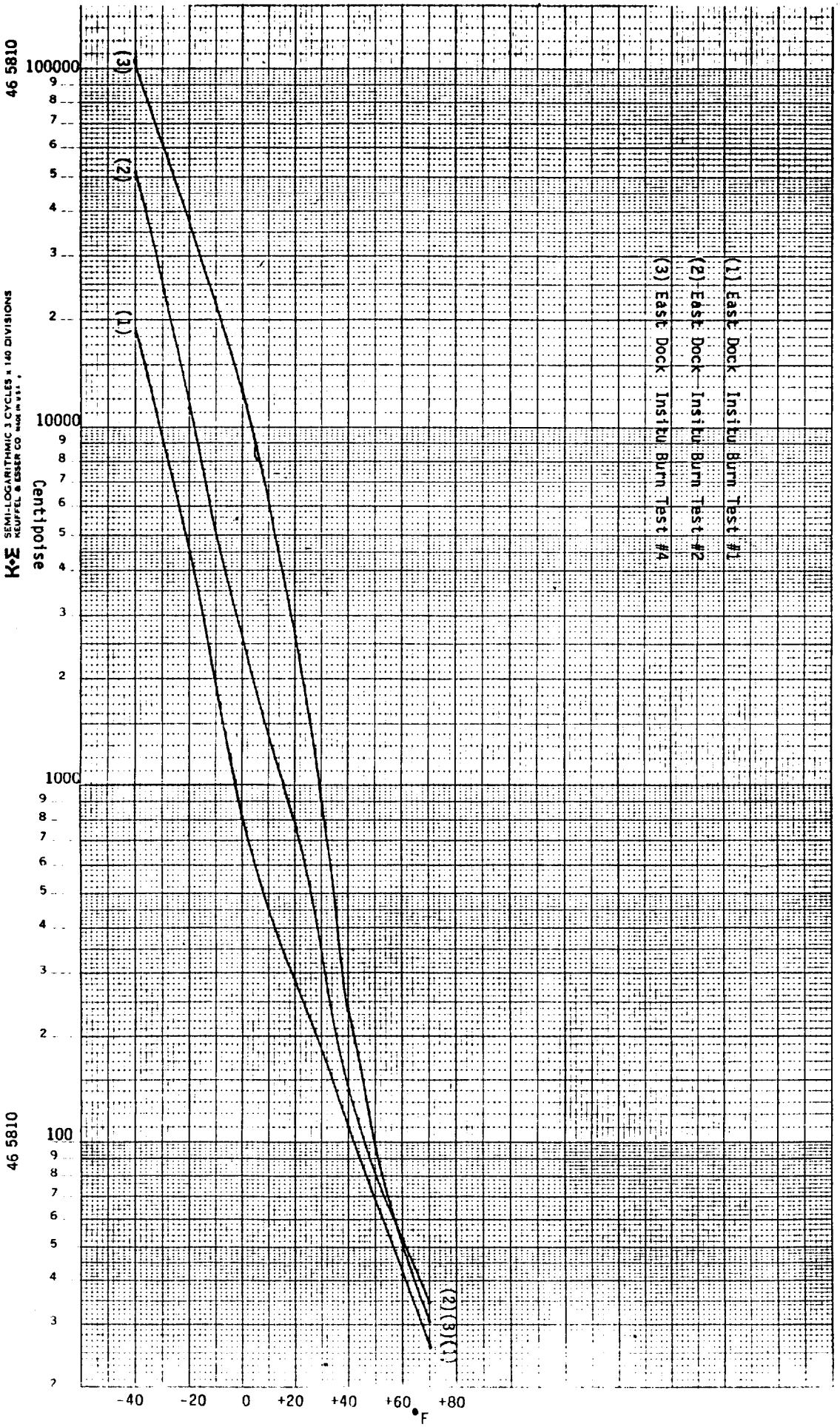
46 5810
SEMI-LOGARITHMIC 3 CYCLES x 140 DIVISIONS
KEUFFEL & ESSER CO
K·E
Centipoise
100000
10000
1000
100
(3)
(2)
(1)
-40
-20
0
+20
+40
+60
+80
°F
(1) East Dock Instu Burn Test #1
(2) East Dock Instu Burn Test #2
(3) East Dock Instu Burn Test #4
(2)(3)(1)

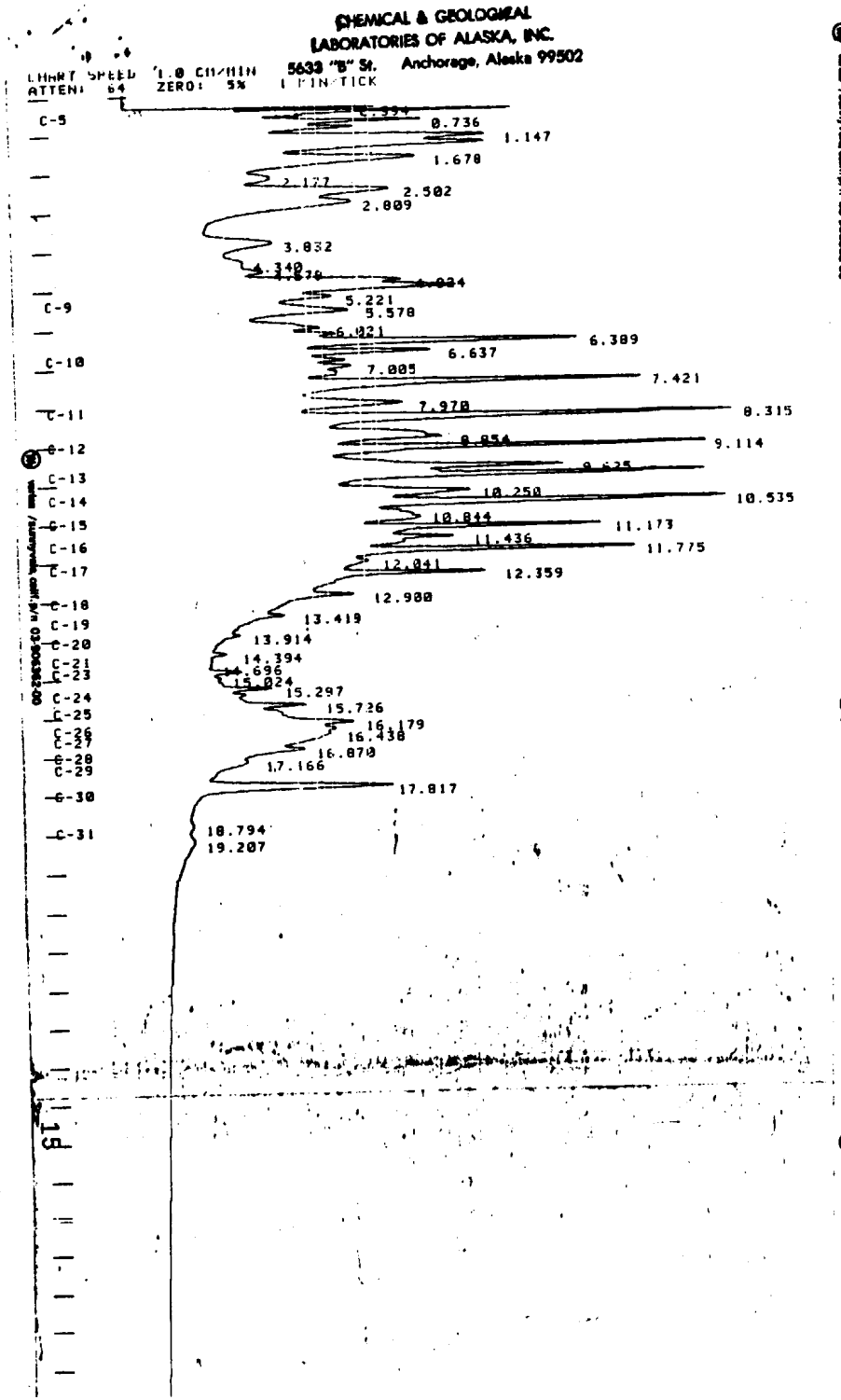

RECALC
TITLE: EAST DOCK BURN TEST#1 9-12-84 10:42 2 OCT 84

CHANNEL NO: 2 SAMPLE: 6558-1C METHOD: 6558-1CM

PEAK NO	PEAK NAME	RESULT A%	TIME (MIN)	TIME OFFSET	AREA COUNTS	SEP CODE		HT 2 (SEC)
1	C-5	0.39	0.394	-0.016	72397	BV		2.55
2		1.06	0.491		197633	VV		5.70
3		0.26	0.578		48798	VV	?	
4		1.30	0.736		242933	VV	?	13.10
5		1.03	0.889		201767	VV	?	6.70
6		2.11	1.147		394301	VV	?	12.30
7	C-7	2.33	1.326	0.056	435887	VV	?	7.20
8		3.04	1.678		568469	VV	?	24.45
9		1.26	2.177		235943	VV	?	14.90
10		2.20	2.502		412071	VV	?	14.60
11	C-8	3.45	2.809	-0.131	646638	VV	?	12.85
12		1.92	3.832		359666	VV	?	15.10
13		0.87	4.340		162031	VV	?	14.40
14		0.96	4.578		180556	VV	?	14.20
15		1.38	4.824		257727	VV	?	13.40
16		1.97	4.987		369524	VV	?	9.65
17	C-9	1.19	5.221	0.031	223561	VV	?	9.00
18		2.16	5.578		405240	VV	?	12.70
19		1.39	6.021		260840	VV	?	14.60
20		0.82	6.178		153149	VV	?	8.60
21		2.53	6.389		474325	VV		11.10
22	C-10	1.46	6.637	-0.093	273306	VV	?	10.10
23		0.97	6.851		181400	VV	?	10.10
24		1.05	7.005		195776	VV	?	8.60
25		0.58	7.152		108319	VV	?	5.50
26		0.62	7.287		115194	VV	?	8.90
27		3.49	7.421		653948	VV	?	10.15
28	C-11	2.65	7.978	0.160	495623	VV	?	14.90
29		3.70	8.315		692409	VV	?	8.05
30	C-12	3.31	8.854	0.124	619028	VV	?	14.50
31		2.95	9.114		553002	VV	?	5.80
32	C-13	3.23	9.625	0.075	604746	VV	?	15.10
33		3.36	9.845		628251	VV	?	12.75
34	C-14	2.76	10.250	-0.050	516761	VV	?	14.80
35		3.16	10.535		590811	VV		11.05
36		1.36	10.844		253800	VV	?	14.90
37	C-15	1.63	10.927	-0.065	304666	VV	?	3.70
38		2.52	11.173		471192	VV	?	10.10
39		1.42	11.436		266557	VV	?	8.40
40	C-16	1.10	11.561	-0.089	205861	VV	?	3.10
41		2.62	11.775		490656	VV		10.55
42		1.77	12.041		331940	VV	?	8.20
43	C-17	3.28	12.359	0.079	615032	VV	?	13.15
44	C-18	2.45	12.980	0.040	458724	VV	?	12.90
45	C-19	1.49	13.419	-0.011	278262	VV	?	7.45
46	C-21	0.94	13.914	-0.186	176533	VV	?	7.30
47		0.34	14.394		63145	VV	?	8.50
48	C-22	0.24	14.548	-0.062	44945	VV	?	5.00
49		0.17	14.696		31928	VV	?	3.35
50		0.40	14.855		73960	VV	?	10.70
51	C-23	0.22	15.024	-0.066	41996	VV	?	7.80
52		0.71	15.297		132576	VV	?	14.90
53	C-24	0.34	15.449	-0.111	63154	VV	?	6.80
54		0.93	15.726		173280	VV	?	14.40
55	C-25	1.95	16.179	0.129	365292	VV	?	29.60
56		0.87	16.350		162261	VV	?	6.90
57	C-26	1.55	16.438	-0.132	289350	VV	?	
58	C-27	1.07	16.870	-0.090	199753	VV	?	8.50
59	C-28	0.90	17.166	-0.064	183116	VV	?	5.40
60	C-30	1.83	17.817	-0.263	342585	VV		11.05
61	C-31	0.26	18.794	0.014	49541	VV	?	15.40
62		0.64	19.207		120695	VB	?	20.45
TOTALS:		100.04		-0.719	18722800			

DETECTED PKS: 62 REJECTED PKS: 0

MULTIPLIER: 1.00000

NOISE: 1.2 OFFSET: -56

ERRORS:
ALL FACTORS = 0
DEFAULT TO A%

NOTES:
SOHIO-ALASKA PETROLEUM CO.
PRUDHOE BAY FIELD
EAST DOCK
IN SITU TEST BURN #1
CRUDE OIL
9-12-84, S. HILLMAN

CHEMICAL & GEOLOGICAL
LABORATORIES OF ALASKA, INC.
5633 "B" St. Anchorage, Alaska 99502

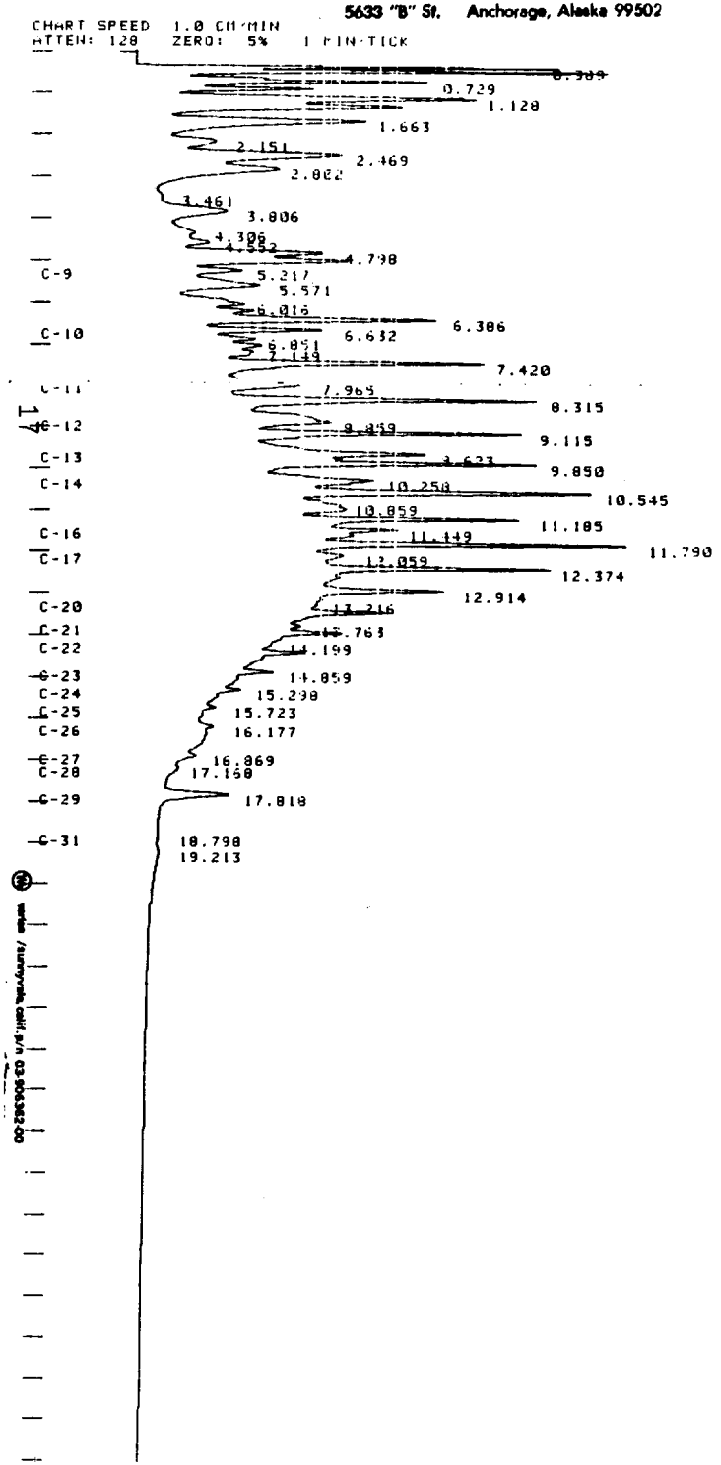

RECALC
TITLE: EAST DOCK TEST BURN#2 9-12-84 12:16 2 OCT 84

CHANNEL NO: 2 SAMPLE: 6558-2C METHOD: 6558-1CM

PEAK NO	PEAK NAME	RESULT A%	TIME (MIN)	TIME OFFSET	AREA COUNTS	SEP CODE	HEIGHT (SEC)
1		0.94	0.389		229867	BV	2.55
2		1.50	0.486		368691	VV	4.20
3	C-6	1.48	0.729	0.029	362315	VV	4.65
4		0.81	0.807		199338	VV	6.00
5		2.23	1.128		547649	VV	8.30
6	C-7	1.76	1.320	0.050	431193	VV	10.20
7		2.25	1.663		552282	VV	11.05
8		0.90	2.151		220846	VV	14.40
9		2.01	2.469		493089	VV	14.10
10	C-8	1.95	2.802	-0.138	477540	VV	13.50
11		0.25	3.461		60978	VV	14.50
12		1.29	3.806		317261	VV	13.55
13		0.68	4.306		166067	VV	15.10
14		0.67	4.552		165555	VV	15.10
15		1.31	4.798		322665	VV	9.30
16		1.46	4.982		358979	VV	8.60
17	C-9	0.78	5.217	0.027	192120	VV	10.10
18		1.49	5.571		364958	VV	12.40
19		1.08	6.016		265497	VV	14.70
20		0.66	6.169		161289	VV	8.30
21		2.03	6.386		497092	VV	5.15
22	C-10	1.11	6.632	-0.098	272968	VV	8.70
23		0.77	6.851		188401	VV	11.80
24		0.82	6.999		201698	VV	8.70
25		0.52	7.149		127982	VV	5.90
26		0.44	7.288		108341	VV	0.20
27		2.86	7.420		702780	VV	4.65
28	C-11	2.19	7.965	0.155	538288	VV	15.00
29		3.29	8.315		807271	VV	5.75
30	C-12	2.99	8.859	0.129	734272	VV	15.10
31		2.66	9.115		653739	VV	4.75
32	C-13	3.08	9.623	0.073	756385	VV	14.80
33		0.50	9.743		122864	VV	2.80
34		2.73	9.850		670434	VV	8.20
35	C-14	2.78	10.258	-0.042	681960	VV	15.00
36		3.32	10.545		813937	VV	9.40
37		0.62	10.767		153330	VV	8.10
38		0.89	10.859		217296	VV	8.70
39	C-15	1.66	10.943	-0.047	406336	VV	6.00
40		2.88	11.185		707399	VV	7.90
41		1.64	11.449		401529	VV	9.10
42	C-16	1.30	11.575	-0.075	320157	VV	4.00
43		3.32	11.790		815856	VV	7.40
44		1.95	12.059		477859	VV	10.30
45	C-17	3.54	12.374	0.094	867984	VV	10.40
46		1.78	12.506		436183	VV	4.80
47	C-18	2.92	12.914	0.054	717532	VV	12.95
48		0.91	13.114		222680	VV	4.10
49		1.08	13.216		264382	VV	2.65
50	C-19	2.82	13.431	0.001	690965	VV	11.00
51	C-20	0.98	13.763	0.173	239467	VV	8.00
52		2.35	13.935		577668	VV	9.50
53	C-21	0.62	14.199	0.099	151120	VV	
54	C-22	2.38	14.403	-0.207	583814	VV	10.40
55		0.94	14.859		229579	VV	9.60
56	C-23	0.97	15.019	-0.071	237729	VV	4.30
57		0.69	15.238		168654	VV	7.80
58	C-24	0.67	15.436	-0.124	165038	VV	2.10
59		0.51	15.723		125508	VV	8.40
60		0.46	15.878		112424	VV	3.95
61	C-25	0.67	16.177	0.127	164573	VV	17.30
62	C-26	1.21	16.338	-0.232	296434	VV	4.60
63	C-27	0.53	16.869	-0.091	130953	VV	7.05
64	C-28	0.56	17.160	-0.062	136203	VV	6.60
65	C-30	1.03	17.818	-0.262	253110	VV	9.05
66	C-31	0.15	18.798	0.018	37894	VV	16.70
67		0.38	19.213		93685	VB	11.90
TOTALS:		100.00		-0.420	24539800		

DETECTED PKS: 67 REJECTED PKS: 0

MULTIPLIER: 1.00000

NOISE: 1.2 OFFSET: 11

ERRORS:
ALL FACTORS = 0
DEFAULT TO A%

NOTES:
SOHIO-ALASKA PETROLEUM CO.
PRUDHOE BAY FIELD
EAST DOCK
IN SITU TEST BURN #2
CRUDE OIL
9-12-84; S. HILLMAN

LABORATORIES OF ALASKA, INC.
5633 "B" St. Anchorage, Alaska 99502

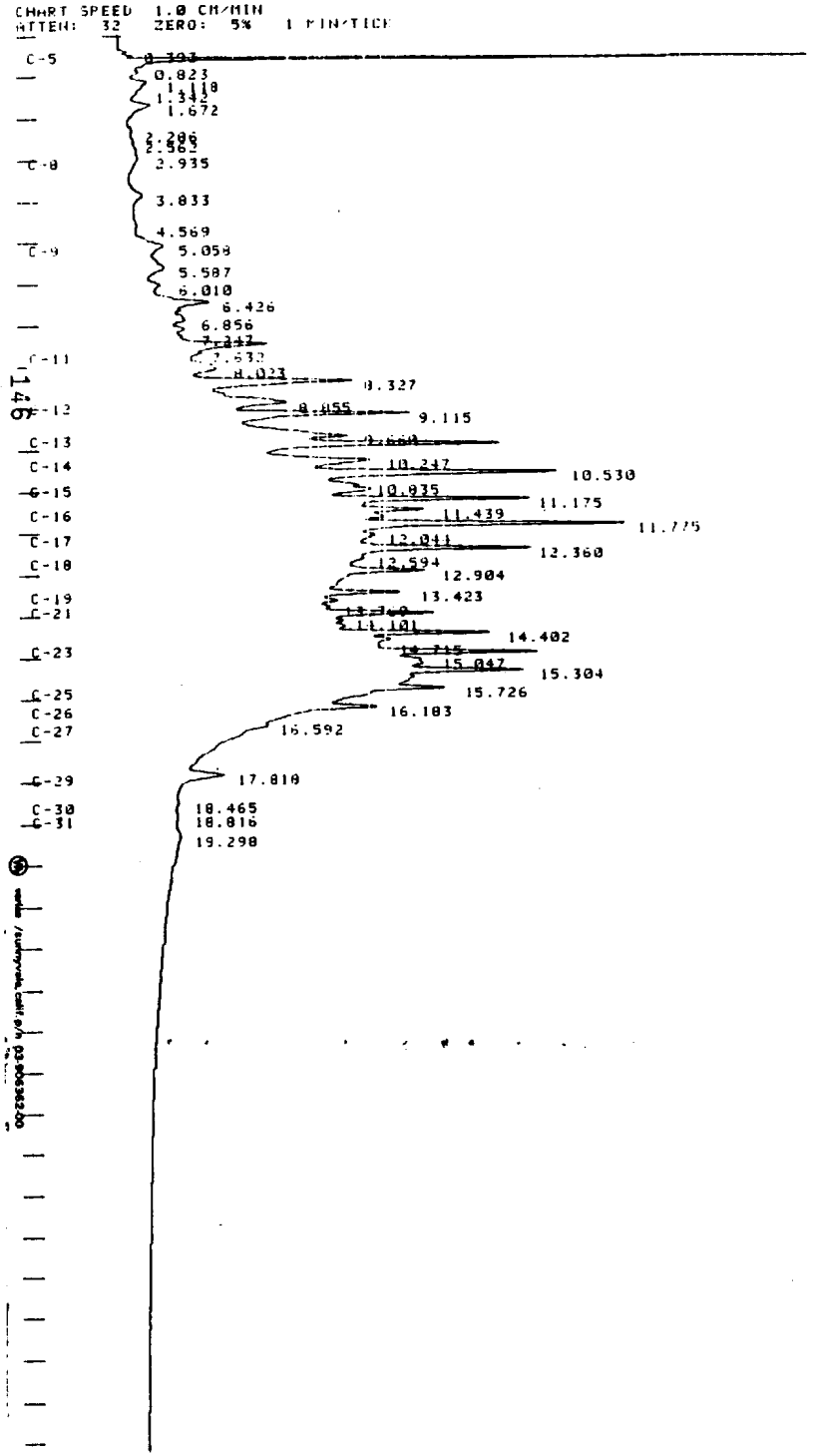

RECALC
TITLE: TEST BURN #2 RESIDUAL 9-12-84 16:41 12 OCT 84

CHANNEL NO: 2 SAMPLE: 6558-2R METHOD: SHT

PEAK NO	PEAK NAME	RESULT A%	TIME (MIN)	TIME OFFSET	AREA COUNTS	SEP CODE	WIDTH (SEC)
1	C-5	0.03	0.393	-0.017	1929	BV	3.6
2		0.04	0.503		2338	VV	7.20
3		3.83	0.561		246169	VV	1.75
4		0.00	0.823		203	T	2.00
5		0.02	0.886		1169	T	3.80
6		0.16	1.118		10158	T	9.50
7		0.04	1.342		2816	T	
8		0.19	1.672		12333	T	16.70
9		0.03	2.206		1836	T	11.10
10		0.04	2.562		2619	T	13.00
11	C-8	0.19	2.935	-0.005	11997	T	13.00
12		0.11	3.833		7254	T	16.50
13		0.02	4.569		998	T	11.50
14	C-9	0.30	5.058	-0.132	18699	T	14.20
15		0.26	5.587		16228	T	12.50
16		0.37	6.010		23578	VV	14.30
17		0.93	6.426		58774	VV	15.10
18	C-10	0.23	6.615	-0.115	14754	VV	2.60
19		0.65	6.856		41160	VV	10.40
20		0.44	7.069		27705	VV	10.70
21		0.23	7.247		14457	VV	7.50
22		1.33	7.441		84027	VV	9.50
23	C-11	0.36	7.632	-0.178	23116	VV	
24		1.34	8.023		84689	VV	14.90
25		1.97	8.327		124886	VV	10.85
26	C-12	2.33	8.855	0.125	147819	VV	14.70
27		2.29	9.115		144469	VV	9.90
28	C-13	2.69	9.660	0.110	170255	VV	14.40
29		3.00	9.843		190162	VV	11.45
30	C-14	2.85	10.247	-0.053	180795	VV	14.50
31		3.49	10.530		221339	VV	13.05
32		1.38	10.835		87326	VV	12.50
33	C-15	1.95	10.943	-0.047	123301	VV	6.30
34		3.03	11.175		192040	VV	9.90
35		2.02	11.439		127902	VV	10.30
36	C-16	1.57	11.611	-0.039	99184	VV	6.35
37		3.84	11.775		243395	VV	13.45
38		2.34	12.044		148513	VV	7.80
39	C-17	4.02	12.360	0.080	254735	VV	18.05
40		1.85	12.594		116969	VV	2.60
41	C-18	5.29	12.904	0.044	334808	VV	12.70
42	C-19	1.98	13.423	-0.007	125592	VV	10.80
43	C-20	1.30	13.617	0.027	82146	VV	7.40
44		0.98	13.769		61814	VV	7.60
45		2.20	13.923		139408	VV	10.30
46	C-21	1.01	14.101	0.001	64106	VV	5.80
47		1.21	14.236		76801	VV	7.60
48		2.21	14.402		139678	VV	10.70
49	C-22	1.78	14.563	-0.047	112529	VV	7.60
50		0.88	14.715		55755	VV	4.10
51		2.78	14.862		175838	VV	12.30
52	C-23	1.26	15.047	-0.043	79957	VV	8.90
53		1.63	15.133		103469	VV	5.60
54		2.70	15.304		170872	VV	10.20
55	C-24	2.59	15.459	-0.101	164268	VV	4.80
56		4.43	15.726		280813	VV	2.50
57	C-25	3.62	16.183	0.133	229089	VV	10.10
58	C-26	3.53	16.592	0.022	223488	VV	56.30
59	C-30	1.43	17.810	-0.262	90693	VV	15.90
60		0.45	18.465		28324	VV	9.90
61	C-31	0.52	18.816	0.036	32885	VV	14.00
62		4.40	19.298		278978	VB	34.70
TOTALS:		99.99		-0.460	6333410		

DETECTED PKS: 62 REJECTED PKS: 0

MULTIPLIER: 1.00000

NOISE: 1.2 OFFSET: -10

ERRORS:
ALL FACTORS = 0
DEFAULT TO A%

NOTES:
SOHIO
EAST DOCK TEST BURN #2
RESIDUAL CRUDE
9-12-84

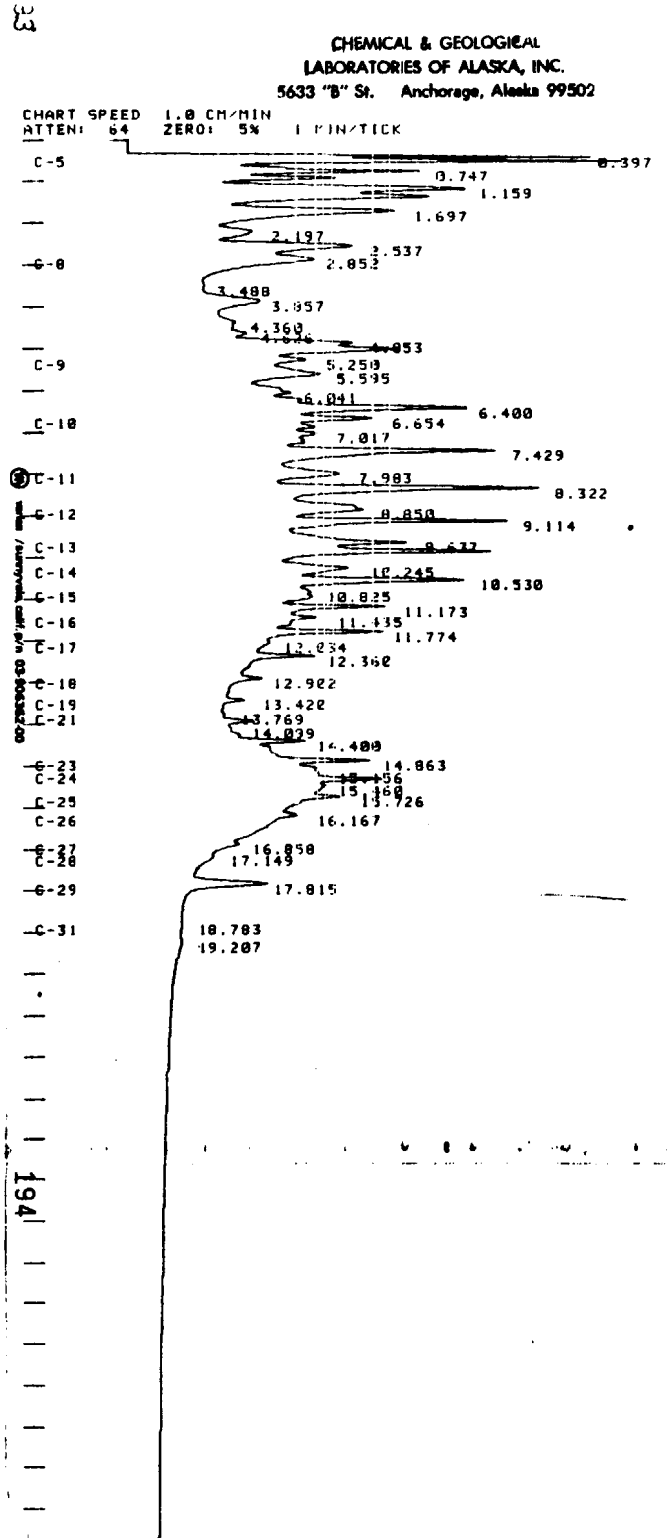

RECALC
TITLE: EAST DOCK BURN TEST#4 9-13-84 13:14 2 OCT 84

CHANNEL NO: 2 SAMPLE: 6558-3C METHOD: 6558-3CM

PEAK NO	PEAK NAME	RESULT A%	TIME (MIN)	TIME OFFSET	AREA COUNTS	SEP CODE		WI 2 (SEC)
1	C-5	1.09	0.397	-0.013	144370	BV		3.15
2		1.92	0.497		254205	VV		5.30
3		1.67	0.747		222012	VV		9.25
4		1.08	0.900		142710	VV	?	10.35
5		2.48	1.159		328524	VV	?	10.30
6		2.28	1.349		301849	VV	?	15.10
7		3.17	1.697		420039	VV		17.30
8		1.47	2.197		194342	VV	?	14.90
9		2.24	2.537		296442	VV	?	13.00
10	C-8	3.11	2.852	-0.000	412054	VV	?	14.30
11		0.59	3.488		78465	VV	?	11.40
12		2.06	3.857		272995	VV	?	14.30
13		1.08	4.360		143700	VV	?	14.40
14		0.35	4.460		46683	VV	?	8.95
15		0.79	4.626		104347	VV	?	11.20
16		1.36	4.853		179818	VV	?	14.20
17		2.03	5.006		275691	VV	?	10.40
18	C-9	1.36	5.250	0.060	180069	VV	?	10.40
19		2.57	5.595		340271	VV	?	14.60
20		1.62	6.041		214395	VV	?	10.40
21		0.83	6.204		110622	VV	?	9.30
22		2.70	6.400		358400	VV	?	14.40
23	C-10	1.64	6.654	-0.076	218089	VV	?	10.50
24		1.07	6.856		141639	VV	?	7.65
25		1.15	7.017		153092	VV	?	8.50
26		0.44	7.161		58940	VV	?	5.00
27		0.81	7.226		107195	VV	?	3.90
28		3.71	7.429		492160	VV	?	16.50
29	C-11	2.74	7.983	0.173	362799	VV	?	14.80
30		3.58	8.322		474175	VV	?	10.95
31	C-12	3.12	8.850	0.120	413687	VV	?	14.80
32		2.77	9.114		366728	VV	?	11.50
33	C-13	2.84	9.637	0.087	377135	VV	?	14.90
34		2.87	9.842		380207	VV	?	16.35
35	C-14	2.30	10.245	-0.055	305449	VV	?	15.10
36		2.45	10.530		324438	VV	?	11.70
37		1.01	10.825		134425	VV	?	12.60
38	C-15	1.26	10.925	-0.065	166953	VV	?	6.15
39		1.75	11.173		232377	VV	?	9.60
40		1.85	11.435		245799	VV	?	9.10
41	C-16	1.76	11.774	0.124	233654	VV	?	12.05
42		1.16	12.034		154219	VV	?	5.90
43	C-17	2.17	12.360	0.000	287255	VV	?	11.65
44	C-18	1.68	12.902	0.042	222532	VV	?	13.10
45	C-19	0.60	13.420	-0.010	79644	VV	?	9.55
46	C-20	0.36	13.577	-0.013	47219	VV	?	3.70
47		0.34	13.769		45080	VV	?	9.90
48		0.62	13.919		82819	VV	?	11.20
49	C-21	0.33	14.039	-0.001	43673	VV	?	7.90
50		0.41	14.260		54740	VV	?	12.90
51		0.87	14.400		114722	VV	?	12.90
52	C-22	0.57	14.574	-0.036	74975	VV	?	9.70
53		1.86	14.863		247132	VV	?	14.80
54	C-23	0.70	15.039	-0.051	93022	VV	?	8.80
55		0.75	15.156		99379	VV	?	8.40
56		1.47	15.304		194319	VV	?	10.90
57	C-24	1.43	15.460	-0.100	189818	VV	?	8.20
58		2.42	15.726		321439	VV	?	9.60
59	C-25	2.79	16.167	0.117	369601	VV	?	7.65
60	C-27	0.71	16.858	-0.102	94790	VV	?	5.50
61	C-28	0.63	17.149	-0.081	83578	VV	?	2.65
62	C-30	0.99	17.815	-0.265	130861	VV		16.90
63	C-31	0.08	18.783	0.003	10940	VV	?	10.80
64		0.05	19.207		6922	VB	?	19.30
TOTALS:		100.01		-0.150	13258800			

DETECTED PKS: 64 REJECTED PKS: 0

MULTIPLIER: 1.00000

NOISE: 1.2 OFFSET: 9

ERRORS:
ALL FACTORS = 0
DEFAULT TO A%

NOTES:
SOHIO-ALASKA PETROLEUM CO.
PRUDHOE BAY FIELD
EAST DOCK
IN SITU TEST BURN #3
CRUDE OIL
9-12-84, S. HILLMAN

CHEMICAL & GEOLOGICAL
LABORATORIES OF ALASKA, INC.
5633 "B" St. Anchorage, Alaska 99502

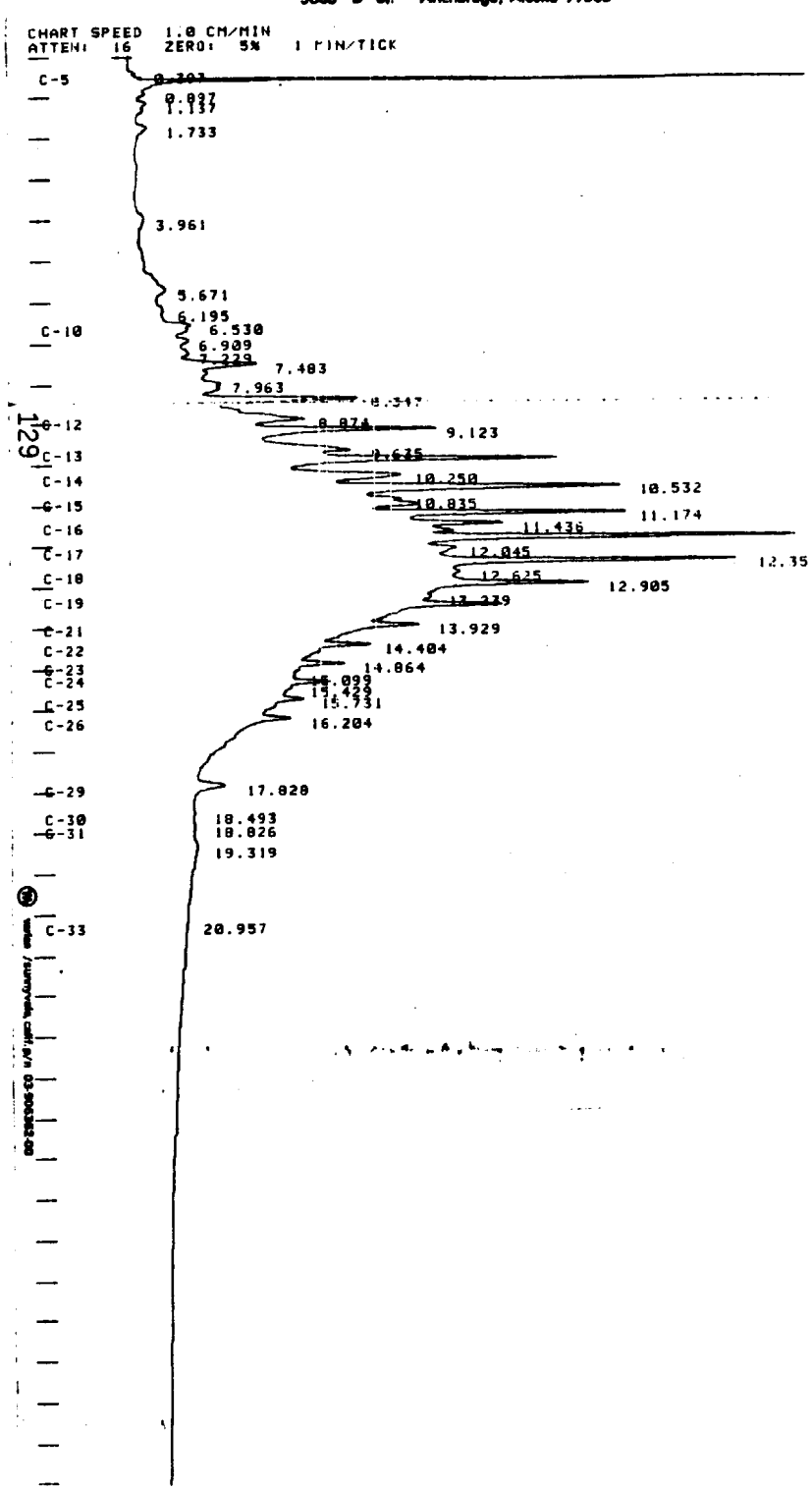

130

RECALC
TITLE: TEST BURN #4 RESIDUAL 9-13-84 14:27 12 OCT 84

CHANNEL NO: 2 SAMPLE: 6558-3R METHOD: SAT

PEAK NO	PEAK NAME	RESULT A%	TIME (MIN)	TIME OFFSET	AREA COUNTS	SEP CODE	HH 2 (SEC)
1	C-5	0.02	0.397	-0.013	478	BV	2.75
2		0.02	0.466		419	VV	2.90
3		2.03	0.569		55144	VV	1.45
4		0.02	0.837		477	T	? 4.40
5		0.07	1.137		1779	T	? 10.00
6	C-7	0.04	1.244	-0.026	1216	T	?
7		0.15	1.733		4165	T	? 19.55
8		0.10	3.961		2828	BB	? 10.60
9		0.45	5.671		12345	BV	? 14.90
10		0.25	6.195		6771	VV	? 13.00
11		0.45	6.530		12271	VV	? 10.30
12	C-10	0.30	6.613	-0.117	8257	VV	?
13		0.47	6.909		12886	VV	? 13.10
14		0.49	7.229		13236	VV	? 10.70
15		1.09	7.483		29781	VV	? 9.20
16	C-11	0.55	7.704	-0.106	15017	VV	? 6.10
17		0.56	7.963		15154	VV	? 12.40
18		0.64	8.076		17544	VV	? 4.15
19		2.07	8.347		56419	VV	11.65
20	C-12	2.47	8.874	0.144	67311	VV	? 14.50
21		2.75	9.123		74854	VV	? 8.50
22	C-13	2.59	9.635	0.085	70435	VV	? 14.60
23		4.12	9.845		112166	VV	9.35
24	C-14	3.31	10.250	-0.050	90024	VV	? 14.80
25		4.74	10.532		128964	VV	12.70
26		1.55	10.835		42160	VV	? 9.90
27	C-15	2.47	10.967	-0.023	67314	VV	? 9.70
28		3.66	11.174		99548	VV	? 8.30
29		3.25	11.436		88596	VV	? 10.80
30	C-16	2.07	11.622	-0.020	56461	VV	? 8.10
31		5.39	11.772		146795	VV	9.30
32		3.47	12.045		94494	VV	? 9.50
33	C-17	6.26	12.357	0.077	170583	VV	? 14.90
34		2.76	12.625		75273	VV	? 7.90
35	C-18	6.82	12.905	0.045	185757	VV	? 12.95
36		2.01	13.239		54751	VV	? 5.50
37	C-19	6.40	13.429	-0.001	174234	VV	? 9.05
38	C-21	4.71	13.939	-0.171	128369	VV	? 9.10
39		1.83	14.404		49904	VV	? 8.65
40	C-22	1.76	14.529	-0.081	47909	VV	?
41		1.55	14.864		42161	VV	? 9.40
42		0.77	14.979		20976	VV	?
43	C-23	0.67	15.099	0.089	18202	VV	?
44		1.54	15.305		41996	VV	? 10.15
45	C-24	1.15	15.429	-0.131	31432	VV	?
46		2.55	15.731		69349	VV	? 10.20
47	C-25	4.33	16.204	0.154	117896	VV	? 10.05
48	C-30	0.99	17.828	-0.252	26921	VV	? 10.70
49		0.30	18.493		8109	VV	? 12.80
50	C-31	0.33	18.826	0.046	9077	VV	? 13.60
51		1.41	19.319		38270	VV	? 34.40
52	C-34	0.24	20.957	-0.113	6645	VB	?
TOTALS:		99.93		-0.552	2723120		

DETECTED PKS: 52 REJECTED PKS: 0

MULTIPLIER: 1.00000

NOISE: 1.2 OFFSET: -11

ERRORS:
ALL FACTORS = 0
DEFAULT TO A%

NOTES:
SAMIN
EAST DOCK TEST BURN #4
RESIDUAL CRUDE
9-14-84

131

129

-134-

U.S. Department of Transportation
United States Coast Guard

Commanding Officer
U.S Coast Guard
Research and Development Center

Avery Point
Groton, CT 06340
Phone:

754154.1
1 FEB 1985

From: Commanding Officer, CG Research and Development Center
To: Commandant (G-DMT)

Subj: ANALYSIS OF PRUDHOE BAY EXPERIMENTAL BURN TEST SAMPLES; REPORT ON

Ref: (a) COMDT (G-DMT-3/54) ltr 3913/3205U of 16 Oct 1984

1. The density measurements and gas chromatographic analysis as requested by reference (a) have been completed. The results of our analyses are summarized below and presented in detail in enclosure (1).

2. Density measurements revealed that in each case the density of the oil increased during the burn test indicating that changes had occurred in the physical properties of the oils involved. However, gas chromatographic analysis did not reveal any significant changes in the chemical composition of the oils attributable to the burn test. Based on these initial results and discussion with LTJG Michele FITZPATRICK, additional analyses were performed. The results of these additional analyses are summarized as follows:

a. Conclusive evidence of any change in the chemical composition of the oil directly attributed to the burn test could not be found. It is our opinion that the burning process occurs at the oil slick surface and any changes in chemical composition may be confined to the surface layer and involves the light (volatile) petroleum fraction. Bulk sampling of the oil slick could easily mask any chemical changes occurring at the slick surface. This opinion is supported by our infrared and fluorescence spectroscopic and gas chromatographic analyses.

b. For future work, different types of high performance liquid chromatographic analyses may provide more information than simple gas chromatographic analyses in these studies.

c. The inconclusive results obtained in this study may be directly attributable to the sampling of the burned oil slick.

3. If these tests are repeated, it is recommended that the burned oil slick residue be sampled as follows:

a. The oil slick surface should be sampled with Teflon^{R} or aluminum foil strips, i.e., the upper 1/8-inch of the oil's surface should be sampled. Adjacent to this surface sampling a bulk sample (i.e., scoop sample which contains both oil and water) should be collected.

b. Dependent on slick size a minimum of two sampling points should be selected to determine the uniformity of the oil slick before and after the burn testing.

754154.1
1 FEB 1985

Subj: ANALYSIS OF PRUDHOE BAY EXPERIMENTAL BURN TEST SAMPLES; REPORT ON

4. It is suggested that selection of appropriate analytical techniques for future studies should be made after consultation with the R&D Center chemistry branch personnel.

SAMUEL F. POWEL, III
By direction

Encl: (1) Analysis Report of Prudhoe Bay Burn Test Samples

Copy: COMDT (G-DMT-3)

ANALYSIS REPORT OF PRUDHOE BAY TEST BURN SAMPLES

I. R&D Center control numbers were assigned to each sample as described in Table 1. All discussions are presented using the R&D Center sample control number.

TABLE 1. SAMPLE INFORMATION

Sample No.	Label Date	Label Information	Comments
1	9-12-84	Prudhoe Bay Crude Burn Residue No.1	In poly bottle
2	9-12-84	In situ Burn Test No.2	In poly bottle
3	9-13-84	Burn Test No.4 *	In poly bottle
4	9-14-84	Burn Test No.5	In mason jar
5	9-14-84	Test Burn No.5 (weathered)	Sample bottle
6	9-12-84	Crude Oil Start No.1	Sample bottle
7	9-12-84	Crude Oil Start No.2	Sample bottle
8	9-12-84	No cap or label on bottle; foil covered; small amount of oil residue in bottom	

II. ANALYSES PERFORMED:

1. Density and gas chromatographic analyses as requested by Commandant (G-DMT-3/54) were performed on all samples received.

2. Further analyses were undertaken after discussion with LTJG Michele FITZPATRICK. It was our concern that the two analyses requested were not sufficient to fully document any changes the samples had undergone as a result of these burn tests. Figure 1 indicates the analysis scheme employed to determine if the physical properties and chemical composition of the oil changed during the burn test. A summary of the information which can be obtained from each technique, as well as the appropriate reference for more detailed information is included within Table 2.

* Test number 5 was conducted by Sohio to assess herding agents and does not relate to the uncontained combustion project.

3. As requested by LTJG FITZPATRICK, a more general discussion of the separation scheme and analytical techniques is included. The four major analytical techniques - Infrared Spectroscopy (IR); Gas Chromatography (GC); Fluorescence (FL); and High Performance Liquid Chromatography (HPLC) - have proven well suited for oil identification work. Fluorescence detects only the small fraction of the sample which is capable of fluorescing upon excitation with ultraviolet light. Infrared analysis produces very characteristic spectra based on the response of different portions, or functional groups, of each constituent molecule to infrared radiation. High performance liquid chromatography separates the components on a time basis, detecting ultraviolet-absorbing molecules, usually only those with an aromatic ring structure. Gas chromatography will only separate components which are volatile at the temperature of the GC column. Non-volatile components precipitate at the head of the column. A pentane extract is therefore used to remove components which would plug the column. This pentane extraction procedure results in the loss of light ends or highly volatile non-aromatic hydrocarbons.

The loss of light ends is an advantage for oil identification, because the effect of weathering is minimized. For the burn residue samples the loss of highly volatile components, as shown in Figure 1, means that analytical information about part of the sample is lost. The loss of volatiles on burning may be inferred from density measurements. The analysis scheme would be sensitive to changes in the chemical composition of the oil samples, as it has proven ability to distinguish among very similar oils.

FIGURE 1. ANALYSIS SCHEME

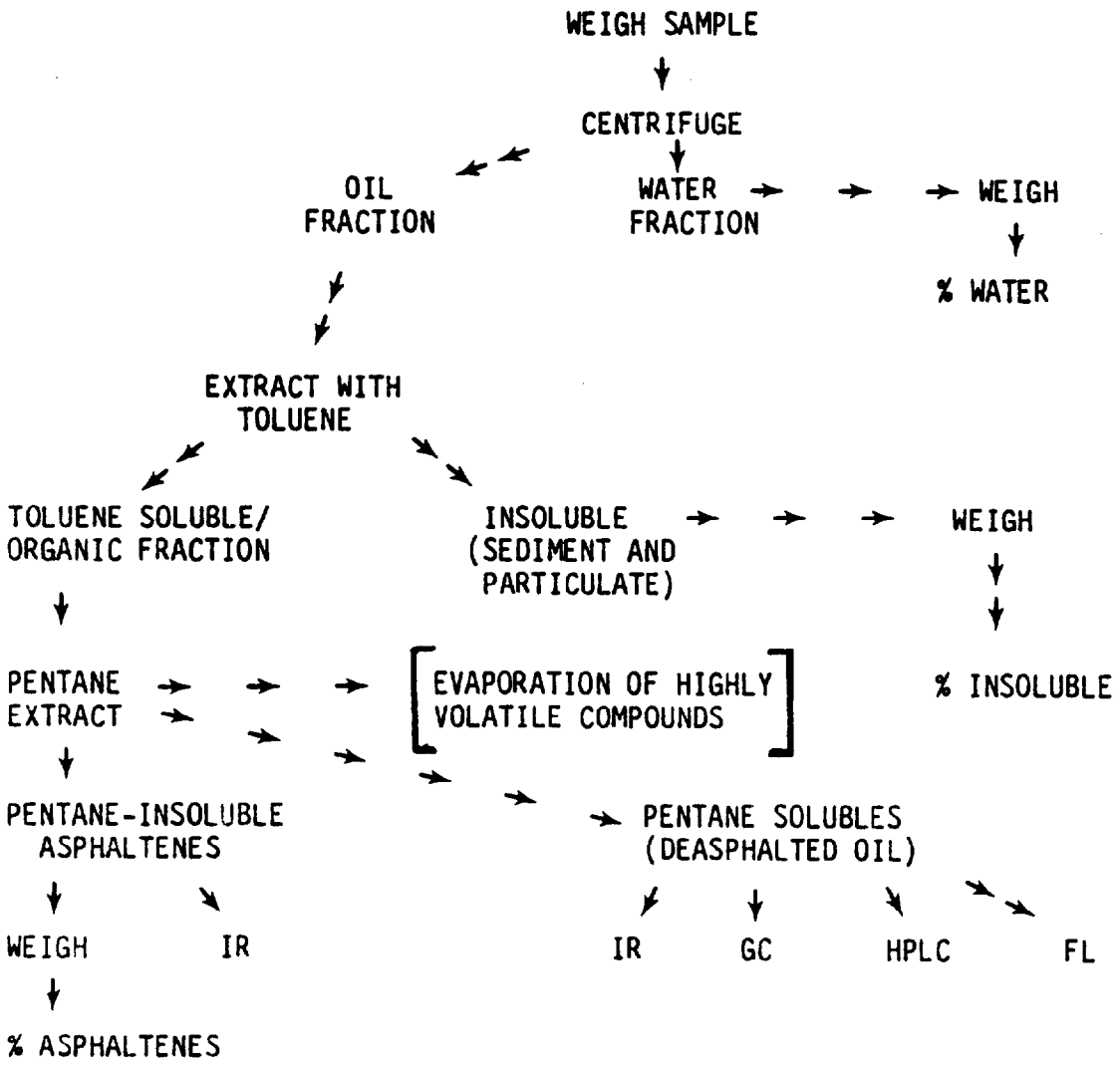

TABLE 2. SEPARATION AND ANALYSIS TECHNIQUES

TECHNIQUE	PURPOSE	REFERENCE
Centrifugation	Separate oil/water emulsion	1977 Oil Spill ID System, page H-7
Toluene Extract	Separate sediment and insoluble residue from organic-soluble components	ASTM standard method of test for sediment in crude and fuel oils by extraction, D473-69
Pentane Extract	Separate deasphalted oil (pentane solubles) from asphaltenes. Procedure results in loss of light ends	1977 Oil Spill ID System, page D-5
Gas Chromatography	Only detects volatile components; separates by molecular weight	1977 Oil Spill ID System, Appendix D
High Performance Liquid Chromatography (Reverse Phase Column)	Detects only aromatic components with UV detector; components must be soluble in mobile phase; separates by polarity of molecule	1977 Oil Spill ID System, Appendix K
Fluorescence Spectroscopy (Synchronous Scan)	Detects only aromatic components which can fluoresce (a small sub-fraction of total sample); separates by aromatic ring size	1977 Oil Spill ID System, Appendix E
Infrared Spectroscopy	Detects specific functional groups; obtains fingerprint for total sample; does not separate complex mixtures	1977 Oil Spill ID System, Appendices G and H

III. RESULTS

A. Density Measurements

The R&D Center is not equipped with the apparatus required to conduct the standard ASTM method of "Test for Density, Specific Gravity or API Gravity of Crude Petroleum Products" (ASTM D1298.67 API Standard 2547). All measurements were simple density determinations using a fixed volume container, i.e., mass/volume at 20°C. The denisty values reported in Table 3 are relative densities of the oil samples, and should not be taken as absolute values.

TABLE 3. RELATIVE DENSITIES OF SAMPLES

SAMPLE NO.	DENSITY @ 20°C (g/ml)
1	.92
2	.90
3	.94
4	.91
5	.80
6	.79
7	.78
8	.76

The samples fall into two groups which are readily distinguishable from each other. The relative standard deviation in these determinations was less than 3%. These relative density measurements performed cannot determine if differences within each group exist. These two groups are:

Group 1 (density range 0.90 through 0.92) Samples 1, 2, 3, and 4

Group 2 (density range 0.76 through 0.80) Samples 5, 6, 7, and 8

The samples representative of the burn residues (Group 1) have a higher density than the unburned oils.

B. Gas Chromatography

The pentane extraction which must precede the gas chromatographic analysis results in the loss of light ends (C_{14} and below). This simulates the loss of the light fraction during natural weathering processes. The gas chromatograms of all the oil samples are similar. The samples may be identified as being the the same oil, with the exception of Sample 5. Polynuclear aromatic compounds were not detectable because of the high concentration of n-alkanes and the overwhelming unresolved envelope.

C. Fluorescence Synchronous Scanning

This analysis was performed only on the pentane extracted fractions of Samples 1 and 6 (burn residue and unburned sample, Test No. 1). This fluorescence analysis indicates similar proportions of fluorescing components based on ring size. The two oils may be identified as originating from the same source. This is a very sensitive test for polynuclear aromatic (PNA) compounds, so it may be concluded that the proportion of PNA's was not affected by burn test No. 1. Dilutions of the oil in cyclohexane were performed to verify that interferences due to fluorescence quenching were not present.

D. High Performance Liquid Chromatographic (HPLC) Analysis

This analysis supported the results obtained from our fluorescence analysis. The HPLC chromatograms of the burn residue and unburned oil sample (Test No. 1) are identical. This analytical procedure allows for the separation of PNA mixtures. The burn test did not result in the formation or loss of large quantities of PNA's.

E. Fraction Composition

Analysis of the composition of the major fractions to determine if any increase in the % water and % sediment (particulates) occurred in the burn residues were inconclusive. A small change in the % of the asphaltene fraction was detected. These small variations in the samples analyzed are shown below.

Sample	Name	Asphaltene % (wt)
1	Residue No. 1	6%
4	Residue Burn Test No. 5	10%
5	Weathered No. 5	2%

Although not all samples were analyzed, the unburned oils should be similar to Sample 5. The burn residue samples were found to contain a higher percentage of toluene-insoluble components.

F. Infrared Analysis

Infrared analysis was performed on the pentane extracts of samples 1, 4, 5, and 6. These analyses showed minor changes in the burn residue samples as compared to the unburned oil samples which are typical for a weathered oil. (The baseline was lowered and two characteristic peaks (at 725 and 745 cm^{-1}) in the fingerprint region were reversed in intensity.) One anomaly which should be noted is that the carbonyl peak at 1750 cm^{-1}, which typically increases on weathering, was absent. The burned oil, while exhibiting some changes characteristic of weathering with the exception of the carbonyl increase, could be readily matched to the unburned oil.

Infrared analysis of the asphaltene fractions of samples 1, 5, and 6 produced identical spectra. Sample No. 4, a burn residue, was similar, but showed two significant differences. A peak at 1605 cm^{-1} increased in intensity and a peak at 1367 cm^{-1} was shifted in wavelength and changed in intensity. Changes in the chemical composition of the asphaltene fraction may be occurring, although they were not observed in sample No. 1, also a burn residue.

IV. CONCLUSIONS

We can readily identify each pair of the unburned oil and burn residue samples as coming from the same source. The significant observation is that burning the crude oil, under the conditions used in these tests, did not affect the oil fingerprinting techniques currently in use by the Central Oil Identification Laboratory (COIL).

If the light ends are lost, as seems highly probably, it does not affect the remainder of the oil for ID purposes based on the samples provided. Increasing the heavy, toluene- insoluble components, also has no effect on the standard oil ID procedure. Infrared spectroscopic analysis of the asphaltene fraction did show chemical differences for one of the burn residue samples.

V. CONSIDERATIONS FOR FUTURE WORK

It is a guideline for analytical chemistry that an analysis can reflect only the quality of the sample submitted for analysis. A good analysis is dependent on a representative sample. If the objective of the study is to compare the average composition of the burn residue with the original oil, large composite samples such as were collected in the previous study are sufficient. This, however, masks changes occurring in a thin layer on the surface of the oil, because the layer becomes mixed in with the bulk oil. If regional changes are of interest, the sample should be collected in a manner which removes the surface preferentially.

If the objective of the study is to determine the extent to which the light ends have been removed, high performance liquid chromatography separation procedures can be developed with other columns and detectors. Comparison of such chromatograms would be more helpful than examining those obtained by gas chromatography, because it would contain information about the total sample.

APPENDIX 4

CHAPTER 7 MODEL FACTORS

Scaling Factors

Dimensionless variables $x \equiv r_s/V_s^{1/3}$; $\tau = t \Big/ \left(\frac{V_s^{1/3}\rho_w}{g\Delta\rho}\right)^{1/2}$

$g = 9.8\ m/s^2$, $\rho_w = 1{,}000\ kg/m^3$, $\Delta\rho = 200\ kg/m^3$

V_s; m^3	r_s; m	t; s
10^{-2}	0.215 x	0.332 τ
1	x	0.714 τ
10^2	4.64 x	1.54 τ
10^4	21.5 x	3.32 τ

Appendix 2. Parameters of Slicks Studied

V_s, m^3	c	u_c, m/s	b	x^*	τ^*	A
10^{-2}	2.6844	0	0	5.142	20.34	-0.4448
		0.01	0.015389	5.03	22.21	-0.33919
1	3.2522	0	0	7.545	43.80	-0.6545
		0.01	0.007143	7.44	46.43	-0.54796
10^2	3.9401	0	0	11.08	94.38	-0.9552
		0.01	0.003315	10.97	98.13	-0.85771
10^4	4.7736	0	0	16.26	203.3	-1.4049
		0.01	0.001539	16.15	208.7	-1.31006

Note that the parameters listed for u_c = 0.01 m/s in each of the four cases were calculated on the basis of ignition with zero delay. Ignition at some intermediate time during the GI regime would yield different values of x^*, t^*, and A.

APPENDIX 5

PROCEDURE FOR MODIFIED ASTM DISTILLATION

APPENDIX

8.0 PROCEDURE FOR MODIFIED ASTM DISTILLATION

8.1 Introduction

The experimental procedure is similar to the standard ASTM distillation method (ASTM D 86). The only major difference is that the oil temperature instead of the vapour temperature is monitored. Distillation data are used to provide the weathering rate of crude oil in the environment.

8.2 Procedure

- Add stirring bar and about 15 ml of glass beads to a 500 ml distillation flask.

- Pour 200 ml of crude oil into the distillation flask.

- Assemble distillation equipment, put aluminum foil around distillation equipment and start cooling water flow.

- Make sure tip of the temperature probe is below oil surface during the experiment.

- Turn stirrer on as fast as possible (without oil splashing).

- Start heating slowly. Condensate should run down the condenser in a dropwise fashion.

- Record initial temperature when the first drop of condensate runs down the curve of the condenser receiver.

- Record temperature at every 2 ml of condensate collected. Stop distillation when oil sample starts to foam, or no more condensate can be collected, or when the oil temperature is above 300 deg C.

- Turn off heater and stirrer. Remove heater and wait for equipment to cool.

- Record atmospheric pressure.

- Cleanup when equipment is cool.

APPENDIX

8.0 PROCEDURE FOR MODIFIED ASTM DISTILLATION (Cont'd)

8.3 Calculations

8.3.1 Atmospheric Pressure Correction

Calculate correction factor:

$$C = 0.00012\ (760 - P)\ (273 + t)$$

where: P = atmospheric pressure in mm Hg
t = thermometer reading in deg C

Add correction factor to thermometer reading and round off readings after decimal point.

8.3.2 Initial Boiling Point and Slope

Convert volume condensed to volume fraction distilled. Plot corrected boiling temperature versus fraction of oil distilled on linear coordinates. Draw a best fit straight line through the data points. Determine the initial boiling point and slope of the line.

Ref.: A Catalogue of Crude Oil and Oil Product Properties
EPS Publication EE-57

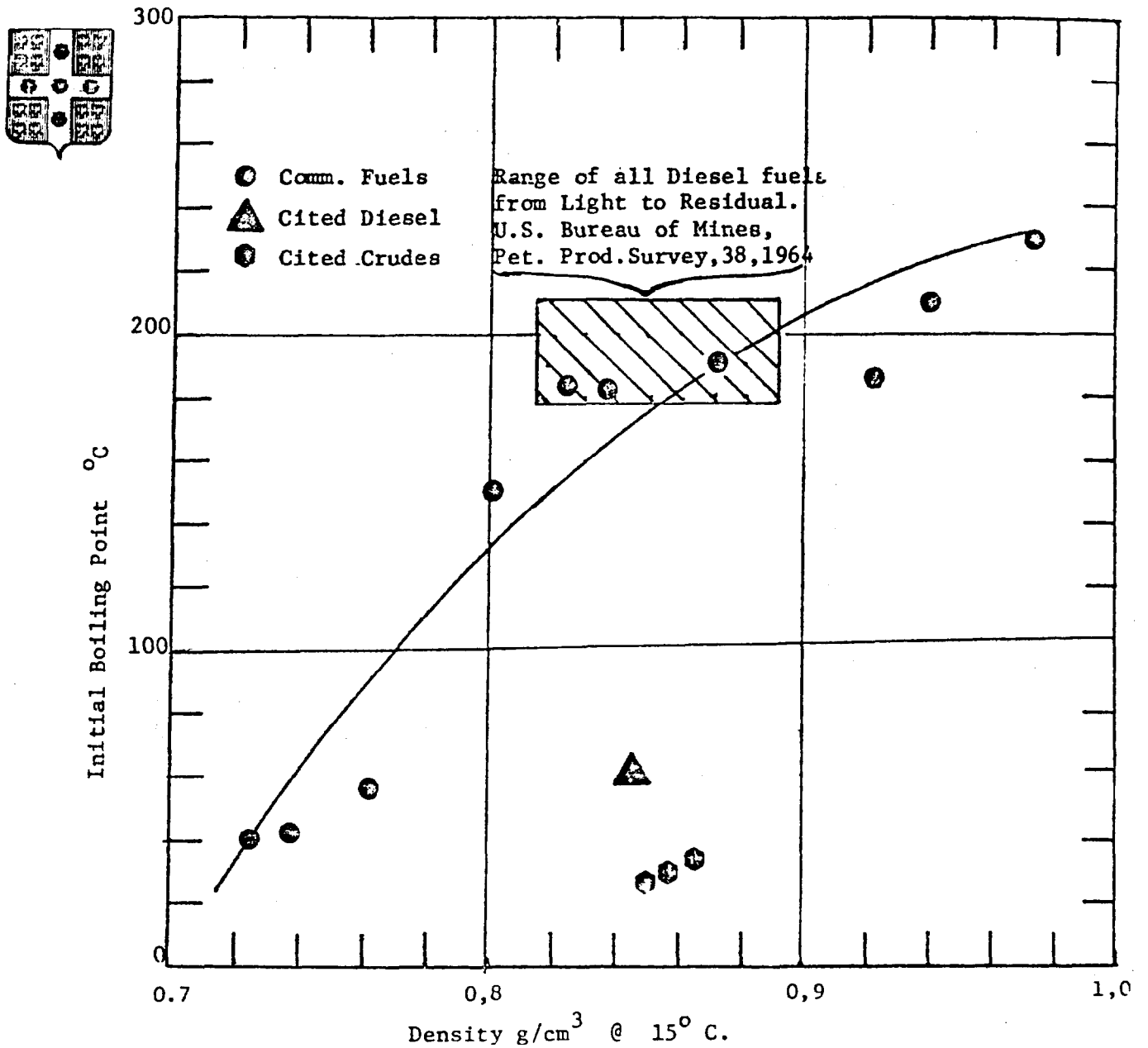

Density / Initial Boiling Point Relationship, Commercial Fuels

Ref.: Prof. J. Odgers, Dept. of Mechanical Engineering
University of Laval, Québec, P.Q.

Fig. 2.